

Electronic Thesis and Dissertation Repository

June 2015

The lung microenvironment influences the metastatic behaviour of breast cancer cells in an innovative 3D ex vivo pulmonary metastasis model

Matt M. Piaseczny, *The University of Western Ontario*

Supervisor: Dr. Alison Allan, *The University of Western Ontario*

A thesis submitted in partial fulfillment of the requirements for the Master of Science degree in Anatomy and Cell Biology

© Matt M. Piaseczny 2015

Follow this and additional works at: <https://ir.lib.uwo.ca/etd>



Part of the [Cancer Biology Commons](#)

Recommended Citation

Piaseczny, Matt M., "The lung microenvironment influences the metastatic behaviour of breast cancer cells in an innovative 3D ex vivo pulmonary metastasis model" (2015). *Electronic Thesis and Dissertation Repository*. 2915.

<https://ir.lib.uwo.ca/etd/2915>

This Dissertation/Thesis is brought to you for free and open access by Scholarship@Western. It has been accepted for inclusion in Electronic Thesis and Dissertation Repository by an authorized administrator of Scholarship@Western. For more information, please contact wlsadmin@uwo.ca.

THE LUNG MICROENVIRONMENT INFLUENCES THE METASTATIC
BEHAVIOUR OF BREAST CANCER CELLS IN AN INNOVATIVE 3D
EX VIVO PULMONARY METASTASIS MODEL

(Thesis format: Monograph)

by

Matthew M. Piaseczny

Graduate Program in Anatomy and Cell Biology

A thesis submitted in partial fulfillment
of the requirements for the degree of
Master of Science

The School of Graduate and Postdoctoral Studies
The University of Western Ontario
London, Ontario, Canada

© Matthew M. Piaseczny 2015

ABSTRACT

Lung metastasis remains a leading cause of death in breast cancer patients. This study established an innovative 3D *ex vivo* pulmonary metastasis assay (PuMA) to test the hypothesis that the lung microenvironment promotes metastatic behaviour of whole population and stem-like ALDH^{hi}CD44⁺ breast cancer cells. Following *in vivo* delivery of breast cancer cells to mice, lungs were excised, maintained in culture and imaged to observe breast cancer growth over time. We observed metastatic progression of breast cancer cells in the PuMA, most notably of ALDH^{hi}CD44⁺ cells which progressed rapidly from single cells to multicellular colonies over 21 days relative to their ALDH^{lo}CD44⁻ counterparts ($p \leq 0.05$). Although soluble lung-derived bFGF induced breast cancer cell proliferation *in vitro*, blocking bFGF in the PuMA showed only a trend towards inhibition of breast cancer cell growth. This model system will be valuable for elucidating the interaction between breast cancer cells and the lung during metastatic progression.

Keywords: Breast cancer, metastasis, organ-specific tropism, pulmonary metastasis assay (PuMA), cancer stem cell, aldehyde dehydrogenase (ALDH), CD44, basic fibroblast growth factor (bFGF).

CO-AUTHORSHIP STATEMENT

Fluorescence activated cell sorting (FACS) and analysis was done by Dr. Kristin Chadwick (London Regional Flow Cytometry Facility, Western University).

Preparation of histological sections and H&E staining was performed by Carl Postenka (Histology Research Technician, London Health Sciences Centre).

ACKNOWLEDGEMENTS

First and foremost, I would like to extend a huge thank you to my supervisor, Dr. Alison Allan. You were kind enough to take me in as a Master's student initially and have continued to provide me with support and guidance. I not only consider you my supervisor, but a friend and a friend that I truly respect and can count on for encouragement and advice. Thank you again for all of the countless hours you put into editing my posters, reports, papers, scholarships and this thesis, ensuring I was adequately prepared and for your help in shaping me into the student I am today. I am truly grateful for this experience.

I would also like to thank all the past and present members of the Allan lab, especially Lori Lowes, Gracie Pio, Ying Xia, Mauricio Rodrigues, Maria Vieito and David Goodale. You guys make work easy to come to and make me look forward to coming into the lab everyday. You have all made life much easier when things didn't quite work out and have always been there to offer friendly advice. I will never forget the stories and laughs we shared. I am so appreciative of the environment that I got to spend my Master's and couldn't have asked for better labmates. I would also like to thank everyone at the London Regional Cancer Program, including professors, students, staff, and admin for all of their guidance and help as well. It was very nice getting to know everyone and I couldn't imagine a better place to learn and work in.

A special thank you also goes to my advisory committee members: Dr. Ann Chambers, Dr. Trevor Shepherd and Dr. Paul Walton for your insight and guidance throughout my Master's. I don't think I could have asked for a better committee. Your continuous constructive criticism, support and encouragement have kept me on track and motivated throughout my project.

A big thank you goes to both my best friend and partner in crime, Julie La. Words cannot describe how influential and important you have been throughout the last seven years and during this degree. I couldn't imagine going through this without you. You've

continued to believe in me through thick and thin and are my biggest supporter. You continue to make me a better person and I am extremely grateful to have shared this experience with you.

Lastly, I'd like to thank both my immediate and extended family. Especially my parents, Michael and Jacqueline, brother Mike and sister Alicia. You guys have supported and believed in me since day one and have continued to help me pursue my dreams. The sacrifices you've made and the help you've landed will never go unnoticed, I am truly blessed. You have all pushed me to be the best I can be and I could not imagine doing this without you guys!

TABLE OF CONTENTS

ABSTRACT	ii
CO-AUTHORSHIP STATEMENT.....	iii
ACKNOWLEDGEMENTS	iv
TABLE OF CONTENTS.....	vi
LIST OF TABLES	ix
LIST OF FIGURES	x
LIST OF APPENDICES	xii
LIST OF ABBREVIATIONS, SYMBOLS, NOMENCLATURE	xiii
1. INTRODUCTION	1
2. LITERATURE REVIEW.....	2
2.1. Cancer	2
2.2. Breast Cancer	3
2.3. Breast Cancer Subtypes	4
2.4. Metastasis.....	5
2.5. Organ-specific Tropism	7
2.6. Importance of Molecular Subtype	8
2.7. Breast Cancer Cell Gene Signature Can Influence Organ Tropism.....	8
2.8. Stem-like Breast Cancer Cells	9
2.9. The “Soil”: Organ Microenvironments.....	10
2.10. Soluble Lung Microenvironment	11
2.11. Insoluble Lung Microenvironment	12
2.12. Techniques for Studying Metastasis in vivo	13
2.13. Ex vivo Pulmonary Metastasis Assay	14

2.14.	Study Rationale	15
3.	HYPOTHESIS AND OBJECTIVES.....	16
3.1.	Hypothesis.....	16
3.2.	Objectives	16
4.	MATERIALS AND METHODS.....	17
4.1.	Cell Culture and Reagents	17
4.1.1.	Generation of Fluorescent Cell Lines	17
4.2.	Fluorescence Activated Cell Sorting.....	19
4.3.	Pulmonary Metastasis Assay.....	21
4.3.1.	Lung Seeding, Harvesting and Culturing	21
4.3.2.	Imaging and Analysis of Lung Sections	27
4.4.	Histology and Immunohistochemistry	29
4.5.	Lung-Conditioned Media, Primary Cell Isolation and Reagents.....	30
4.5.1.	Animals and Lung Harvesting	30
4.5.2.	Lung-Conditioned Media Generation.....	30
4.6.	Assessment of bFGF Concentration	31
4.6.1.	bFGF Immunodepletion from Lung-Conditioned Media	31
4.7.	In vitro Transwell Migration Assay	33
4.8.	In vitro BrdU Incorporation Assay	34
4.9.	Blocking of bFGF and CD44 in the PuMA	35
4.10.	Statistical Analysis	37
5.	RESULTS	38
5.1.	Pulmonary Architecture Remains Structurally and Microscopically Intact in the PuMA over 21 days	38
5.2.	Whole Population MDA-MB-468, SUM149 and MDA-MB-231 Breast Cancer	

	Cell Lines Demonstrate Differential Growth Progression Within the PuMA	40
5.3.	Highly Metastatic MDA-MB-231 Cells Proliferate in the PuMA.....	43
5.4.	Stem-like ALDH ^{hi} CD44 ⁺ MDA-MB-231 Breast Cancer Cells Progress Relative to ALDH ^{lo} CD44 ⁻ Cells within the PuMA	43
5.5.	ALDH ^{hi} CD44 ⁺ Breast Cancer Cells Progress from Single Cells to Micrometastases to Macrometastases in the PuMA while the Majority of ALDH ^{lo} CD44 ⁻ Cells Remain as Single Cells.....	47
5.6.	Basic Fibroblast Growth Factor is Present in Lung-conditioned Media and Increases in vitro Breast Cancer Cell Proliferation, but not Migration	50
5.7.	Basic Fibroblast Growth Factor is Present in the Intact Lung Microenvironment	55
5.8.	Blocking bFGF or CD44 on Whole Population MDA-MB-231 Cells Does Not Decrease Cellular Growth in the PuMA	57
6.	DISCUSSION.....	60
6.1.	Summary of Experimental Findings	61
6.2.	Advantages of the PuMA as a Model for Metastasis	62
6.3.	ALDH ^{hi} CD44 ⁺ Breast Cancer Cells Drive Metastatic Progression Within the Lung Microenvironment.....	64
6.4.	The Complexity of the Lung Microenvironment.....	66
6.5.	bFGF in the Lung Microenvironment.....	67
7.	POSSIBLE LIMITATIONS OF THE STUDY.....	71
8.	FUTURE DIRECTIONS.....	73
9.	FINAL CONCLUSIONS.....	76
	BIBLIOGRAPHY.....	78
	APPENDICES.....	92
	CURRICULUM VITAE.....	93

LIST OF TABLES

Table 1. Cell lines and culturing conditions.....	18
Table 2. Media formulations for lung tissue used in the PuMA	26
Table 3. Proportion of SUM149 ALDH ^{hi} CD44 ⁺ and ALDH ^{lo} CD44 ⁻ colony sizes in the PuMA.....	49
Table 4. Proportion of MDA-MB-231 ALDH ^{hi} CD44 ⁺ and ALDH ^{lo} CD44 ⁻ colony sizes in the PuMA	51

LIST OF FIGURES

Figure 1. The metastatic cascade.....	6
Figure 2. Aldefluor™ Assay.....	20
Figure 3. Isolation strategy for tdTomato expressing stem-like human breast cancer cells from the SUM149 breast cancer cell line.....	22
Figure 4. Isolation strategy for tdTomato expressing stem-like breast cancer cells from the MDA-MB-231 human breast cancer cell line.....	24
Figure 5. Pulmonary Metastasis Assay (PuMA)	28
Figure 6. Lung-conditioned media generation and bFGF immunodepletion.....	32
Figure 7. Blocking strategy for bFGF and CD44 in the PuMA.....	36
Figure 8. Pulmonary architecture remains structurally and microscopically intact in the PuMA over 21 days	39
Figure 9. Whole population MDA-MB-468, SUM149 and MDA-MB-231 human breast cancer cell lines differentially progress within the PuMA	41
Figure 10. Highly metastatic MDA-MB-231 cells proliferate in the PuMA.....	44
Figure 11. Stem-like ALDH ^{hi} CD44 ⁺ MDA-MB-231 breast cancer cells progress relative to ALDH ^{lo} CD44 ⁻ cells within the PuMA	45
Figure 12. ALDH ^{hi} CD44 ⁺ breast cancer cells progress from single cells to micromets to macromets while the majority of ALDH ^{lo} CD44 ⁻ cells remain as single cells.....	48
Figure 13. Depletion of bFGF from lung-conditioned media reduces breast cancer cell proliferation but not migration.....	53
Figure 14. Basic fibroblast growth factor is present in the intact lung microenvironment.	56

Figure 15. Blocking bFGF and CD44 has no effect on growth reduction of whole population MDA-MB-231 cells in the PuMA58

LIST OF APPENDICES

Appendix 1. Approved animal use protocol.....	92
--	----

LIST OF ABBREVIATIONS, SYMBOLS, NOMENCLATURE

3D	3-Dimensional
4-PL	Four-parameter Logistic
7-AAD	7-aminoactinomycin A
α MEM	Minimum Essential Media Alpha
ALDH	Aldehyde Dehydrogenase
AML	Acute Myeloid Leukemia
ANOVA	Analysis of Variance
APC	Allophycocyanin
BAAA	BODIPY-aminoacetaldehyde
bFGF	Basic Fibroblast Growth Factor
BLI	Bioluminescence
BM	Basal Media
BrdU	bromodeoxyuridine
BSA	Bovine Serum Albumin
CCR	Chemokine (C-C motif) Receptor
CD	Cluster of Differentiation
CM	Conditioned Media
CSC	Cancer Stem Cell
CT	Computed Tomography
CTC	Circulating Tumour Cell
d	Day(s)
DAB	3,3'-Diaminobenzidine
DAPI	4',6-diamidino-2-phenylindole
DCIS	Ductal Carcinoma <i>in situ</i>
DEAB	Diethylaminobenzaldehyde
DMEM	Dulbecco's Modified Eagle Medium
DNA	Deoxyribonucleic Acid

ECM	Extracellular Matrix
EDTA	Ethylene diamine tetraacetic acid
EGF	Epidermal Growth Factor
EGFR	Epidermal Growth Factor Receptor
ELISA	Enzyme-linked Immunosorbant Assay
ER	Estrogen Receptor
EREG	Epiregulin
FACS	Fluorescent Activated Cell Sorting
FBS	Fetal Bovine Serum
FGF	Fibroblast Growth Factor
FGF-2	Fibroblast Growth Factor Receptor-2
FITC	Fluorescein Isothiocyanate
FOV	Field of View
G	Gauge
H	Hour(s)
HBSS	Hank's Balanced Salt Solution
H&E	Hematoxylin and Eosin
HER2,3,4	Human Epidermal Growth Factor Receptor-2,3,4
HMW	High Molecular Weight
HRP	Horseradish Peroxidase
IVM	Intravital Microscopy
LCIS	Lobular Carcinoma <i>in situ</i>
LMW	Low Molecular Weight
LN	Lymph Node(s)
M199	Media 199
min	Minute(s)
MMP1	Matrix Metalloproteinase-1
MRI	Magnetic Resonance Imaging

NLS	Nuclear Localization Sequence
O/N	Overnight
OI	Optical Imaging
OPN	Osteopontin
PBS	Phosphate Buffered Saline
PDGF	Platelet Derived Growth Factor
PE	Phycoerythrin
PET	Positron Emission Tomography
PR	Progesterone Receptor
PuMA	Pulmonary Metastasis Assay
RFP	Red Fluorescent Protein
RT	Room Temperature
SELL	L-selectin
SEM	Standard Error of the Mean
TCGA	The Cancer Genome Atlas
TGF α	Transforming Growth Factor alpha
TN	Triple Negative
VM	Video Microscopy

1. INTRODUCTION

Despite earlier screening and ongoing research in the areas of cancer treatment and prevention, cancer remains the leading cause of death in developed countries worldwide. Interestingly, cancer prevalence is also increasing in developing areas of the world as a result of population growth and aging as well as the adoption of risk-factor associated lifestyles (smoking, inactivity, “westernized” diets) [1, 2].

Breast cancer is the second most common cancer in the world and ranks number one in terms of most frequent cancer diagnoses amongst women and the second leading cause of cancer related deaths in North America [1-4]. Over the past 25 years we have seen a drastic increase in overall 5-year survival rates for patients with breast cancer, largely due to improvements in treatment and the widespread use of mammography [5]. Breast cancer caught early on results in 5-year survival rates of 98.6% and 84.4% for localized and regional breast cancers, respectively [6]. However, survival rate significantly declines to less than 25% in women diagnosed with late-stage metastatic spread [6, 7]. Therefore, the majority of deaths associated with breast cancer are not due to the burden of the primary tumour, but rather the later stages following metastatic spread, especially towards the lungs [8, 9].

The focus of this thesis is to investigate the importance of the native lung microenvironment on the behaviour of both whole population and stem-like breast cancer cells using an innovative 3D animal model, so we can better understand which aspects of the lung make it a permissible environment for breast cancer to grow and progress.

2. LITERATURE REVIEW

2.1. Cancer

Cancer is a complex set of diseases characterized by the failure of cellular growth regulation. Loss in regulation most often occurs by means of genetic disruption, eventually resulting in loss of homeostasis and subsequent aberrant growth and unlimited proliferative capacity. Fundamentally, characteristics acquired during cancer growth and progression include self-sufficiency in growth signalling, insensitivity to anti-growth signals, acquisition of limitless replicative capacity, ability to promote and sustain angiogenesis, evasion of apoptosis and tissue invasion and metastasis [10, 11].

Malignant transformation of normal cells can often be linked to disruptions in two different categories of genes: oncogenes and tumour suppressor genes. Oncogenes are those that promote cell growth and reproduction and are tumour-promoting when over stimulated. When constitutively activated, oncogenes cause cells destined for apoptosis or cell death to survive and continue to proliferate [12]. In contrast, tumour suppressor genes are those that inhibit cell division and survival and promote apoptosis and cell cycle arrest [13]. Typically, mutations or epigenetic changes in several genes are needed to transform a healthy cell into a malignant one [14, 15].

Cancers are typically classified according to the cell type in which they resemble and therefore most likely derive from. For example, carcinomas are cancers derived from epithelial cells, sarcomas from connective tissue, lymphoma or leukaemia from hematopoietic origin, germ-line tumours from germ-line cells and blastomas from embryonic cells [16]. Benign tumours are those which remain contained within the tissue of origin and are not usually life-threatening. In contrast,

malignant tumours are life threatening and are able to invade surrounding tissues and move to distant areas of the body separate from the primary tumour [12].

2.2. Breast Cancer

The principle structure of the breast is the mammary gland. The mammary gland is composed of alveoli lined with milk-producing cuboidal epithelia surrounded by a layer of myoepithelia. Many alveoli join together to form groups called lobules, each having a lactiferous duct responsible for draining to the nipple, composed of ductal epithelia surrounded by myoepithelia [17, 18]. Breast cancer is neoplastic formation originating from breast tissue, most commonly from the ducts that carry milk or the lobules that supply them. The susceptibility of these structures to benign and malignant transformations are in part a consequence of cycling hormonal stimulation throughout life leading to increased cell turnover and accumulation of genetic defects [19, 20].

Cancer originating from the milk ducts and lobules are referred to as ductal carcinoma or lobular carcinoma, respectively [21]. Ductal carcinoma represents the most commonly diagnosed breast tumour, accounting for approximately 75% of breast cancer cases [22, 23]. Breast cancer can often be classified according to different schemas. Histopathological analysis is commonly used when determining the class of breast cancer. Tumours confined within the ducts or lobules that have not spread beyond their borders are referred to as either ductal carcinoma *in situ* (DCIS) or lobular carcinoma *in situ* (LCIS). Both DCIS and LCIS are non-invasive in nature and lack invasion into surrounding tissues [24, 25]. Therefore, when breast cancer remains *in situ*, traditional treatments are highly effective if required [26]. Prognosis worsens for patients with invasive ductal or lobular carcinoma; characterized by tumour that has infiltrated surrounding tissues [27]. Invasive disease often leads to further cancer dissemination throughout the body, leading to distant metastatic disease. Many of the traditional methods for treating breast cancer often fail once the cancer has reached the metastatic setting [28]. Therefore, the majority of deaths associated with breast cancer are attributed to cancer that has spread from the initial

region of the breast to distant organs [8, 9], necessitating a deeper understanding of this complex metastatic process.

2.3. Breast Cancer Subtypes

In addition to histopathological classification, breast cancer can also be categorized according to molecular subtype [22]. Genomic profiling and immunohistochemical markers have revealed the presence of specific molecular subtypes with predictable clinical behaviours. The Cancer Genome Atlas (TCGA) classifies breast cancer subtypes into one of four specific groups: luminal A, luminal B, HER2-enriched or basal-like (triple negative; TN) [29-31]. Although a complex molecular and genetic profile is needed to determine exact subtype, most subtypes can be roughly defined by hormone receptor status (estrogen and progesterone), HER2/neu status (a member of the epidermal growth factor receptor family) and proliferation rate [32, 33]. Luminal A tumours resemble the inner linings of mammary ducts and tend to be ER⁺/PR⁺ and HER2⁻. Since these tumours are often ER⁺, they respond well to hormone therapy and often have favourable prognoses and survival rates associated with them [34, 35]. Luminal B tumours also resemble the inner linings of mammary ducts and tend to be ER⁺/PR⁺ but are highly positive for the proliferative marker Ki-67 and/or HER2⁺. Women diagnosed with these tumours also tend to have fairly high survival rates, but not as high as those with luminal A tumours [35, 36]. HER2-enriched tumours are most commonly ER⁻/PR⁻ and HER2⁺, although a small percentage of this subtype are HER2⁻. These tumours often have a poorer prognosis and are prone to metastasis and frequent recurrence [31, 32, 37]. HER2⁺ tumours can however be treated with the targeted therapy Herceptin (trastuzumab), which targets the HER2 surface receptor on breast cancer cells, slowing growth and progression [38]. Basal-like or TN breast tumours share features with the outer lining of mammary ducts and are defined as ER⁻/PR⁻ and HER2⁻. Most TN breast cancers are highly aggressive and have a poor prognosis and relatively low 5-year survival rates [32, 39, 40].

Traditionally, molecular subtype classification has been involved with aiding clinical treatment decisions for patients, particularly in terms of targeted therapies. However, breast tumour populations are often heterogeneous in nature and therefore are comprised of cells with varying molecular subtypes. Therefore, molecular subtype classification should not be used exclusively as a means of treatment consideration, especially as we continue to appreciate the vast heterogeneity that exists within solid breast tumours [41].

2.4. Metastasis

Metastasis is a complex process by which a series of cellular events are ultimately responsible for tissue invasion and distant tumour establishment [42]. The metastatic process consists of a series of coordinated steps in a prototypical cascade. Over time, rare subsets of tumour cells acquire a more invasive phenotype and break off from the primary tumour. Invasive tumour cells attach to basement membranes and release extracellular matrix (ECM) degrading enzymes and factors, which facilitate infiltration into surrounding tissues and entry into the circulation or lymphatics [43]. As primary tumours grow and develop, they require a supply of oxygen to support metabolic needs, and therefore promote angiogenesis or the recruitment of new blood vessels. Angiogenesis and the proximity of a blood supply to the tumour also provide a route by which tumour cells can invade the vasculature and spread [28, 44]. Once in the circulation, tumour cells need to survive, which often represents a rate limiting step for metastasis. Successful circulating tumour cells (CTC) remain in the circulation until they extravasate into a new tissue where they ultimately initiate and establish a secondary tumour, distant from the primary tumour [28, 45, 46] (**Figure 1**). Metastasis is an inherently inefficient process as only a small subset of invading tumour cells are able to successfully establish secondary tumours and survive within the tissue [47]. Although this process is relatively inefficient, it still remains one of the most important issues regarding cancer related deaths. Many conventional anti-cancer therapies such as surgery, radiotherapy, and hormone therapy are fairly successful when treating cancers detected and diagnosed prior to

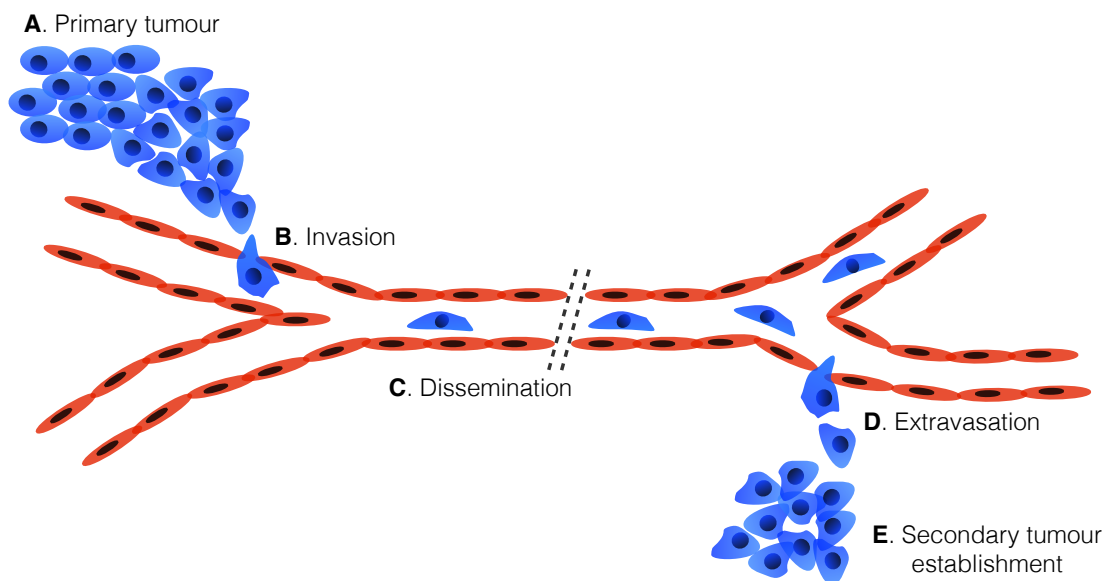


Figure 1. The metastatic cascade. Metastasis is a complex process by which tumour cells spread to distant sites throughout the body. This occurs by a series of coordinated cellular events: (A) Development of a primary tumour, (B) a subset of primary tumour cells invade and enter surrounding tissue and vasculature, (C) tumour cells disseminate within the blood and/or lymphatics, (D) tumour cells attach to vessel walls and extravasate into a secondary tissue, (E) tumour cells establish a secondary tumour distant from the primary tumour site. The final step represents a metastatic lesion.

distant metastasis. However, most current therapies ultimately fail with respect to metastatic tumours, for reasons still poorly understood [28]. Therefore, metastatic progression illustrates a fundamental event for understanding during the progression of cancer.

2.5. Organ-specific Tropism

Although most cancers have the potential to spread to multiple organs, they usually prefer certain sites in relation to others. The preference of particular cancers to metastasize to specific organs is termed “organ tropism” and it has been well established that breast cancer exhibits this phenomenon [28, 29, 48, 49]. Clinically, the most common sites for breast cancer to spread to are the lung, bone, liver, brain and lymph nodes (LN). Metastasis to the lung is of particular interest due to its poor prognosis and lethality in breast cancer patients [29].

Multiple theories have been developed to explain the process of organ-specific tropism, including Stephen Paget’s seminal “seed and soil” hypothesis in 1889, and Ewing’s mechanical arrest theory [50]. Paget’s original theory suggested that organ-specific patterns of metastasis are the result of favourable interactions between tumour cells (the ‘seed’) and their respective organ microenvironment in the secondary site (the ‘soil’) [51]. Paget’s theory therefore predicts that certain cancer cells can survive and proliferate only in secondary sites that produce appropriate factors to sustain growth and survival. In contrast, Ewing’s theory some forty years later postulates that metastatic dissemination is strictly the result of mechanical factors caused by the nature of the vascular system, meaning that cells are mechanically arrested in the first capillary beds they encounter [52]. It is likely that these two theories operate in concert rather than alone to produce and maintain secondary tumour growth, as evidence has shown both theories hold true. That is, breast cancer cells invade the local vasculature, are taken to the heart via the venous circulation and subsequently delivered to the lungs where they mechanically arrest in the first capillary beds they encounter. While there, successive initiation, growth and

maintenance of secondary tumours within the lung is influenced, at least in part, by specific lung-derived factors [53].

2.6. Importance of Molecular Subtype

It is widely believed that as a result of genomic instability within tumour populations, large-scale cellular heterogeneity develops in cancer. As a consequence, tumour cell variants with augmented metastatic capabilities arise through selective pressures [54-56]. Several studies have demonstrated specific genetic signatures or molecular characteristics associated with organ-specific patterns of metastasis in breast cancer [53]. As mentioned previously, breast cancers are often classified into one of four major molecular subtypes (luminal A/B, HER2-enriched or TN) based on genetic and immunohistochemical markers [29, 30]. One particular study by Kennecke and colleagues examined the metastatic dissemination patterns for patients with different breast cancer subtypes. Using 15-year cumulative incidence rates according to metastatic site, they concluded that certain subtypes were associated with particular patterns of metastatic spread. In particular, they found more aggressive subtypes (HER2⁺ and TN) had a propensity for the lungs whereas less aggressive subtypes preferred the bone as a metastatic site. Importantly, this disparity supports the idea that certain molecular characteristics associated with breast cancer cells may be involved in promoting organ-specific patterns of spread [29, 53].

2.7. Breast Cancer Cell Gene Signature Can Influence Organ Tropism

In addition to specific patterns of metastatic spread based on molecular subtype, work done by Joan Massagué's group has also supported the notion that molecular characteristics are in part responsible for organ-tropism. Their experimental studies set out to determine a specific gene signature associated with patterns of lung-specific metastasis in breast cancer. Using a mouse model of lung metastasis, their group was able to successfully generate a lung-seeking variant of the aggressive TN human breast cancer cell line MDA-MB-231 through multiple rounds of *in vivo* selection [56]. Following transcriptome analysis of both parental and lung-seeking variants, their work revealed a gene signature associated with lung-specific

metastasis distinct from a previously identified bone-specific signature. Interestingly, many genes identified had not been previously linked to metastasis. Genes that did correlate with metastasis were comprised of extracellular and receptor proteins including a HER receptor ligand (epiregulin; EREG), adhesion receptors (ROBO1), specific chemokines (CXCL1), secreted proteases (MMP1), and transcriptional regulator proteins (ID1, ID3) [45, 57, 58]. These important findings suggest an intimate relationship between cancer cells, their genetic signature and specific organ microenvironments most permissive to their growth and survival. However, it remains relatively unclear as to when and why subsets of tumour cells acquire these gene signatures during the progression of cancer.

2.8. Stem-like Breast Cancer Cells

Recent studies have described a unique subpopulation of cancer cells within solid tumours termed “cancer stem cells” (CSC) [59, 60]. These cells represent a small subset of cells within the tumour characterized by stem-like properties including self-renewal and multi-lineage differentiation [61]. The cancer stem cell model suggests that CSCs represent a distinct population of tumour cells ultimately responsible for tumour initiation, metastatic spread and therapy resistance [60]. The first evidence to support this hypothesis was provided in 1994 by John Dick and colleagues, who demonstrated that human acute myeloid leukemia (AML) was organized as a hierarchy that originates from a primitive leukemia-initiating hematopoietic cell [62, 63]. In breast cancer, tumour-initiating cells or CSCs have been isolated from patient tumours and various breast cancer cell lines based on a CD44⁺CD24⁻ phenotype and/or high aldehyde dehydrogenase (ALDH) activity [64-67]. CD44 is a cell surface glycoprotein with well-defined roles in cell-cell interactions, cell adhesion, migration and metastasis [68]. The ALDH superfamily of intracellular enzymes is involved in the detoxification of aldehydes [67, 69, 70] with ALDH1A1 and ALDH3A1 isoforms having defined roles in normal stem cell function and self-protection [71]. Interestingly, high expression of ALDH1 has been associated with a poorer prognosis in breast cancer patients as well as an increased risk of metastatic progression [72, 73]. Previous work done by Alysha Croker in our

lab demonstrated that high ALDH activity in addition to CSC surface marker expression (CD44⁺CD24⁻) selects for a highly enriched population of stem-like breast cancer cells with enhanced metastatic properties and therapy resistance [67]. In this study, ALDH^{hi}CD44⁺ breast cancer cells isolated from MDA-MB-468 and MDA-MB-231 breast cancer cell lines demonstrated enhanced cell growth, colony formation, migration, and invasion *in vitro* as well as enhanced tumourigenicity and metastasis *in vivo* [67]. This data demonstrates the functional importance of ALDH^{hi}CD44⁺ breast cancer cells in promoting many of the events that accompany metastatic progression.

2.9. The “Soil”: Organ Microenvironments

It is becoming increasingly clear that specific organ microenvironments have a profound influence on the biology of tumour growth and survival. The end result of the metastatic cascade (development of clinically relevant macrometastases) depends greatly on the interactions between metastatic cells and host homeostatic mechanisms [48, 57]. Previous studies have conclusively demonstrated in animal models that tumour cells are able to reach the microvasculature of many organs but sustained growth, survival and progression only occurred within specific organs [74, 75]. These studies support the role of certain organ microenvironments in promoting and sustaining metastases within a secondary environment. Once tumour cells reach distant organs, they must proliferate to establish a successful secondary tumour. To accomplish this, tumour cells can usurp physiological growth factors produced by the microenvironment. In addition, the organ microenvironment can also influence how metastases respond to common means of clinical intervention, including chemotherapy and radiation [76]. For example, previous studies by Wilmanns *et al.* have observed that murine fibrosarcomas or colon carcinomas grown subcutaneously in syngeneic mice were sensitive to systemic administration of doxorubicin, whereas lung or liver metastases were not [59]. Therefore, new therapeutic approaches for metastasis should be targeted not only against tumour cells but also against host factors favourable to tumour metastasis, growth, and survival.

2.10. Soluble Lung Microenvironment

Previous work done in our lab by Jenny Chu has led to the development and establishment of a comprehensive *ex vivo* murine model for studying the influence of organ-derived soluble factors on breast cancer cell metastatic behaviour. Organs representing common clinical sites of breast cancer metastasis (lung, bone, liver, brain, LN) were harvested from female nude mice and cultured for the purposes of generating organ conditioned media (CM) [52]. Using this model, Chu demonstrated that different human breast cancer cell lines show specific chemotactic and proliferative behaviours in response to various organ-CM, reflective of their metastatic behaviours *in vivo* [50, 53]. Specifically, the most aggressive of the cell lines, MDA-MB-231, showed increased migration patterns towards bone, lymph node, and lung-CM. The second most aggressive cell line, SUM159, displayed enhanced migration towards the bone, brain, LN, and while the two least aggressive cells lines (SUM149 and MDA-MB-468) demonstrated increased migration to lung-CM only. More specifically, Chu's work has also shown that stem-like ALDH^{hi}CD44⁺ breast cancer cells exhibit preferential migration towards lung-CM over all other organ conditions, complementing Croker's previous work demonstrating that these cells preferentially migrate to the lung *in vivo* [52, 67]. In addition to increased migratory patterns, MDA-MB-231 and MDA-MB-468 cell lines demonstrated cell line specific patterns of proliferation in response to organ-CM. MDA-MB-231 cells showed increased proliferation in the presence of liver and lung-CM and MDA-MB-468 cells showed increased proliferation in the presence of lung-CM [52]. These results indicate the potential of the lung microenvironment in promoting metastatic progression of breast cancer cells as demonstrated by enhanced patterns of migration and proliferation in response to lung-CM.

Protein array analysis of lung-CM identified numerous soluble factors within the lung microenvironment possibly contributing to breast cancer metastasis. Many of these factors have implications during metastasis, migration, growth and adhesion. One protein identified and of particular interest to our group is basic fibroblast growth factor (bFGF or FGF-2) [52]. bFGF is one of 22 mitogenic members of the FGF family, involved in wound healing, tissue repair, and embryonic development [77-79].

Both low molecular weight (LMW) and high molecular weight (HMW) isoforms of bFGF have been characterized, representing alternative translation products from a single mRNA. The 18 kDa LMW isoform is primarily localized to the cytoplasm and is the secreted form, whereas HMW (21-23 kDa) bFGF contains a nuclear localization sequence (NLS)-like domain and is targeted to the nucleus [80-83]. Most stimulatory effects induced by bFGF occur through the secreted LMW isoform and canonically signal through the specific transmembrane fibroblast growth factor receptors (FGFR). There are four tyrosine kinase FGF receptors (FGFR1-4), with bFGF preferentially binding to FGFR1 or FGFR2 with higher affinity than FGFR3/4. Non-canonically, bFGF also interacts and signals through alternative receptors, including CD44 and $\alpha v\beta 3$ [77, 83].

bFGF has been implicated in cancer previously, as a proliferation-inducing signal and during angiogenesis [81, 84, 85]. bFGF is of particular interest to us due to its potent mitogenic capacity, as well as its ability to signal through the CD44 receptor, which is present on stem-like breast cancer cells [52, 67, 70]. However, its role in the metastatic progression of breast cancer within the lung has not previously been explored. This coupled with the fact that this protein has been previously identified in our lab as a soluble factor present in lung-CM has led our interest as to the influence of bFGF during metastatic progression of breast cancer in the lung.

2.11. Insoluble Lung Microenvironment

The role of the lung microenvironment during cancer initiation and progression is for a large part, poorly understood. The lung is composed of over 60 different cell types involved in various functions including sensory, mechanical, secretory and transport [86]. While the soluble microenvironment is much more intuitive to think of as a contributor to cancer progression, we cannot disregard the influence the insoluble microenvironment may play in this dynamic process. In the lung specifically, about 15% of alveolar tissue and 50% of non-alveolar tissue is noncellular, or ECM [87]. The ECM is composed of a myriad of structural proteins including collagen and elastin, specialized proteins such as fibronectin and laminin, as well as high-

molecular weight proteoglycans, which function to support surrounding parenchymal cells [88-90].

Many types of epithelial and endothelial cells are dependent upon adhesion to the ECM for their continued survival and often undergo apoptosis when this adhesion is disrupted [91]. Although cancer cells are characterized by their unique ability to progress and grow in the absence of ECM adhesion, solid tumours often exist in a dynamic relationship between anchorage-dependence and independence [92]. One potential implication of this is that tumour cells bound to the ECM may be relatively protected from chemotherapy compared to non-adhered cells. Therefore, the insoluble lung microenvironment in addition to soluble microenvironmental factors may have a profound impact on the growth and therapy response patterns of cancer cells in the lung.

2.12. Techniques for Studying Metastasis *in vivo*

Traditionally, most metastasis-related research revolves around endpoint analysis, e.g. after a detectable tumour has formed within a secondary site. While this research sheds important light in terms of how and where tumours grow once they metastasize, there often exists a lack of mechanistic knowledge as to how these cells actually escape the primary tumour, invade and exit the vasculature, and ultimately establish a secondary colony from the single cell stage. There exists a biological black box during the metastatic progression from single tumour cells to the formation of gross metastatic lesions [93]. Several attempts have been made to understand these important initial steps of metastatic progression by imaging the early stages of metastasis *in vivo*. Many of these modalities include techniques that mirror methods for human imaging, including computer tomography (CT), micro-positron emission tomography (PET), and magnetic resonance imaging (MRI) [94, 95]. However, techniques also exist that lack a human correlate such as optical imaging (OI) of bioluminescence (BLI) or fluorescence (intravital video microscopy; IVM). OI represents a unique tool for whole body imaging in small animals. For example, BLI-based imaging has been used to monitor the development and progression of bone metastases in living animals with a high degree of sensitivity [96, 97]. Similarly,

IVM-based cellular imaging techniques are powerful tools for the continuous monitoring of cellular processes in a living animal/tissue with a high degree of resolution, something not currently possible with all OI techniques. IVM has been used for measuring the heterogeneity within tumour populations and interactions among subsets of cells within a tumour. It has provided tremendous insight into various steps of metastasis including cell-cell interactions and the migration of cancer cells [98]. Another potential method for understanding the cellular processes of metastasis is *in vivo* video microscopy (IVVM). This provides a dynamic approach to visualizing labelled tumour activity within the microcirculation in living animals [99] and has provided valuable knowledge in terms of the inefficiency associated with the metastatic process [100]. Findings using IVVM have shown that post-extravasation growth of individual tumour cells contribute significantly to metastatic inefficiency and not earlier steps in metastasis as once previously thought [101]. While these techniques are certainly promising and can potentially uncover many key processes underlying the process of metastatic progression, they are time consuming, often require highly sophisticated and expensive imaging systems and do not allow serial assessment at secondary sites [93, 95].

2.13. *Ex vivo* Pulmonary Metastasis Assay

In 1992, Siminski and colleagues first established a method by which pulmonary parenchyma could be maintained in serum-free conditions for up to 9 weeks. This unique *ex vivo* model system involved cutting murine whole lungs into thin slices (~1-2 mm thick) and growing them in culture [102]. This model was later adapted and modified by Mendoza *et al.* to study the influence of the lung parenchyma on metastatic osteosarcoma, in an assay they described as a Pulmonary Metastasis Assay (PuMA) [93]. The main advantage of this assay over traditional *in vitro* techniques is that it recapitulates the native cellular and microenvironmental complexity of the lung within the native 3D lung architecture. It allows valuable insight into the progression of metastasis since cellular interactions between cancer cells and both the lung parenchyma and ECM are maintained and can be

experimentally investigated and/or targeted in an “open box” system, something not always feasible *in vivo*.

2.14. Study Rationale

Breast cancer remains the leading cause of cancer diagnosis and the second leading cause of cancer-related deaths among women. If detected relatively early, traditional therapies often prove highly effective. However, many conventional therapies fail following the metastatic spread of breast cancer. Thus, the majority of deaths associated with breast cancer are due to metastasis, and not the primary tumour, particularly in patients with lung metastasis. Previous work in our lab has demonstrated that stem-like ALDH^{hi}CD44⁺ breast cancer cells display preferential migration patterns towards lung-derived soluble factors and an increased propensity to metastasize to the lung *in vivo*. However, the exact role of the lung microenvironment in supporting growth and progression of breast cancer from a single cells stage remains poorly understood.

3. HYPOTHESIS AND OBJECTIVES

3.1. Hypothesis

Whole population breast cancer cells exhibit growth and progression within an innovative *ex vivo* pulmonary metastasis (PuMA) model. More specifically, stem-like ALDH^{hi}CD44⁺ breast cancer cells demonstrate increased growth and progression from a single cell stage to micrometastases to macrometastases within the native lung microenvironment in relation to their non stem-like ALDH^{lo}CD44⁻ counterparts.

3.2. Objectives

1. Establish a 3D *ex vivo* model system for investigating the role of the lung microenvironment on breast cancer cell metastatic behaviour.
2. Evaluate the growth and progression patterns of whole population and ALDH^{hi}CD44⁺ breast cancer cells in the 3D model.
3. Determine the interaction between lung-derived soluble factor(s) and their respective receptors on whole population and ALDH^{hi}CD44⁺ breast cancer cells.

4. MATERIALS AND METHODS

4.1. Cell Culture and Reagents

Commercial cell lines and culturing conditions are listed in **Table 1**. Dulbecco's Modified Eagle Medium/Nutrient Mixture F-12 (DMEM/F12), HAM'S:F12, Modified Eagle Medium alpha (α MEM) used for cell culture and Medium 199 (M199) used for culturing mouse lung tissue were purchased from Invitrogen (Burlington, ON, Canada). Fetal bovine serum (FBS) was purchased from Sigma (St. Louis, MO, USA). Tissue culture plates used were purchased from Nunc™ (Fisher Scientific, Ottawa, ON, Canada). Trypsin was purchased from Invitrogen and used at a concentration of 0.25% in citrate saline. Ethylene diamine tetraacetic acid (EDTA) was purchased from Bioshop Canada Inc. (Burlington, ON, Canada) and used at a concentration of 1 mM in deionized water. Cells were cultured and maintained under normal conditions of 37°C and 5% CO₂ and used at low passages.

4.1.1. Generation of Fluorescent Cell Lines

Cell lines were generated to express tdTomato (excitation 554 nm, emission 581 nm). MDA-MB-468, SUM149 and MDA-MB-231 breast cancer cell lines were transduced with lentivirus containing a tdTomato vector (pLVX-IRES-tdTomato), a kind gift from Dr. Hon Sing Leong (London Health Sciences Centre). Stable tdTomato-expressing cells were maintained in culture using puromycin (Invitrogen) as a selection agent (0.25 μ g/mL for MDA-MB-468 and SUM149, 0.5 μ g/mL for MDA-MB-231).

Table 1. Cell lines and culturing conditions.

Cell line/Tissue	Culturing conditions	Source and References
SUM149	HAM'S F:12 + 5% FBS, 2.5 mL insulin, 500 μ L hydrocortisone, 5 mL HEPES	Asterand Inc. (Detroit, MI, USA) [110]
SUM149-tdTomato	HAM'S F:12 + 5% FBS, 2.5 mL insulin, 500 μ L hydrocortisone, 5 mL HEPES + 0.25 μ g/mL puromycin	Generated in-house
MDA-MB-231	DMEM:F12 + 10% FBS	American Type Culture Collection (ATCC: Manassas, VA, USA) [108]
MDA-MB-231-tdTomato	DMEM:F12 + 10% FBS + 0.5 μ g/mL puromycin	Generated in-house
MDA-MB-468	α MEM + 10% FBS	MD Anderson Cancer Center (Houston, TX, USA) [109]
MDA-MB-468-tdTomato	α MEM + 10% FBS + 0.25 μ g/mL puromycin	Generated in-house

4.2. Fluorescence Activated Cell Sorting

Fluorescence activated cell sorting (FACS) was used to isolate stem-like ALDH^{hi}CD44⁺ and non stem-like ALDH^{lo}CD44⁻ subpopulations from both the MDA-MB-231 and SUM149 breast cancer cell lines. The Aldefluor™ assay kit (StemCell Technologies, Vancouver, BC, Canada) was used to assess ALDH activity in cellular populations. The Aldefluor™ kit uses an uncharged fluorescent ALDH substrate (BODIPY-aminoacetaldehyde (BAAA) that passively diffuses into cells. Cellular ALDH activity converts uncharged BAAA molecules to negatively charged BAA⁻ molecules, which prevents diffusion out of the cell. The trapped BAA⁻ molecule labels ALDH^{hi} cells green. Cells are kept on ice prior to sorting to prevent the active efflux of BAA⁻ from labeled cells (**Figure 2**). Roughly 2×10^8 cells were harvested, washed in PBS, centrifuged at 1000g for 5 min, and resuspended in assay buffer. Suspended cells were incubated with Aldefluor substrate (1 μ L BAAA/ 10^6 cells). A control sample was also prepared in which diethylaminobenzaldehyde (DEAB; 1.5 mM), a specific ALDH inhibitor, was co-incubated with Aldefluor. DEAB allows BAAA to remain in its uncharged form and therefore passively diffuse out of the cell. During FACS analysis, ALDH⁺ cells were characterized based upon having higher levels of fluorescence than the DEAB control. Both Aldefluor only and Aldefluor plus DEAB samples were incubated for 50 minutes at 37°C. Following incubation, samples were centrifuged (1000g for 5 min), resuspended with provided assay buffer and labelled with a CD44-allophycocyanin (APC; BD Biosciences) antibody at 4°C for 30 min. Cells were again centrifuged (1000g for 5 min) and resuspended in assay buffer. Following resuspension, 7-aminoactinomycin D (7-AAD; BD Biosciences) was added to sample tubes for monitoring of cell viability during FACS, and stored on ice for immediate transport to the London Regional Flow Cytometry Facility for FACS. To remove cellular clumping during transportation, cell suspensions were filtered through a 70 μ m mesh filter preceding FACS analysis. Sorting was accomplished using a 4-colour analysis protocol on a FACSAria I or II (Bd Biosciences) at the London Regional Flow Cytometry Facility. ALDH activity

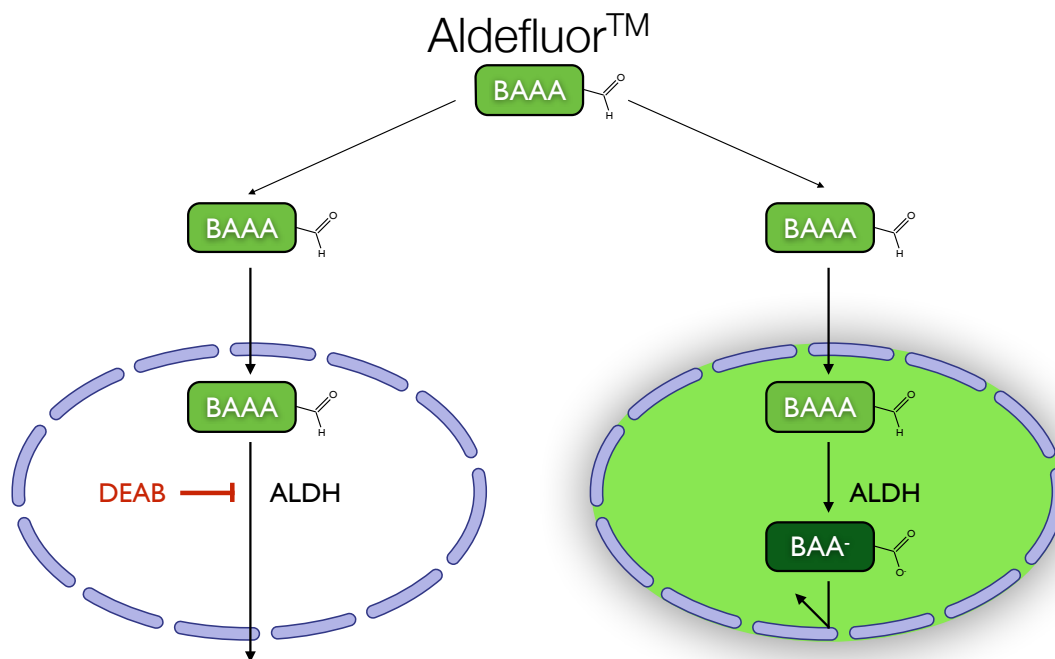


Figure 2. Aldefluor™ Assay. The Aldefluor™ assay is a fluorometric assay used to detect human cells that express high levels of aldehyde dehydrogenase 1 (ALDH1). The fluorescent neutrally charged BODIPY-aminoacetaldehyde (BAAA) molecule is taken up by intact and viable cells by passive diffusion. In the presence of ALDH, BAAA is converted into BODIPY-aminoacetate (BAA^-) which is unable to diffuse out of the cell due to its negative charge. Active removal of BAA^- by ATP binding cassettes is inhibited by the use of provided assay buffer and cold temperature (2-8°C). Resulting fluorescence is proportional to ALDH activity and cells can be isolated using a cell sorter. A specific inhibitor of ALDH, diethylaminobenzaldehyde (DEAB), is used to control for background fluorescence. The population in the DEAB negative control provides an appropriate gate for $ALDH^{hi}$ cells, whereby only cells demonstrating higher levels of fluorescence than the DEAB control are included.

was used as the primary sort criteria (ALDH^{hi} = top 20%, ALDH^{lo} = bottom 20%), after which 50% of the ALDH^{hi} cells were selected for the CD44⁺ phenotype and 50% of the ALDH^{lo} cells selected for the CD44⁻ phenotype (**Figures 3, 4**). The resulting isolated ALDH^{hi}CD44⁺ and ALDH^{lo}CD44⁻ populations were transported back to the London Regional Cancer Centre and used immediately for injections in the PuMA assay.

4.3. Pulmonary Metastasis Assay

4.3.1. Lung Seeding, Harvesting and Culturing

The pulmonary metastasis assay (PuMA) represents an innovative *ex vivo* model for growing sections of lung in culture. This model allows real-time assessment of metastatic progression, from single cells to micrometastatic to macrometastatic colonies. A main advantage of this assay is that it provides the unique ability to study the interactions between cells and the local host microenvironment. Serum-free conditions are used for lung culture and were first described by Siminski and colleagues [102] and later modified by Mendoza and colleagues [93] (**Table 2**).

Healthy 5-7 week old female athymic nude mice (Hsd: Athymic Nude-*Foxn1*^{nu}; Harlan Sprague-Dawley, Indianapolis, IN) were purchased and maintained under the guidelines of the Canadian Council of Animal care as outlined by the protocol approved by the University of Western Ontario Council on Animal Care (protocol #2009-064). TdTomato-expressing tumour cells were harvested, suspended in either PBS (MDA-MB-468) or Hank's Balanced Salt Solution (HBSS; Invitrogen) (SUM149 and MDA-MB-231) and delivered by tail-vein injection to female athymic nude mice. Within 15 minutes of cell injection, mice were euthanized by CO₂ inhalation. Using sterile surgical conditions, the trachea was snipped and cannulated with an 18G blunt needle. The lungs were infused under gravitational pressure with 1.2 mL of equal amounts of well-mixed lung medium 1/low melting agarose solution (0.6%, 40°C). The trachea, lungs, and heart were carefully removed *en bloc* and immediately placed in ice-cold PBS containing 100 U/ml penicillin and 100 µg/ml

Figure 3. Isolation strategy for tdTomato expressing stem-like human breast cancer cells from the SUM149 breast cancer cell line. Fluorescence activated cell sorting (FACS) was used to isolate both ALDH^{hi}CD44⁺ and ALDH^{lo}CD44⁻ cell populations labelled with 7-AAD, CD44-APC and the Aldefluor™ assay kit. Cell subsets were isolated using a four-colour protocol on a FACS ARIA I or III and subsequently used for the PuMA. (A) Cells were first selected based on expected light scatter, (B) viability based on 7-AAD exclusion, (C) and tdTomato positivity. (D) Cells were further divided into ALDH^{hi} (top ~20% most positive of ALDH⁺ population) and ALDH^{lo} (bottom ~20% of ALDH⁺ population) populations. (E) Finally, cells were further selected based on a CD44⁺ phenotype (~50% of the ALDH^{hi} population), or (F) a CD44⁻ phenotype (~50% of the ALDH^{lo} population). Resulting subsets were designated as either stem-like (ALDH^{hi}CD44⁺) or non stem-like (ALDH^{lo}CD44⁻) and were used immediately for injection into the PuMA.

SUMI49

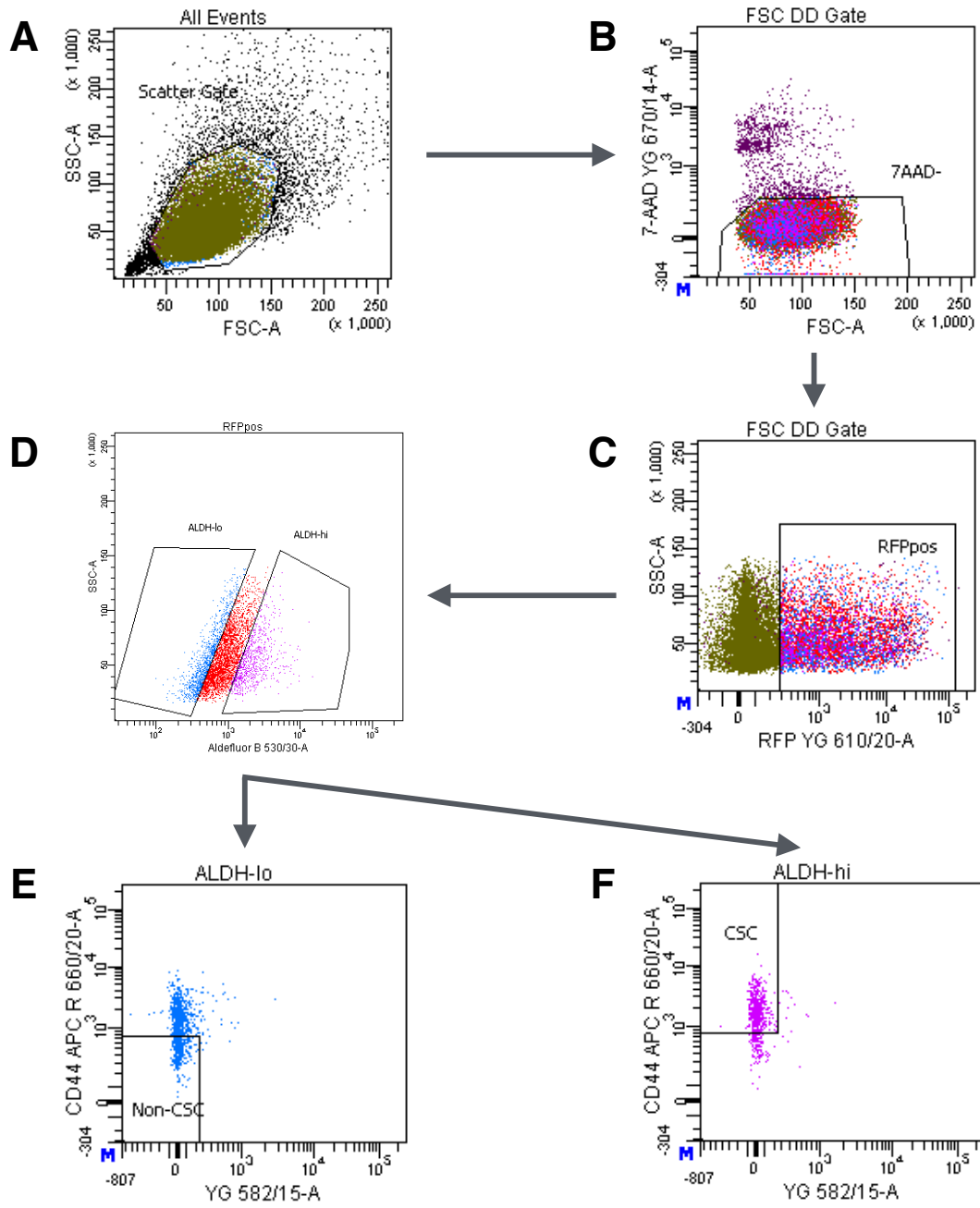


Figure 4. Isolation strategy for tdTomato expressing stem-like breast cancer cells from the MDA-MB-231 human breast cancer cell line. Fluorescence activated cell sorting (FACS) was used to isolate both ALDH^{hi}CD44⁺ and ALDH^{lo}CD44⁻ cell populations labelled with 7-AAD, CD44-APC and the Aldefluor™ assay kit. Cell subsets were isolated using a four-colour protocol on a FACS ARIA I or III and subsequently used for the PuMA. (A) Cells were first selected based on expected light scatter, (B) viability based on 7-AAD exclusion, (C) and tdTomato positivity. (D) Cells were further divided into ALDH^{hi} (top ~20% most positive of ALDH⁺ population) and ALDH^{lo} (bottom ~20% of ALDH⁺ population) populations. (E) Finally, cells were further selected based on a CD44⁺ phenotype (~50% of the ALDH^{hi} population), or (F) a CD44⁻ phenotype (~50% of the ALDH^{lo} population). Resulting subsets were designated as either stem-like (ALDH^{hi}CD44⁺) or non stem-like (ALDH^{lo}CD44⁻) and were used immediately for injection into the PuMA.

MDA-MB-231

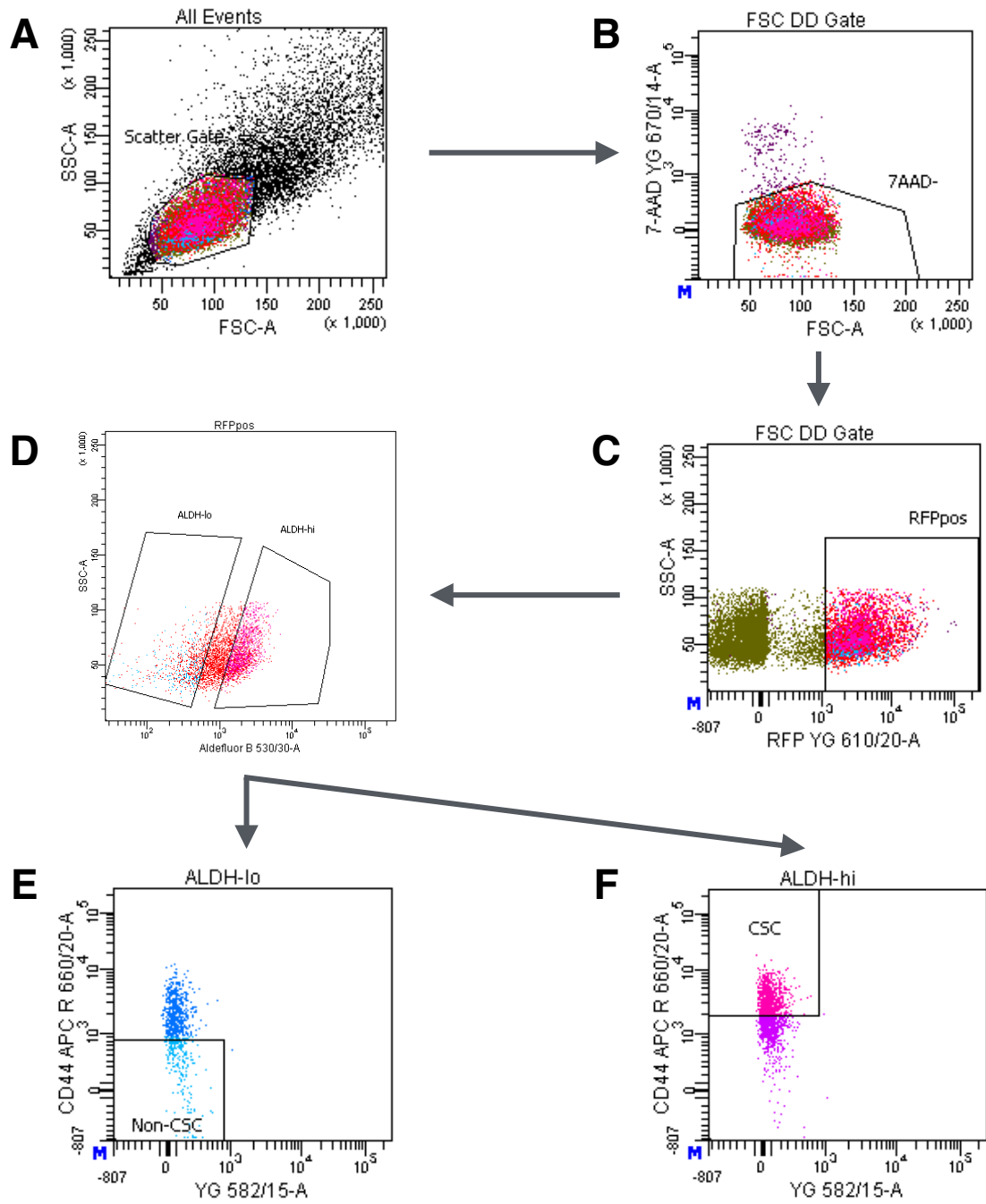


Table 2. Media formulations for lung tissue used in the PuMA.

Lung Media 1 (perfusion)	Lung Media 2 (culturing)
2X M199 Media	1X M199 Media
2.0 µg/mL bovine insulin	1.0 µg/mL bovine insulin
0.2 µg/mL hydrocortisone	0.1 µg/mL hydrocortisone
0.2 µg/mL retinyl acetate	0.1 µg/mL retinyl acetate
200 U/mL penicillin	100 U/mL penicillin
200 µg/mL streptomycin	100 µg/mL streptomycin
7.5% sodium bicarbonate	7.5% sodium bicarbonate

streptomycin and stored at 4°C for 20 minutes to solidify the medium/agarose solution within the lung. Transverse lung sections (1–2 mm in thickness) were cut from each lobe using a scalpel blade. This typically gives 12–20 sections per lung. Lung sections were carefully placed on a single sterile piece of Gelfoam (~1 cm x 1 cm) that had been preincubated for 1-2 hours in a 6-well plate with lung medium 2. Lung sections were grown in culture for 21 days at 37°C in 5% CO₂. Lung medium 2 was replaced every other day and lung tissue sections turned over carefully with tweezers (**Figure 5**).

4.3.2. Imaging and Analysis of Lung Sections

Seeded sections of lung were imaged at days 0, 7, 14 and 21 post-injection for cancer cell growth and progression. Lung sections were first removed from culture on their given day and fixed overnight in 10% buffered formalin phosphate (Fisher Scientific) plus 25% sucrose (w/v) to preserve fluorescent signal. The following day, sections were rinsed with PBS three times and carefully placed on a glass slide with a glass coverslip gently sitting on top. Images were acquired using an upright Nikon A1R confocal microscope at 20X objective (Nikon), with a 591 nm emission laser (Melles Griot, Carlsbad, CA, USA). Three separate lung sections were imaged per time point with five images taken per lung section. Growth and progression of cellular populations within the lung was determined by measuring the mean fluorescent area per field of view (FOV) for each section of lung (μm^2) using ImageJ software (NIH, Bethesda, WA, USA). Data were normalized to 1000 μm^2 at day 0 to account for variability in cellular delivery during tail-vein injection. Three mice were injected for each cellular population with each replicate using cell populations from different days.

To determine the relative degree of metastatic progression for each cell population, we characterized the percentage of colonies present per image taken as either single cells, micrometastatic lesions or macrometastatic lesions according to measured diameter. We have set thresholds for single cells as 50 μm or smaller.

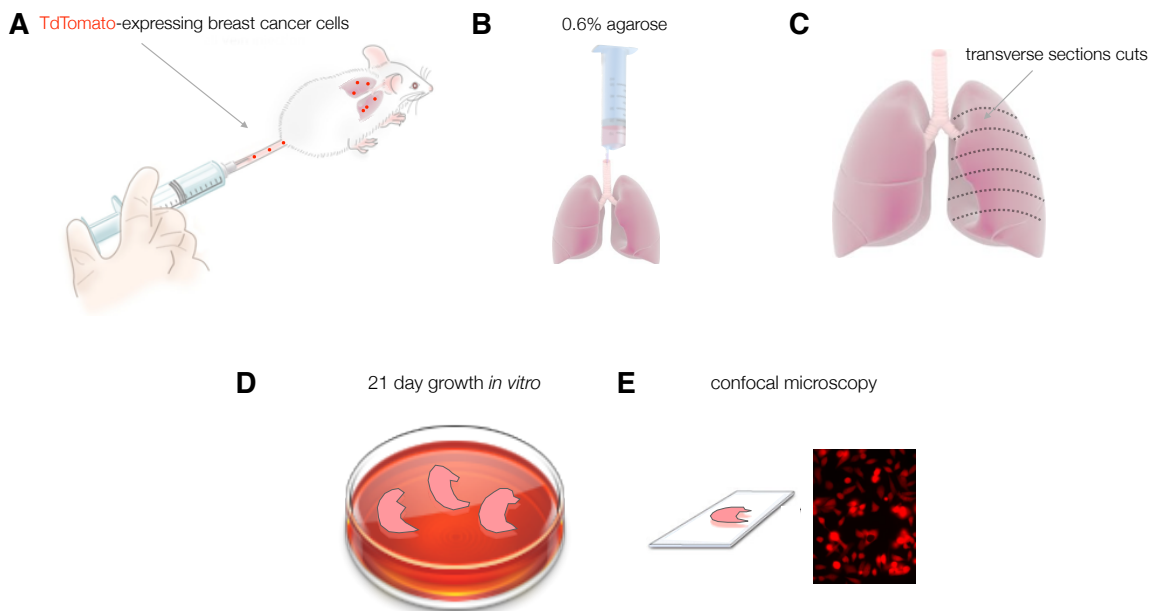


Figure 5. Pulmonary Metastasis Assay (PuMA). The PuMA offers a real time assessment of breast cancer cell growth from a single cell stage to multicellular colonies in a metastatic setting. (A) Female nude mice are injected tail-vein with tdTomato-expressing breast cancer cells. (B) Mice are sacrificed 15 min post injection by CO₂ inhalation. The trachea is carefully cut and cannulated with an 18G blunt needle. The lungs are infused with an agarose/lung media 1 solution using gravity perfusion. (C) Lungs are carefully removed *en bloc* and cut into ~1 mm transverse sections. (D) Lung sections are grown on Gelfoam[®] pre-incubated with Lung Media 2 and grown in culture for 21-days. (E) Sections are removed from the PuMA at days 0, 7, 14 and 21 and fixed in formalin for approximately 24 h prior to imaging. Sections are imaged for each time point using confocal microscopy to determine metastatic growth, progression and colony size.

Traditionally, clinical micrometastases in breast carcinoma are defined anywhere between 200 μm - 2 mm [103, 104]. We have therefore set the threshold for micrometastatic lesions within the PuMA as being between 100-400 μm . There exists much less consensus as to what clinically constitutes a macrometastatic lesion and as a limitation to the size we can quantitatively measure in a given area of the images acquired by confocal microscopy, we have set the threshold for macrometastases as anything greater than 400 μm . Using the images taken for growth and progression analysis for each time point, we determined the average proportion of colony sizes per lung section using ImageJ software (NIH, Bethesda, MD, USA).

4.4. Histology and Immunohistochemistry

Lung sections from the PuMA were fixed for at least 24 h in 10% buffered formalin phosphate (Fisher Scientific), paraffin-embedded and sectioned at 5 μm on a transverse plain. Hematoxylin and eosin (H&E) staining was carried out by Carl Postenka (Histology Research Technician, London Health Sciences Centre). Masson's Trichrome Connective Tissue Stain kit was used according to the manufacturer's instructions to evaluate muscle fibre and collagen presence within sections of lung (Abcam, Cambridge, MA, USA). Expected Trichrome staining results were as follows: collagen (blue), muscle fibres (red) and nuclei (black/blue).

Determination of proliferation competency within the PuMA was accomplished using Ki-67 staining of seeded lung sections. Sections were rehydrated in xylene followed by a series of graded ethanol incubations (100%, 95%, 80%, 70%). Sections underwent antigen retrieval in sodium citrate buffer (10 mM sodium citrate, 0.05% Tween-20, pH 6.0) in a 100°C water bath for 20 min, then cooled at RT for an additional 20 min. Staining was performed using the Mouse and Rabbit Specific HRP/DAB (ABC) Detection Kit (Abcam) according to the manufacturer's instructions. Purified mouse monoclonal anti-Ki-67 antibody (1:75; Dako, Burlington, ON, CA) was diluted in blocking buffer (1% BSA in PBS) and incubated with tissue sections in a humid container O/N at 4°C. Detection of bFGF within normal unseeded lung sections was accomplished using a rabbit polyclonal anti-FGF

basic antibody (1:300; Abcam) which was diluted in blocking buffer (1% BSA in PBS) and incubated with tissue sections in a humid container O/N at 4°C. Staining was achieved using the same Mouse and Rabbit Specific HRP/DAB (ABC) Detection Kit (Abcam). A negative antibody control (no primary) and negative tissue control (mouse liver tissue) were used to rule out non-specific binding of primary antibody. Following staining for Ki-67 and bFGF, tissues were dehydrated in a series of graded ethanol (70%, 80%, 95%, 100%) ending in xylene, mounted with coverslips and imaged using the Scanscope® CS System (Aperio, Vista, CA, USA).

4.5. Lung-Conditioned Media, Primary Cell Isolation and Reagents

4.5.1. Animals and Lung Harvesting

Healthy 5-7 week old female athymic nude mice (Hsd: Athymic Nude-*Foxn1*^{nu}; Harlan Sprague-Dawley, Indianapolis, IN) were purchased and maintained under the guidelines of the Canadian Council of Animal care as outlined by the protocol approved by the University of Western Ontario Council on Animal Care (protocol #2009-064). Mice were euthanized by CO₂ inhalation and their lungs removed aseptically. The heart was carefully removed and the lungs were placed in a pre-weighed 50 mL conical tube containing 30 mL PBS.

4.5.2. Lung-Conditioned Media Generation

Following the harvesting of lungs (n=4 mice per session), the total weight of lungs + PBS was determined using an electronic balance. Harvested lungs were washed three times in ice cold PBS before being minced into ~1 mm³ fragments using two sterile scalpel blades in a 60 mm² glass petri dish. Lungs were weight-normalized by re-suspension in a 4:1 media to tissue (v/w) ratio in DMEM:F12 supplemented with Mito⁺ serum extender (1X; BD Biosciences, Mississauga, Canada) and penicillin-streptomycin (50 U/mL penicillin-50 µg/mL streptomycin; Invitrogen). Lung fragments and media were incubated at 37°C and 5% CO₂ for 24 h. Following incubation, conditioned media (CM) was removed from lung fragments, diluted by a further three volumes of media and centrifuged at 1000g for 15 min to remove

residual cell debris [43]. CM was filtered by a 0.22 μm syringe filter (Fisher Scientific), aliquoted and stored at -80°C until use (**Figure 6A**).

4.6. Assessment of bFGF Concentration

To measure the concentration of soluble bFGF in lung-CM, the Quantikine[®] ELISA Mouse/Rat FGF Basic Kit was used (R&D Systems, Minneapolis, MN, USA). Basal media, lung-CM and lung-CM depleted of bFGF were added to the supplied pre-coated microplate and carried out according to the manufacturer's instructions to measure the concentration of bFGF in lung-CM and the efficiency of bFGF immunodepletion.

The Mouse/Rat FGF Basic Kit was also used to determine the concentration of soluble bFGF secreted by normal unseeded lung tissue grown in the PuMA. Surrounding media and Gelfoam[®] sections were collected for each time point (days 0, 7, 14, 21) and centrifuged at 1000g for 10 min to sediment the Gelfoam[®]. The supernatant was collected and added to the microplate and carried through according to the manufacturer's instructions to measure the concentration of soluble bFGF at each time point throughout the assay. A standard curve was used for each experiment and concentrations of bFGF were calculated using a four-parameter logistic (4-PL) curve-fit software (elisaanalysis.com/app).

4.6.1. bFGF Immunodepletion from Lung-Conditioned Media

To determine the influence of soluble bFGF on *in vitro* migration and proliferation of breast cancer cells, bFGF was depleted from lung-CM using Dynabeads[®] Protein G (Life Technologies). Lung-CM (1 mL) was added to a 1.5 mL microfuge tube with 5 μL of neutralizing monoclonal bFGF antibody (1 mg/mL, clone bFM-1; EMD Millipore, Etobicoke, ON, CA). The microfuge tube was inverted twice and placed on a nutating mixer (VWR, Radnor, PA, USA) for 30 min at RT. Following nutation, Dynabeads[®] were resuspended in the vial by vortexing for 30 sec. 50 μL (1.5 μg) Dynabeads[®] were transferred to a clean 1.5 mL microfuge tube and placed in a magnetic rack (Invitrogen) for 2 min to separate beads from solution.

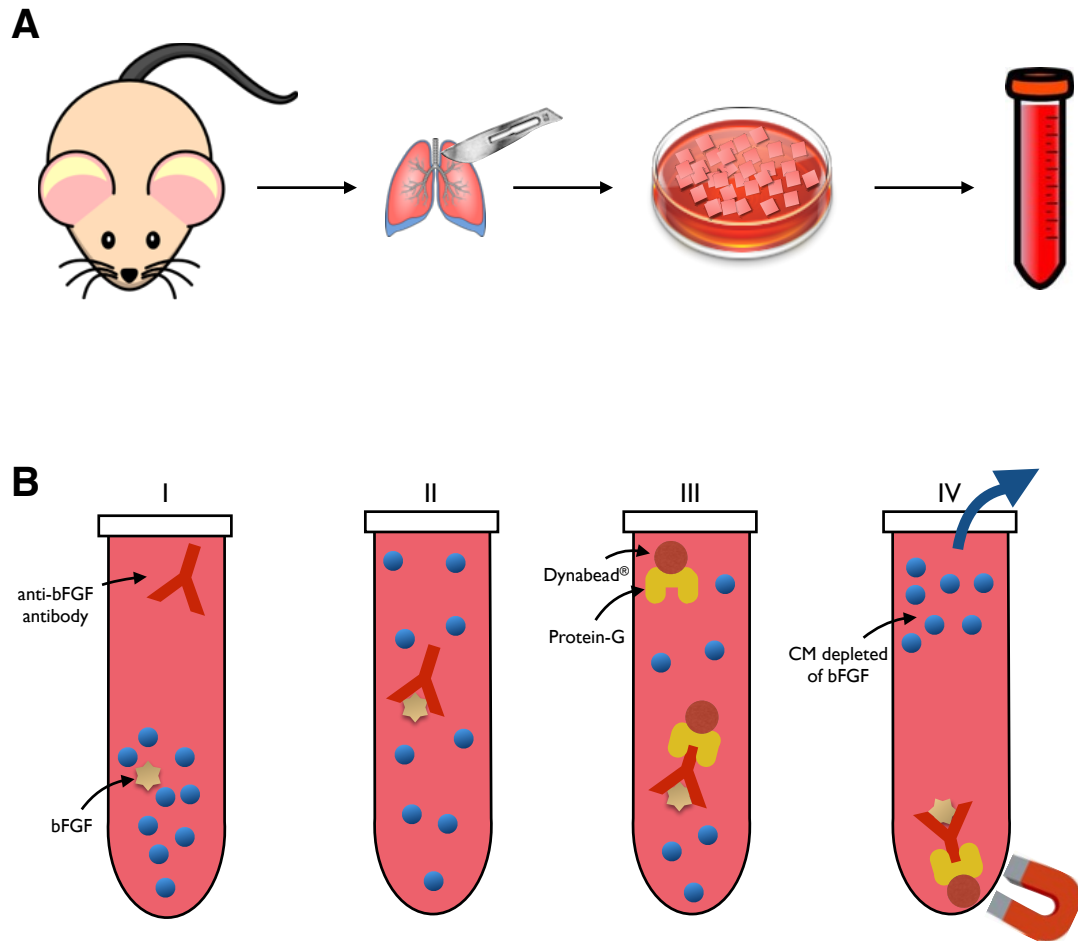


Figure 6. Lung conditioned media generation and bFGF immunodepletion. (A) Healthy female nude mice were euthanized by CO₂ inhalation and their lungs removed aseptically. Harvested lungs were washed, minced into ~1 mm³ fragments, and resuspended in a 4:1 media to tissue (v/w) ratio for incubation at 37°C and 5% CO₂ for 24 h. Following incubation, lung fragments were further diluted by three volumes of media, centrifuged and CM filtered prior to use. (B) Immunodepletion of bFGF from lung-CM was accomplished using magnetic Protein-G Dynabeads[®]. *I.* A neutralizing antibody specific to bFGF was added to lung-CM. *II.* Lung-CM/bFGF antibody was mixed for 30 min whereby antibody bound free bFGF protein present in lung-CM. *III.* Lung-CM/bFGF antibody mixture was added to magnetic Dynabeads[®] and mixed for 20 min. *IV.* After mixing, a magnet was used to separate lung-CM from the bFGF antibody/Dynabeads[®] mixture.

The supernatant was carefully removed and 1 mL of lung-CM/bFGF antibody mixture was added to the magnetic beads. The lung-CM/bFGF antibody/beads solution was inverted twice and placed on a nutating mixer for 20 min at RT. After mixing, the tube was placed in a magnetic rack for 2 min to separate lung-CM from the bFGF antibody-beads mixture. Lung-CM depleted of bFGF was transferred to a new tube and filtered by 0.22 μm syringe filtration (Fisher Scientific), aliquoted and stored at -80°C until use (**Figure 6B**). For bFGF rescue experiments involving re-addition of bFGF to immunodepleted lung-CM, recombinant bFGF (Sigma) at a concentration of 0.3 $\mu\text{g}/\text{mL}$ was added to depleted media prior to cell seeding. This amount was equal to the concentration of bFGF determined to be present in normal lung-CM.

4.7. *In vitro* Transwell Migration Assay

Patterns of MDA-MB-231 and SUM149 whole population cellular migration towards lung-CM were assessed using transwell migration assays. Prior the start of the assay, 300 μL of gelatin (Bioshop) was warmed to 60°C for 20 min and further diluted with 1500 μL of sterile water. Transwell inserts (24-well, 6.4 mm polyethylene terephthalate membrane, 8 μm pore size; BD Falcon, Mississauga, ON, CA) were then coated with diluted gelatin (6 $\mu\text{g}/\text{well}$) and allowed to dry at RT in a sterile environment O/N. Immediately prior to the assay, gelatin was reconstituted with control media (DMEM:F12 + Mito⁺ + 0.1% BSA; Bioshop) and agitated for 1.5 h at RT. Following reconstitution, SUM149 or MDA-MB-231 whole cell populations were harvested, washed twice with PBS and suspended at a concentration of 5×10^5 cells/mL in control media. Excess media from the top of the transwells was carefully removed with a pipette and 600 μL of negative basal media, lung-CM or lung-CM depleted of bFGF was added to the bottom wells of a 24-well dish. Cells (5×10^4 cells/mL) were seeded onto the top portion of each transwell chamber. Chambers containing cells were placed on top of the wells containing chemoattractant and incubated for 18 h at 37°C , 5% CO_2 . Following incubation, transwell chambers were removed, inverted and fixed with 1% glutaraldehyde (Fisher Scientific) in PBS for 20

min. Fixed cells were washed with sterile water and 0.1% Triton-X-100 (Acros Organics, NJ, USA) in PBS for 10 min. Cells were washed again with sterile water and non-migrated cells were removed from the inner portion of the transwell chamber with a cotton swab. Membranes were carefully cut out from the transwell chambers, placed on a microscope slide and mounted with Vectashield with DAPI (Vector Laboratories, Burlingame, CA, USA). Five high powered fields of view (FOV) were captured for each well, and a mean number of migrated cells/FOV was calculated using ImageJ software.

4.8. *In vitro* BrdU Incorporation Assay

Proliferative responses of the human breast cancer cell lines SUM149 and MDA-MB-231 to human lung-CM were assessed using a bromodeoxyuridine (BrdU) incorporation assay. Whole population (1.5×10^4 /well) were plated on 8-well chamber slides (Lab-tek; Fisher Scientific) and allowed to adhere for 24 h, after which cells were washed once with PBS and serum starved for 72 h. Media was then replaced with lung-CM, negative control media (basal media; DMEM:F12 + Mito⁺), or positive control media (DMEM:F12 + Mito⁺ + 10% FBS) for 24 h. Following incubation, BrdU (5 μ g/mL; Amersham Cell Proliferation Labelling Reagent; GE Healthcare, Piscataway, NJ, USA) was added for 30 min. Following BrdU incorporation, cells were washed with PBS and fixed with 10% neutral-buffered formalin (Fisher Scientific) for 5 min. Cells were then incubated with 0.1% Triton X-100 (Sigma) in PBS for 10 min to permeabilize cell membranes and subsequently treated with 2N HCl (Fisher Scientific) for 10 min to denature DNA. Slides were blocked for 30 min in 5% bovine serum albumin (BSA) in 0.1% Triton X-100 in PBS. An anti-BrdU primary antibody (BD Biosciences) was added (1:75 dilution) in 5% BSA/0.1% Triton X-100 in PBS for 1 h at RT. Slides were washed with PBS and a FITC-conjugated anti-mouse IgG secondary antibody (H+L made in horse; Vector, Burlington, ON, Canada) was added (1:100 dilution) in 5% BSA + 0.1% Triton X-100 in PBS for 1 h at RT. Slides were washed with PBS to remove unbound antibody, mounted with ProLong Gold with DAPI (Invitrogen) and allowed to cure

O/N in the dark at RT. Images were taken (5 FOV/well) and nuclei counted using ImageJ. Results were expressed as a percentage of BrdU positive cells to total nuclei.

4.9. Blocking of bFGF and CD44 in the PuMA

To determine the effect of bFGF present within the lung microenvironment in the context of the PuMA, antibody mediated blocking of either bFGF alone or its non-canonical receptor, CD44 was used. Highly aggressive MDA-MB-231 breast cancer cells were chosen as they were shown to progress to the greatest degree within the PuMA. TdTomato-expressing MDA-MB-231 whole population cells were harvested and first split into two groups: one group incubated at RT for 30 min in HBSS and the other to incubate at RT in the presence of a rat monoclonal anti-CD44 antibody (1:50; Abcam) in HBSS for 30 min (**Figure 7A**). Following incubation, cells were delivered to female nude mouse lungs by tail vein injection (5×10^5 cells/mouse, n=3 mice) (**Figure 7B**). Lungs seeded with cells pre-incubated with an anti-CD44 antibody were infused with the normal agarose/lung media 1 solution and excised as per the PuMA protocol. Lungs seeded with cells not pre-incubated with HBSS only were either infused with the normal agarose/lung media 1 solution or agarose/media 1 solution plus a neutralizing monoclonal bFGF antibody (1:200, clone bFM-1; EMD Millipore) before following the remainder of the PuMA protocol (**Figure 7C**). Sections were cultured in serum-free conditions for 21 days, removed from culture on their given day (0, 7, 14, 21) and fixed O/N in 10% buffered formalin phosphate (Fisher Scientific) plus 25% sucrose (w/v) to preserve fluorescent signal. The following day, sections were imaged for cancer cell growth and progression. Three separate lung sections were imaged per time point with five images taken per lung section. Growth and progression of cellular populations within the lung was determined by measuring the mean fluorescent area per FOV for each section of lung (μm^2) using ImageJ software (NIH). Data were normalized to $1000 \mu\text{m}^2$ at day 0 to account for variability in cellular delivery during tail-vein injection. Three mice were injected for each experimental group using cell populations from different days.

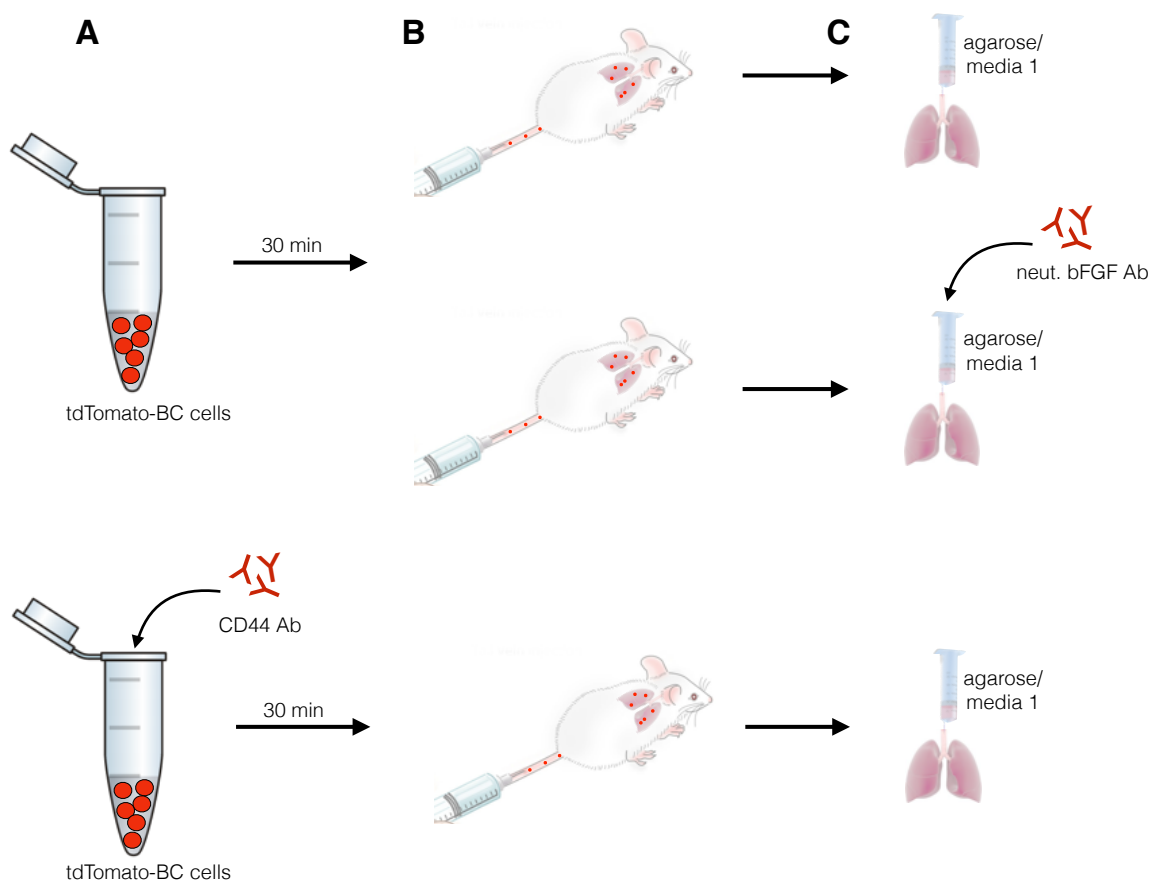


Figure 7. Blocking strategy for bFGF and CD44 in the PuMA. Both bFGF and CD44 were blocked to determine the effect of bFGF on breast cancer cell growth in the context of the PuMA. (A) TdTomato-expressing MDA-MB-231 whole population cells were harvested and either incubated in HBSS or incubated in the presence of an anti-CD44 antibody in HBSS. (B) Following incubation, cells were delivered female nude mouse lungs by tail vein injection. (C) Lungs seeded with cells pre-incubated with an anti-CD44 antibody were infused with the normal agarose/media 1 solution. Lungs seeded with cells not pre-incubated with an anti-CD44 body were either infused with the normal agarose/media 1 solution or in agarose/media 1 solution plus a neutralizing bFGF antibody. Resulting lungs were sliced into transverse sections and grown in culture according to the PuMA.

4.10. Statistical Analysis

All experiments were performed using a minimum of three biological replicates with internal triplicates, unless otherwise noted. Statistical analysis was done using GraphPad Prism 6.0 (San Diego, CA, USA) and data are presented as mean \pm standard error of the mean (SEM). A one-way analysis of variance (ANOVA) was used to compare data with multiple means and a two-way ANOVA used to compare multiple means between different groups. Either a Dunnett's, Tukey's or Bonferroni, or Sidak's post-hoc test was used to confirm significance, as noted. P-values less than 0.05 were deemed statistically significant.

5. RESULTS

5.1. Pulmonary Architecture Remains Structurally and Microscopically Intact in the PuMA over 21 days

The PuMA represents an innovative model to study the behaviour of cancer cells within the lung microenvironment in an open-box manner. We first wanted to determine if sections of female nude mouse lungs could remain viable and healthy throughout the duration of the PuMA. Unseeded slices of lung from healthy mice were maintained according to the PuMA protocol. Lung slices were fixed, paraffin embedded, sectioned and stained at days 0, 7, 14 and 21 with H&E for routine histological examination and Masson's Trichrome stain to evaluate connective tissue components (**Figure 8**). H&E staining demonstrated that the lung remained structurally intact with normal lung appearance throughout the 21 day period. Alveoli were uniformly expanded throughout the lung for the duration of the assay with no evidence of alveolar collapse. A thin outline of solidified agarose could be identified within the alveoli and larger airways, which indicated successful infusion of the agarose/media solution prior to the start of the PuMA. Alveoli, airways and large vessels remained expanded with no evidence of collapse seen in the pulmonary architecture. Both type I and type II pneumocytes were present at each time point throughout the assay and could be appropriately identified. There was a decrease in overall cellularity as evidenced by a qualitative reduction in total nuclei present at days 14 and 21 compared to earlier time points. However, the overall lung microarchitecture was remarkably unchanged throughout the duration of the assay (**Figure 8A**). Sections of unseeded lung from the PuMA were also stained with Masson's Trichrome stain to evaluate the presence of connective tissue during the PuMA. Over the course of 21 days, muscle tissue was present surrounding arteries and larger airways. Collagen fibres could also be identified at each time point and were present surrounding vasculature. Although collagen was present throughout the

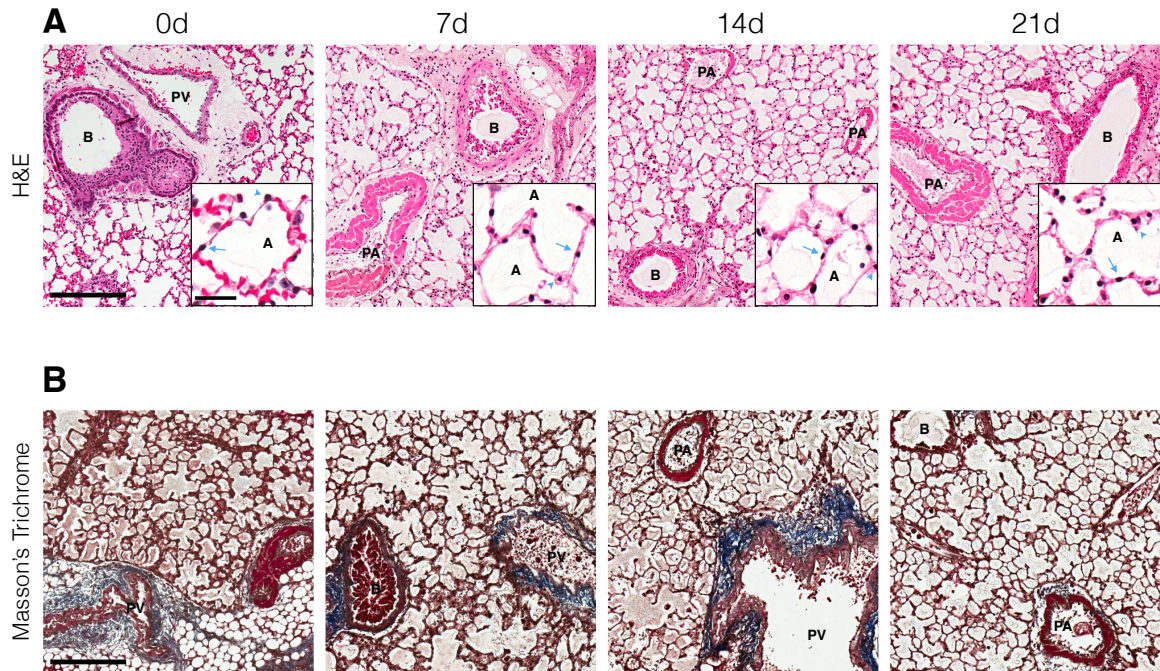


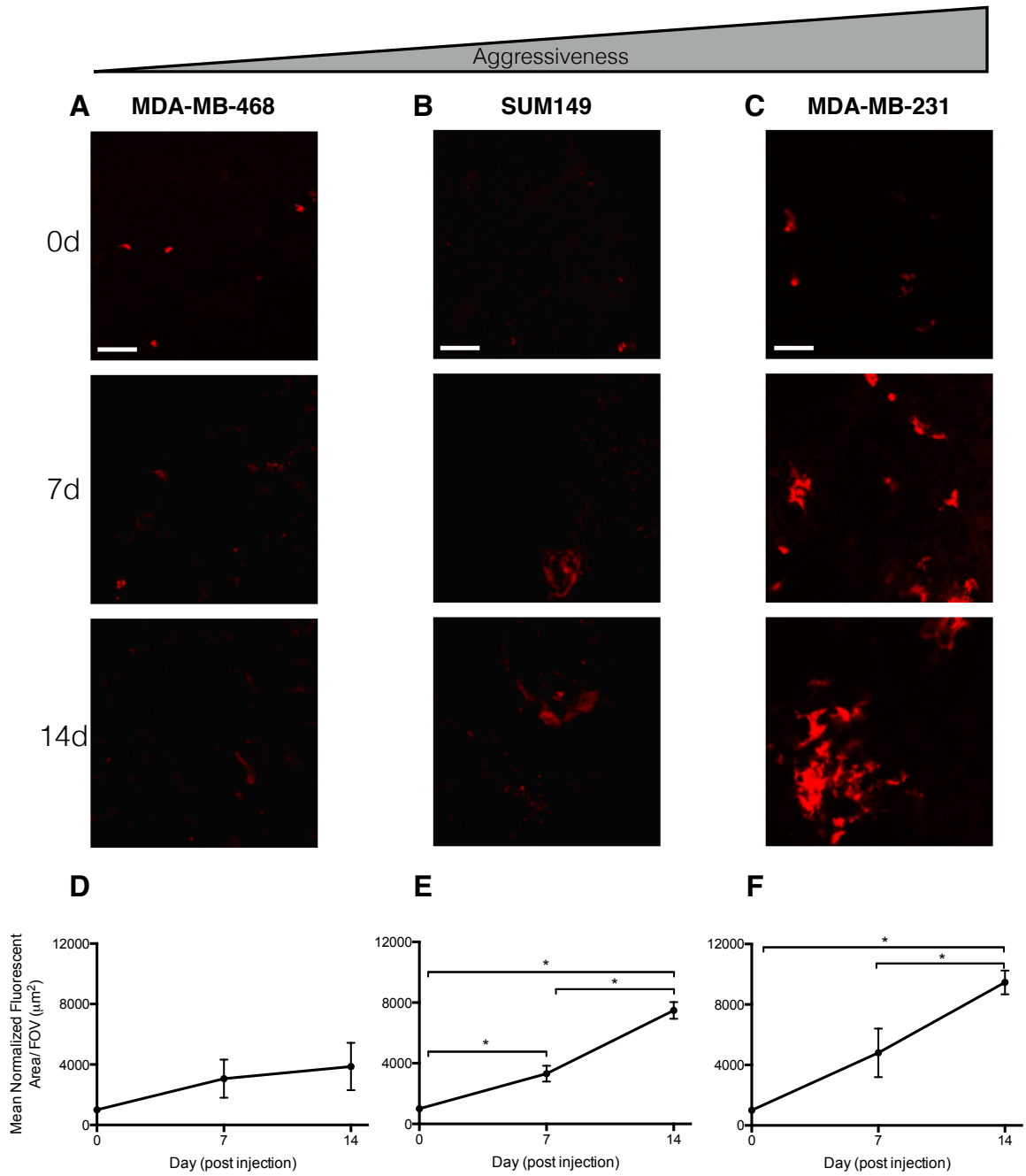
Figure 8. Pulmonary architecture remains structurally and microscopically intact in the PuMA over 21 days. To demonstrate the viability of the PuMA, normal unseeded female mouse lungs were cultured according to the PuMA, fixed, paraffin embedded, sectioned and stained. **(A)** H&E staining revealed the lung microarchitecture remained relatively healthy and intact throughout the 21 day period. Alveoli (A), airways (B) and large vessels (PA, pulmonary arteries; PV, pulmonary veins) throughout the lung remained expanded and were of normal diameter. Overall, gross cellularity decreased at days 14 and 21 compared to earlier time points. (*Inset*) Type I (blue arrows) and type II (blue arrowheads) pneumocytes were present at each time point throughout the assay and could be identified. Scale bar: 25 μm . **(B)** Masson's Trichrome stain was used to evaluate connective tissue components in the lung. Over the course of 21 days, muscle tissue (red stain) and collagen tissue (blue stain) remained visibly present with a slight reduction in collagen staining at day 21. Each component was present and could be identified at each time. Scale bars: 200 μm .

duration of the assay, there appeared to be a slight reduction in collagen staining by day 21 relative to earlier time points (**Figure 8B**). Each of these components was present and could be identified at each time point.

5.2. Whole Population MDA-MB-468, SUM149 and MDA-MB-231 Breast Cancer Cell Lines Demonstrate Differential Growth Progression Within the PuMA

To first determine the growth potential of whole population breast cancer cells within the lung, we used three different breast cancer cell line models with varying degrees of metastatic behaviour *in vivo*: very weakly metastatic MDA-MB-468, weakly metastatic SUM149 and highly metastatic MDA-MB-231 breast cancer cells. Cells were delivered to female nude mouse lungs by tail vein injection according to the PuMA protocol. Sections were cultured in serum-free conditions for 14 days and imaged at days 0, 7 and 14 using confocal microscopy to evaluate cellular growth and progression. Only SUM149 and MDA-MB-231 cells demonstrated increased fluorescence area at later time points compared to earlier time points (**Figure 9B,C**), whereas very weakly metastatic MDA-MB-468 cells failed to progress into larger colonies (**Figure 9A**). Highly metastatic MDA-MB-231 cells showed a greater progression in growth area compared to the weakly metastatic SUM149 cell line. Single cells could be seen in sections of lung in similar numbers at day 0 for each cell line, demonstrating successful delivery of cells to the lungs. Single cells progressed during the assay to small multicellular colonies by day 7 (SUM149, MDA-MB-231) and even larger colonies by day 14 (MDA-MB-231). However, little to no growth was observed for the very weakly metastatic MDA-MB-468 cell line over 14 days (**Figure 9B, C, D**). Cellular growth of SUM149 cells indicated by fluorescent area was significantly increased at day 7 ($p \leq 0.05$) and 14 ($p \leq 0.001$) relative to day 0, and day 14 ($p \leq 0.01$) relative to day 7 (**Figure 9E**). Growth of MDA-MB-231 cells was significantly increased at day 14 relative to days 7 ($p \leq 0.05$) and 0 ($p \leq 0.01$) (**Figure 9F**). Statistical significance was determined by one-way ANOVA with a Tukey's post test. Error bars represent \pm SEM.

Figure 9. Whole population MDA-MB-468, SUM149 and MDA-MB-231 human breast cancer cells differentially progress within the PuMA. To determine if breast cancer cells were able to grow and progress within the PuMA, very weakly metastatic MDA-MB-468, weakly metastatic SUM149 and highly metastatic MDA-MB-231 breast cancer cells were injected (n=3 mice). **(A, B, C)** Representative images for each cell line are shown. Five random images were taken for each of three lung sections for each time point. Single cells are seen within the lung at day 0, which progress to multicellular colonies by day 7 and 14 in the SUM149 and MDA-MB-231 populations only. Scale bars represent 100 μm . A mean normalized fluorescent area (μm^2) per image was measured and averaged for each time point. **(D)** MDA-MB-468 cells fail to grow into larger colonies. **(E)** SUM149 cell growth increased at day 7 ($p \leq 0.05$) and 14 ($p \leq 0.001$) relative to day 0, and day 14 ($p \leq 0.01$) relative to day 7. **(F)** MDA-MB-231 cell growth increased at day 14 relative to days 7 ($p \leq 0.05$) and 0 ($p \leq 0.01$). * indicates statistical significance. Error bars represent \pm SEM.



5.3. Highly Metastatic MDA-MB-231 Cells Proliferate in the PuMA

To assess the proliferative competency of breast cancer cells within the PuMA, sections of lung seeded with highly metastatic MDA-MB-231 whole population cells were fixed, sectioned and stained for the proliferative marker, Ki-67. Positive Ki-67 staining was present at day 0 once cells had arrived to the lung and throughout the duration of the assay (days 7, 14). Positive staining for Ki-67 was most notable at day 14 in larger multicellular colonies (**Figure 10B**). Positive staining was compared to a negative control (unseeded lung section from PuMA at day 14) (**Figure 10A**). Serial sections from the same lung tissue from each time point were also stained with H&E to confirm proliferative competency of breast cancer cells (versus surrounding lung tissue). Indeed, H&E staining demonstrated a concentrated presence of tumour cells corresponding to areas of Ki-67 positivity. Similar to Ki-67 staining, the most notable areas of tumour cells were seen in larger multicellular colonies at day 14 relative to earlier time points (**Figure 10C**). To qualitatively determine if these areas of tumour cells seen in seeded sections of lung were in fact areas of tumour cells, seeded H&E sections were compared to an unseeded lung section from the PuMA at day 14 (**Figure 10A**).

5.4. Stem-like ALDH^{hi}CD44⁺ MDA-MB-231 Breast Cancer Cells Progress Relative to ALDH^{lo}CD44⁻ Cells within the PuMA

After demonstrating the ability of whole breast cancer cell populations to grow within the lung in the PuMA, we wanted to determine the growth differences between stem-like and non stem-like breast cancer cells. To assess growth patterns of weakly aggressive SUM149 and highly aggressive MDA-MB-231 cells, both cell lines underwent FACS to isolate both stem-like ALDH^{hi}CD44⁺ and non stem-like ALDH^{lo}CD44⁻ populations. Immediately following isolation, 5×10^5 ALDH^{hi}CD44⁺ or ALDH^{lo}CD44⁻ tdTomato-expressing SUM149 or MDA-MB-231 breast cancer cells were delivered to female mouse lungs by tail vein injection (n=3 mice) and cultured for 21 days following the PuMA protocol. Initial cellular delivery was similar for both stem-like and non stem-like populations for each cell line injected. Single cells were present within the lung at day 0 for both ALDH^{hi}CD44⁺ and ALDH^{lo}CD44⁻ populations in each cell line. Weakly aggressive SUM149 ALDH^{hi}CD44⁺ cells

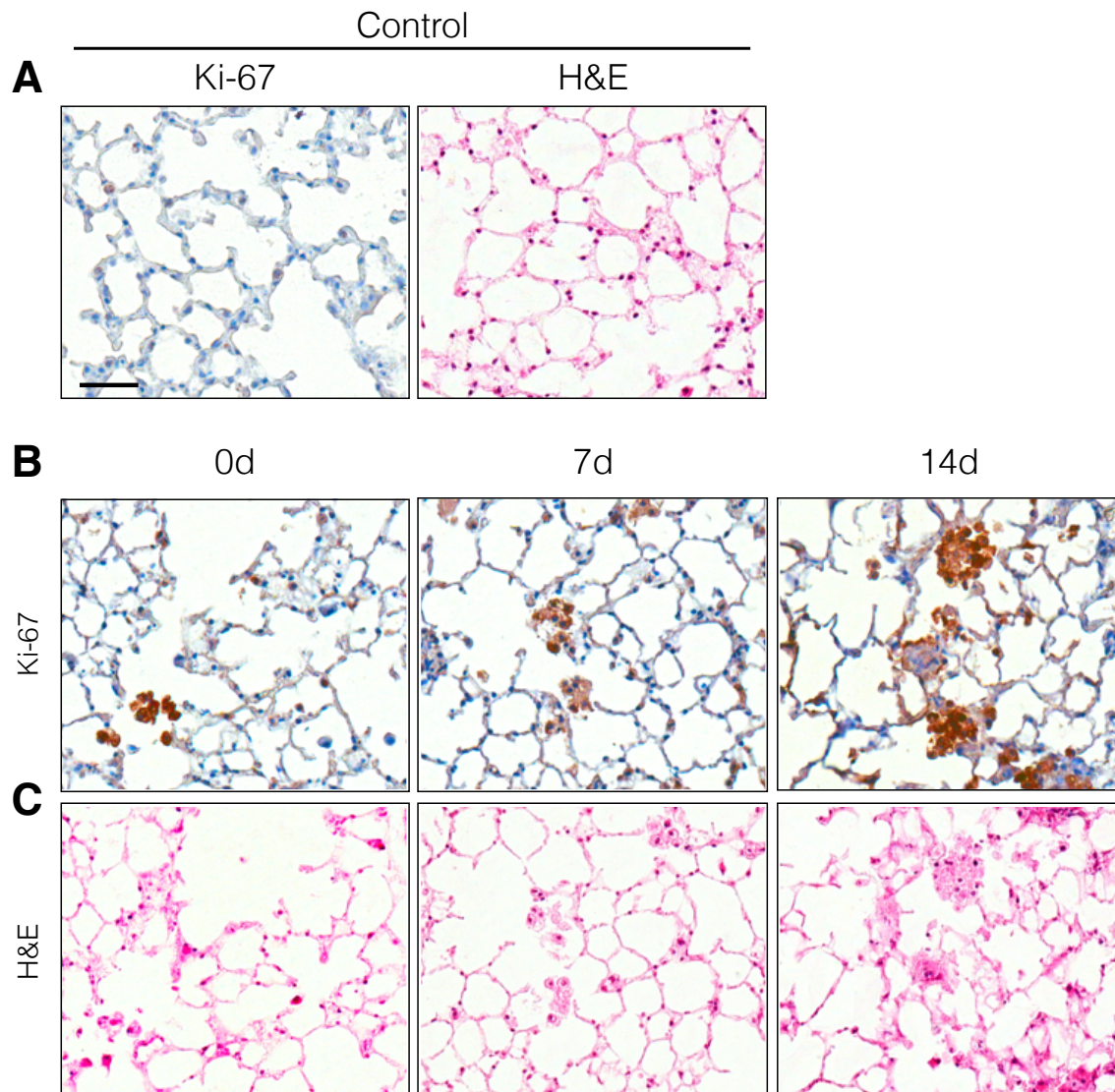
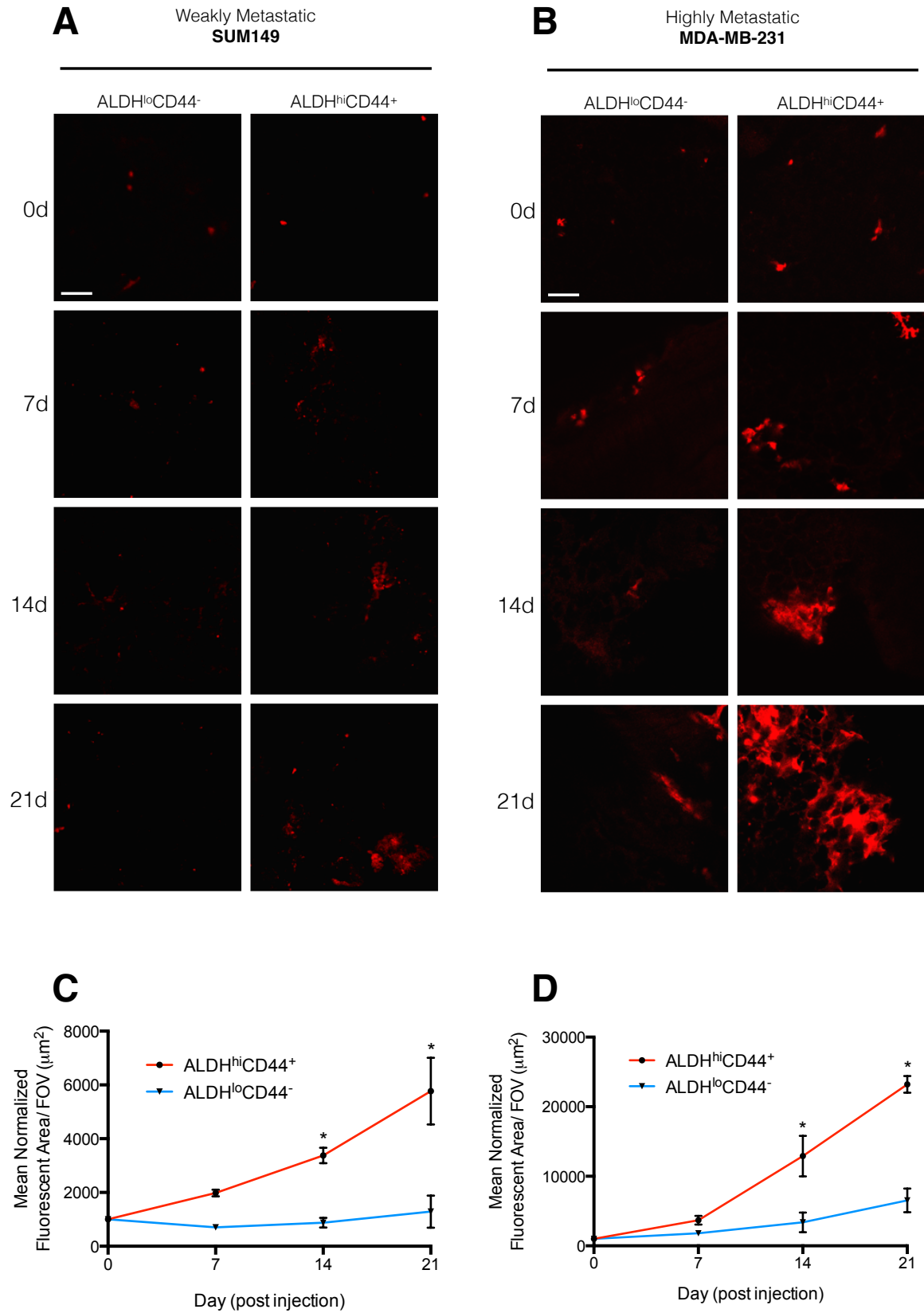


Figure 10. Highly metastatic MDA-MB-231 proliferate in the PuMA. To assess the proliferative competency of breast cancer cells grown in the PuMA, both normal unseeded and seeded sections of lung with highly aggressive MDA-MB-231 cells were stained for the proliferative marker Ki-67. (A) Negative control for both Ki-67 and H&E staining (unseeded lung section from day 14 in PuMA). (B) Seeded sections of lung with highly aggressive MDA-MB-231 cells in the PuMA show positive staining for Ki-67 in cells present in the lung at day 0 through day 14. Positive staining is most notable at day 14. (C) H&E staining of serial sections of seeded lungs confirmed proliferative competency of highly metastatic cells within the PuMA, as seen with Ki-67 staining. Scale bars represent 50 μ m.

Figure 11. Stem-like ALDH^{hi}CD44⁺ MDA-MB-231 breast cancer cells progress relative to ALDH^{lo}CD44⁻ cells within the PuMA. To determine growth patterns between stem-like and non stem-like breast cancer cells in the PuMA, ALDH^{hi}CD44⁺ and ALDH^{lo}CD44⁻ cells were isolated by FACS from SUM149 and MDA-MB-231 human breast cancer cell lines and injected into the PuMA (n=3 mice). (A, B) Representative images for each population are shown. Five random images were taken per lung section (n=3 lung sections) for each time point. Single cells are seen within the lung at day 0 for both populations, which progress to increasingly larger multicellular colonies by day 21 only in the stem-like ALDH^{hi}CD44⁺ population. Scale bars represent 100 μm . A mean normalized fluorescent area (μm^2) per FOV was measured and averaged for each time point. (C) SUM149 cellular growth was increased in the ALDH^{hi}CD44⁺ population relative to the ALDH^{lo}CD44⁻ population at day 14 ($p \leq 0.05$) and day 21 ($p \leq 0.0001$). (D) MDA-MB-231 growth was increased in the ALDH^{hi}CD44⁺ population compared to the ALDH^{lo}CD44⁻ population at day 14 ($p \leq 0.001$) and day 21 ($p \leq 0.0001$). * indicates statistical significance between stem-like and non stem-like populations at a given time point. Error bars represent \pm SEM.



progressed to small multicellular colonies by day 21, whereas non stem-like ALDH^{lo}CD44⁻ cells remained predominantly as single cells throughout the duration of the assay (**Figure 11A**). Highly aggressive MDA-MB-231 stem-like ALDH^{hi}CD44⁺ cells progressed to much larger multicellular colonies by day 21 compared to non stem-like ALDH^{lo}CD44⁻ cells which remained primarily as single cells. Scale bars represent 100 μm (**Figure 11B**). SUM149 cellular growth increased in the ALDH^{hi}CD44⁺ population relative to the ALDH^{lo}CD44⁻ population at day 14 ($p \leq 0.05$) and day 21 ($p \leq 0.0001$) (**Figure 11C**). Similarly, MDA-MB-231 cellular growth increased in the ALDH^{hi}CD44⁺ population compared to the ALDH^{lo}CD44⁻ population at day 14 ($p \leq 0.001$) and day 21 ($p \leq 0.0001$) (**Figure 11D**). Significance between both populations at a given time point was determined by two-way ANOVA with a Sidak's post test. Error bars represent \pm SEM.

5.5. ALDH^{hi}CD44⁺ Breast Cancer Cells Progress from Single Cells to Micrometastases to Macrometastases in the PuMA while the Majority of ALDH^{lo}CD44⁻ Cells Remain as Single Cells

To further quantify the differences in progression within the lung between stem-like ALDH^{hi}CD44⁺ and non stem-like ALDH^{lo}CD44⁻ breast cancer cells, we measured and classified the size of colonies present in the PuMA. Three groups were used to classify the sizes of multicellular colonies in the PuMA according to diameter: diameter: single cells ($\leq 50 \mu\text{m}$), micrometastases (100-400 μm) or macrometastases ($>400 \mu\text{m}$). Data were presented as a mean percentage of specific colony size (single cells, micrometastases, or macrometastases) per image. Stem-like ALDH^{hi}CD44⁺ cells from the weakly metastatic SUM149 cell line progressed from single cells at day 0 (100.0% \pm 0.0 single cells, 0.0% \pm 0.0 micrometastases, 0.0% \pm 0.0 macrometastases) to micrometastases by day 21 (89.3% \pm 4.7 single cells, 10.7% \pm 2.6 micrometastases, 0.0% \pm 0.0 macrometastases). In contrast, the majority of non stem-like ALDH^{lo}CD44⁻ cells remained as single cells from day 0 (100.0% \pm 0.0 single cells, 0.0% \pm 0.0 micrometastases, 0.0% \pm 0.0 macrometastases) throughout the duration of the assay to day 21 (98.0% \pm 2.0 single cells, 1.3% \pm 1.3 micrometastases, 0.0% \pm 0.0 macrometastases) (**Figure 12A, Table 3**). As predicted, Highly aggressive MDA-MB-231 stem-like ALDH^{hi}CD44⁺ cells grew to a greater

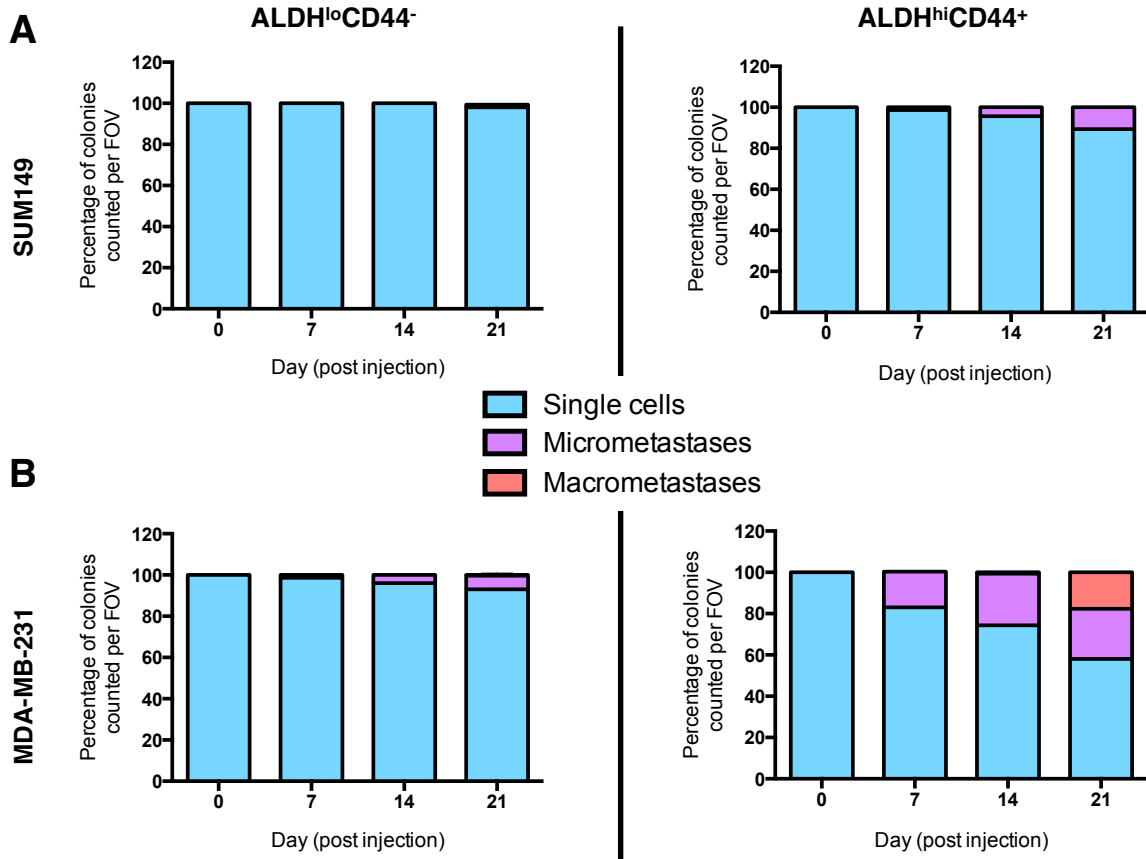


Figure 12. ALDH^{hi}CD44⁺ breast cancer cells progress from single cells to micromets to macromets while the majority of ALDH^{lo}CD44⁻ cells remain as single cells. Colonies present in lung sections grown in the PuMA were classified in diameter as single cells ($\leq 50 \mu\text{m}$), micromets (100-400 μm) or macromets ($>400 \mu\text{m}$). Five random images were taken per lung section ($n=3$ lung sections) for each time point. (A) Only SUM149 ALDH^{hi}CD44⁺ cells progressed from single cells at day 0 to micromets. (B) MDA-MB-231 ALDH^{hi}CD44⁺ cells progressed from single cells at day 0 through micromets to macromets whereas ALDH^{lo}CD44⁻ cells remained predominantly as single cells.

Table 3. Proportion of SUM149 ALDH^{hi}CD44⁺ and ALDH^{lo}CD44⁻ colony sizes in the PuMA.

	Day 0	Day 7	Day 14	Day 21
Single cells ($<50 \mu\text{m}$)	100.0 \pm 0.0 100.0 \pm 0.0	98.7 \pm 0.3 100.0 \pm 0.0	95.7 \pm 0.9 100.0 \pm 0.0	89.3 \pm 4.7 98.0 \pm 2.0
Micromets (100-400 μm)	0.0 \pm 0.0 0.0 \pm 0.0	1.3 \pm 2.6 0.0 \pm 0.0	4.3 \pm 0.3 0.0 \pm 0.0	10.7 \pm 2.6 1.3 \pm 1.3
Macromets ($>400 \mu\text{m}$)	0.0 \pm 0.0 0.0 \pm 0.0	0.0 \pm 0.0 0.0 \pm 0.0	0.0 \pm 0.0 0.0 \pm 0.0	0.0 \pm 0.0 0.0 \pm 0.0

Bold Font = Stem-like ALDH^{hi}CD44⁺ population

Regular Font = Non stem-like ALDH^{lo}CD44⁻ population

proportion of larger multicellular colonies compared to weakly aggressive SUM149 cells. MDA-MB-231 ALDH^{hi}CD44⁺ cells progressed from single cells at day 0 (100.0% ± 0.0 single cells, 0.0% ± 0.0 micrometastases, 0.0% ± 0.0 macrometastases) through micrometastases to macrometastases by day 21 (58.0% ± 2.0 single cells, 24.0% ± 2.2 micrometastases, 17.7% ± 4.3 macrometastases). Similar to patterns observed with SUM149 cells, non stem-like MDA-MB-231 ALDH^{lo}CD44⁻ cells remained mainly as single cells throughout the duration of the assay. Single cells present at day 0 (100.0% ± 0.0 single cells, 0.0% ± 0.0 micrometastases, 0.0% ± 0.0 macrometastases) progressed to few micrometastasis sized colonies by 21 (93.0% ± 2.5 single cells, 6.7% ± 2.9 micrometastases, 0.3% ± 0.3 macrometastases) (**Figure 12B, Table 4**). Overall, stem-like ALDH^{hi}CD44⁺ cells isolated from both cell lines progressed to larger sized colonies by day 21 faster and in greater numbers compared to their non stem-like ALDH^{lo}CD44⁻ counterparts.

5.6. Basic Fibroblast Growth Factor is Present in Lung-conditioned Media and Increases *in vitro* Breast Cancer Cell Proliferation, but not Migration

Previous work in our lab has identified the presence of many lung-derived soluble factors present in the lung microenvironment that could potentially contribute to the metastatic behaviour of breast cancer cells. Many of these soluble factors are proteins that have well-characterized roles in cellular adhesion, migration and neoplasia. In addition, many of the soluble factors identified in the lung are CD44-associated proteins [52]. One specific protein of interest previously identified is basic fibroblast growth factor (bFGF) due to its potent mitogenic effect, well-characterized role in the maintenance of normal stem cells and its interaction with the cell surface receptor, CD44 [83, 105]. Therefore, we wanted to determine the influence of bFGF on breast cancer cell migration and proliferation. Conditioned media was generated from healthy female mouse lungs, bFGF protein levels were assessed, and bFGF was removed from lung CM by means of immunodepletion (**Figure 13**). bFGF protein levels were determined by ELISA in basal media (BM), lung-CM, lung-CM exposed to Dynabeads Protein G only, and lung-CM exposed to Dynabeads plus an anti-mouse bFGF antibody. Data indicated that the concentration of bFGF present in lung-CM was significantly higher than bFGF present in BM ($p \leq 0.0001$). Immunodepletion of

Table 4. Proportion of MDA-MB-231 ALDH^{hi}CD44⁺ and ALDH^{lo}CD44⁻ colony sizes in the PuMA.

	Day 0	Day 7	Day 14	Day 21
Single cells ($<50 \mu\text{m}$)	100.0 \pm 0.0 100.0 \pm 0.0	83.0 \pm 4.0 98.7 \pm 0.9	74.3 \pm 1.5 96.0 \pm 2.5	58.0 \pm 2.5 93.0 \pm 2.5
Micromets (100-400 μm)	0.0 \pm 0.0 0.0 \pm 0.0	17.3 \pm 3.8 1.3 \pm 0.9	25.0 \pm 1.2 4.0 \pm 2.5	24.0 \pm 2.2 6.7 \pm 2.9
Macromets ($>400 \mu\text{m}$)	0.0 \pm 0.0 0.0 \pm 0.0	0.0 \pm 0.0 0.0 \pm 0.0	0.7 \pm 0.3 0.0 \pm 0.0	17.7 \pm 4.3 0.3 \pm 0.3

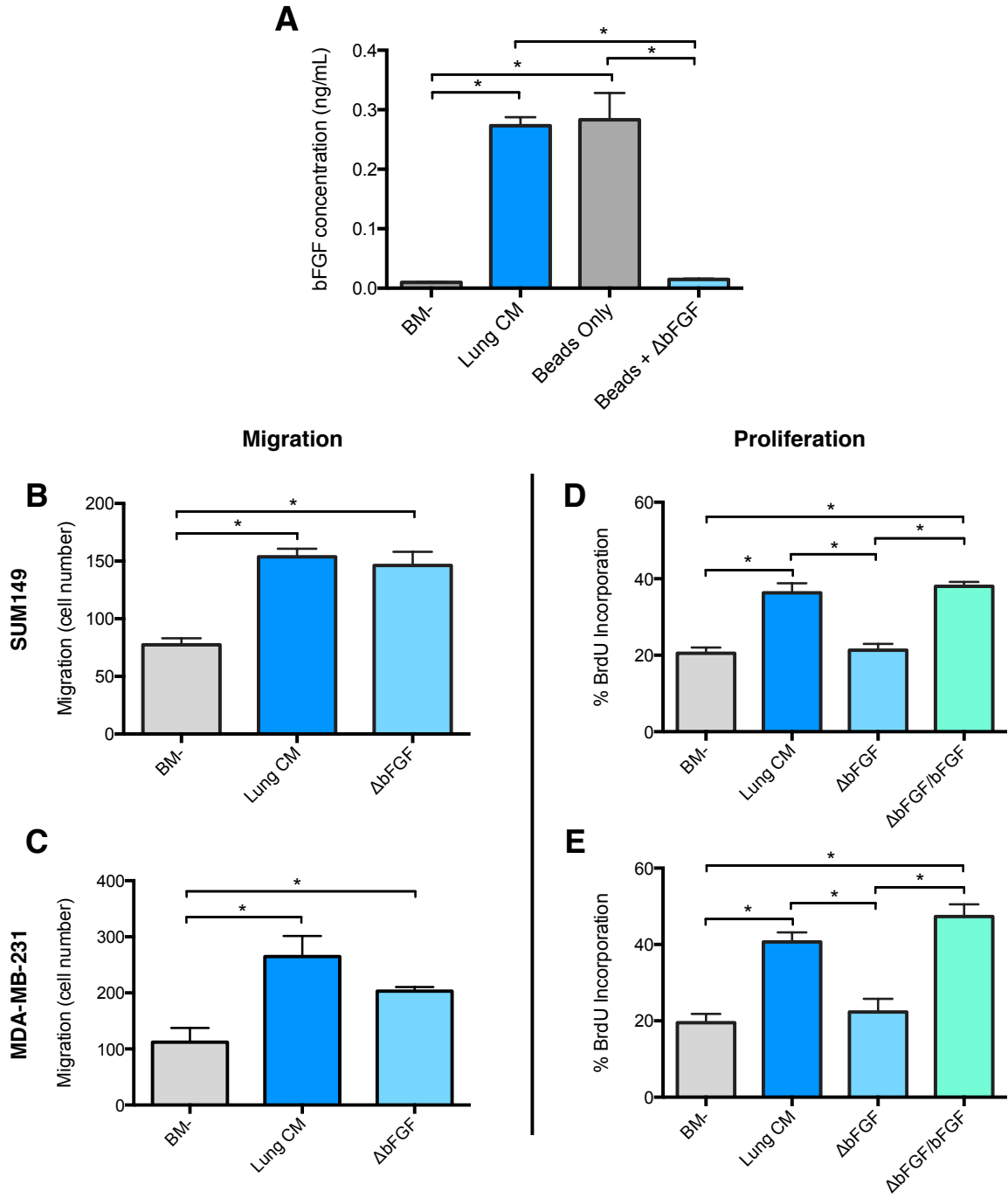
Bold Font = Stem-like ALDH^{hi}CD44⁺ population

Regular Font = Non stem-like ALDH^{lo}CD44⁻ population

bFGF was successful and resulted in lung-CM with significantly decreased bFGF levels compared to lung-CM alone ($p \leq 0.0001$). These levels were in line with the BM control. Dynabeads Protein G only in the absence of an anti-bFGF antibody had no effect on bFGF depletion (**Figure 13A**). Data are presented as mean bFGF concentration \pm SEM ($n = 3$). To assess the influence of lung-derived bFGF on breast cancer cell migration, whole population SUM149 or MDA-MB-231 cells were plated in triplicate on top of gelatin-coated transwells. Transwells were placed in basal media (DMEM:F12 + Mito⁺), normal lung-CM or lung-CM depleted of bFGF and incubated for 18 hr at 37°C and 5% CO₂. SUM149 cells showed a significantly increased number of migrated cells exposed to lung-CM relative to BM ($p \leq 0.01$), although this migration was not impacted by depletion of bFGF (**Figure 13B**). MDA-MB-231 cells demonstrated a similar pattern to SUM149 cells with a significantly increased number of migrated cells exposed to lung-CM relative to BM-, with no influence of bFGF ($p \leq 0.001$) (**Figure 13C**).

To determine the influence of bFGF on cellular proliferation, SUM149 or MDA-MB-231 cells were plated in triplicate in 8-well chamber slides and incubated for 24 hr at 37°C and 5% CO₂ ($n = 3$) prior to incubation with BrdU. SUM149 cells showed a significantly increased number of BrdU positive cells when exposed to lung-CM relative to BM- ($p \leq 0.0001$), and this effect could be abrogated by depletion of bFGF ($p \leq 0.0001$) to levels consistent with the BM- control (**Figure 13D**). MDA-MB-231 cells displayed similar BrdU incorporation patterns to SUM149 cells, with a significantly increased number of BrdU positive cells exposed to lung-CM relative to BM ($p \leq 0.001$) and abrogation of this effect with depletion of bFGF ($p \leq 0.001$) to levels consistent with the BM control (**Figure 13E**). To determine if bFGF was in fact increasing cellular proliferation, recombinant bFGF was added to immunodepleted lung-CM. The re-addition of bFGF to immunodepleted lung-CM rescued the reduction of cellular proliferation to levels consistent with non-depleted lung-CM. This effect was apparent in both SUM149 and MDA-MB-231 cell lines.

Figure 13. Depletion of bFGF from lung conditioned media reduces breast cancer cell proliferation but not migration. To determine the effect of bFGF on breast cancer cell migration and proliferation, bFGF was immunodepleted from lung-CM. (A) CM was generated from healthy female mouse lungs and bFGF immunodepleted. Resulting bFGF protein levels were determined by ELISA in basal media (BM), lung-CM, lung-CM exposed to Dynabeads only, and lung-CM exposed to beads plus an anti-mouse bFGF antibody. Data indicate bFGF is present in lung-CM and not in BM ($p \leq 0.0001$). Immunodepletion of bFGF from lung-CM was successful ($p \leq 0.0001$). Data are presented as mean bFGF concentration \pm SEM ($n = 3$). (B, C) SUM149 and MDA-MB-231 cells showed an increased number of migrated cells exposed to lung-CM relative to BM ($p \leq 0.01$, $p \leq 0.001$). No migratory differences are seen for cells exposed to lung-CM compared to lung-CM depleted of bFGF. (D, E) SUM149 and MDA-MB-231 cells show a significantly increased number of BrdU positive cells exposed to lung-CM relative to BM ($p \leq 0.0001$, $p \leq 0.001$). SUM149 and MDA-MB-231 cells exposed to lung-CM depleted of bFGF (Δ bFGF) showed significantly less BrdU positive cells compared to lung-CM ($p \leq 0.0001$, $p \leq 0.001$). Re-addition of recombinant bFGF to depleted lung-CM (Δ bFGF/bFGF) rescued the effect on proliferation for both cell lines to levels consistent with lung-CM alone. * indicates statistical significance. Data are presented as mean number of migrated cells/FOV or percentage of BrdU positive cells per total cells counted \pm SEM ($n = 3$).



5.7. Basic Fibroblast Growth Factor is Present in the Intact Lung Microenvironment

To further determine the presence of bFGF within the intact lung microenvironment in the context of the PuMA, sections of normal unseeded lung from healthy mice were immunohistochemically stained for bFGF at each time point of the assay (days 0, 7, 14, 21) (**Figure 14A**). Sections of lung were grown in culture according to the PuMA protocol, fixed, paraffin embedded and sectioned into 5 μm slices for staining with an anti-mouse bFGF antibody. Unseeded sections of lung in the PuMA consistently showed diffuse positive staining for bFGF at day 0 through day 21. The highest levels of staining for bFGF corresponded to the basement membrane surrounding vasculature within the lung. A negative control stained with secondary antibody only was used to assess any non-specific binding of secondary antibody. Furthermore, tissue from mouse liver was also used as a control to determine if the anti-bFGF antibody simply bound to any tissue of mouse origin. Staining shows that there is very weak signal for bFGF present in the liver whereas signal in the lung is diffusely present throughout the tissue.

To further evaluate the presence of bFGF in the context of the PuMA, surrounding media and Gelfoam® were collected for each time point in the PuMA on which normal unseeded sections of lung were grown (**Figure 14B**). Media and Gelfoam® were centrifuged together and the supernatant collected to measure the concentration of secreted mouse bFGF by ELISA. Basal media (M199 media) alone contained no soluble bFGF and day 0 contained negligible amounts of bFGF. By day 7, a small amount of bFGF is present in the Gelfoam® and surrounding media. At days 14 and 21, this amount is more pronounced, with a significant increase in bFGF at day 14 relative to day 0 ($p \leq 0.05$) and media only ($p \leq 0.05$), and day 21 relative to day 0 ($p \leq 0.05$) and media alone ($p \leq 0.05$). This increase coincided with the length of time that lung sections spent on the Gelfoam® throughout the duration of the PuMA. Statistical significance at a given time point was determined by one-way ANOVA with a Tukey's post test. Data was presented as bFGF concentration ($\mu\text{g/mL}$) \pm SEM.

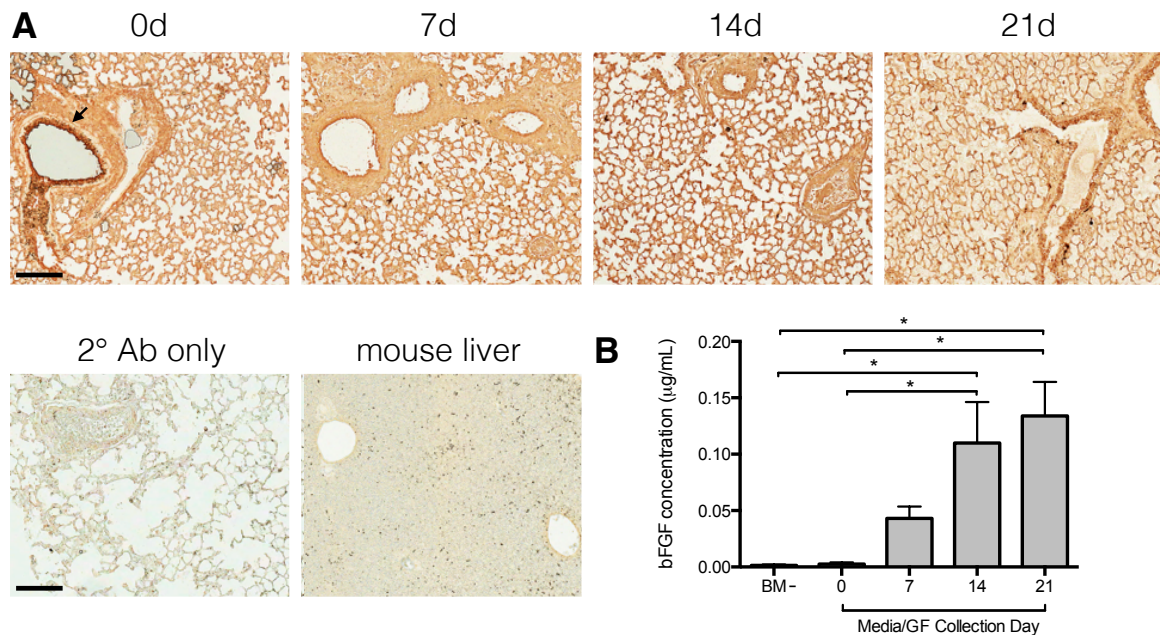
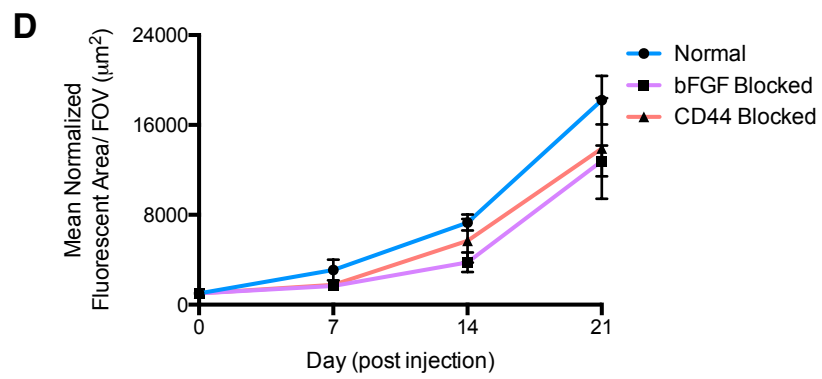
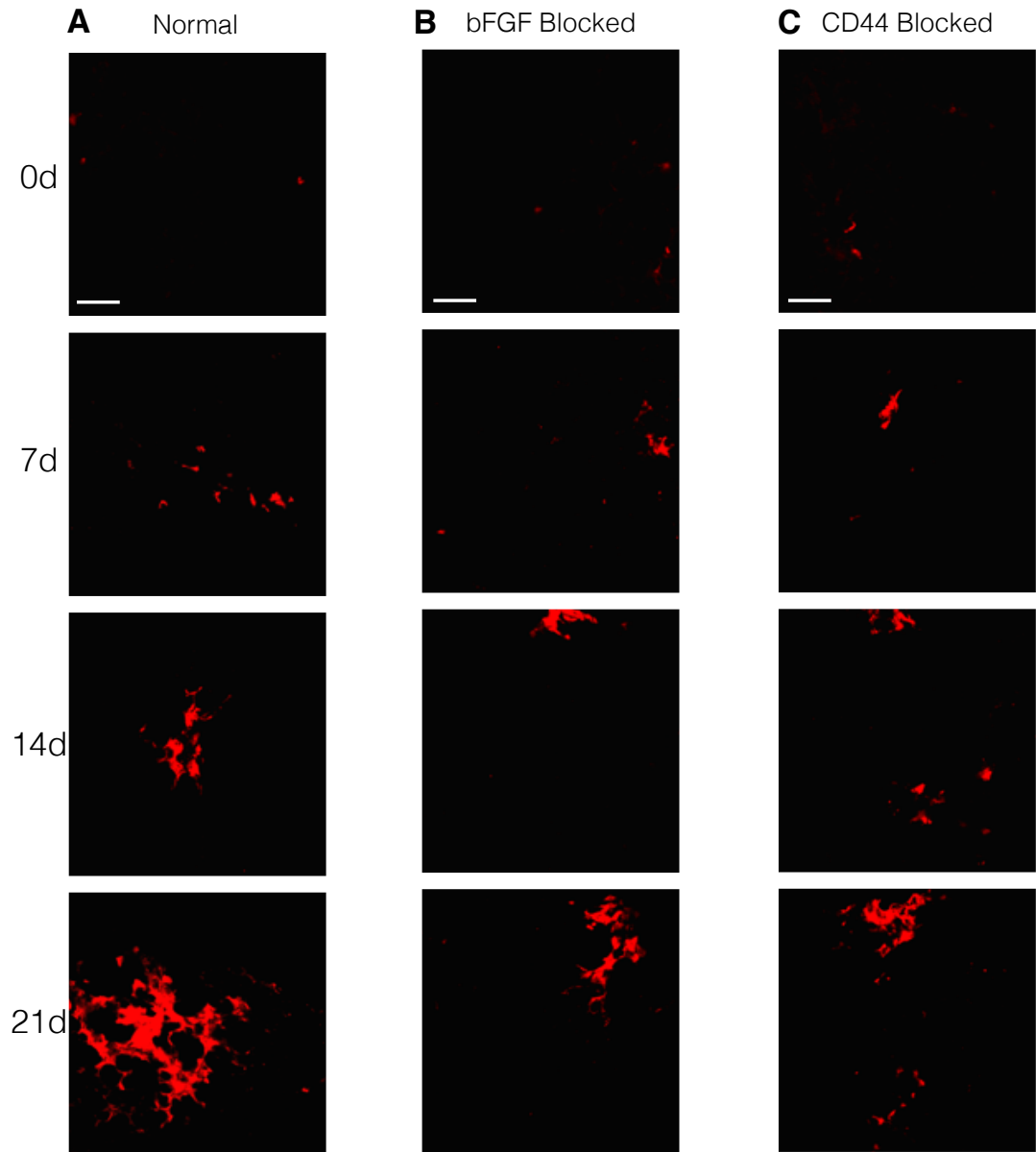


Figure 14. Basic fibroblast growth factor is present in the intact lung microenvironment. To determine the presence of bFGF within the lung in the context of the PuMA, sections of normal unseeded lung grown in the PuMA were immunohistochemically stained for bFGF. (A) Unseeded sections of lung consistently show diffuse positive staining for bFGF at days 0 through day 21. Positive staining is most notable around the basement membranes of airways and vasculature (*black arrow*). A antibody negative control consisted of the section stained with secondary antibody only. Mouse liver tissue was used as a tissue control to determine the specificity of the anti-bFGF antibody. Scale bars represent 200 μm . (B) Surrounding media/Gelfoam® were collected for each time point in the PuMA which normal sections of lung were grown. Basal media (BM) alone contained no soluble bFGF and day 0 contained negligible amounts. By day 7, a small amount of bFGF is present in the Gelfoam and surrounding media. At days 14 and 21, this amount is more pronounced with an increase in bFGF at day 14 relative to day 0 ($p \leq 0.05$) and BM ($p \leq 0.05$), and day 21 relative to day 0 ($p \leq 0.05$) and BM ($p \leq 0.05$). * Indicates statistical significance. Data is presented as bFGF concentration ($\mu\text{g/mL}$) \pm SEM.

5.8. Blocking bFGF or CD44 on Whole Population MDA-MB-231 Cells Does Not Decrease Cellular Growth in the PuMA

We next wanted to determine the influence of bFGF on cellular growth and proliferation in the native lung microenvironment in the context of the PuMA. Using the highly metastatic MDA-MB-231 whole cell population, cells were either pre-incubated with an anti-CD44 antibody in HBSS or in HBSS alone prior to injection. Cells were then delivered to female nude mouse lungs by tail vein injection (5×10^5 cells/mouse, $n=3$ mice). Lungs seeded with cells pre-incubated with an anti-CD44 antibody were infused and excised as per the PuMA protocol (**Figure 7**). Lungs seeded with cells pre-incubated with HBSS only were either infused with normal agarose/media 1 solution or agarose/media 1 solution plus a neutralizing bFGF antibody before following the remainder of the PuMA protocol. Sections were cultured in serum-free conditions and imaged at days 0, 7, 14 and 21 using confocal microscopy to evaluate cellular growth and progression. Following imaging, there was a slight decrease in cellular growth and progression for bFGF blocked or CD44 blocked groups compared to normal seeded lungs by day 21 (**Figure 15A,B,C**). There was a trend towards decrease in overall growth in the presence of a neutralizing bFGF antibody or in cells pre-incubated with an anti-CD44 antibody at days 7, 14, and 21, although this did not reach statistical significance ($p>0.05$) (**Figure 15D**). Significance between experimental groups at a given time point was determined by two-way ANOVA with a Sidak's post test. Error bars represent \pm SEM.

Figure 15. Blocking bFGF and CD44 has no effect on growth reduction of whole population MDA-MB-231 cells in the PuMA. To determine the influence of bFGF on breast cancer growth in the context of the PuMA, both bFGF and one of its receptors on breast cancer cells, CD44, were blocked. For bFGF blocking, cells were injected as per the PuMA assay with the exception that lungs were infused with a neutralizing bFGF antibody within the agarose/lung media 1 solution. For CD44 blocking, cells were pre-incubated with an anti-CD44 antibody prior to injection. The PuMA was carried out as described above. **(A,B,C)** Representative images for normal seeded lungs, normal seeded lungs infused with a neutralizing bFGF antibody and seeded lungs pre-incubated with an anti-CD44 antibody. Scale bars represent 100 μm . A mean normalized fluorescent area (μm^2) per image was measured and averaged for each time point for each experimental group. **(D)** A trend towards decrease in overall growth is seen for cells grown in the presence of a neutralizing bFGF antibody or cells pre-incubated with an anti-CD44 antibody at days 7, 14, and 21, however this did not reach statistical significance ($p>0.05$). Error bars represent \pm SEM.



6. DISCUSSION

Breast cancer incidence has remained relatively constant over the past 10-15 years, with a general decline in the number of individuals succumbing to this type of cancer. Despite the decreasing deaths rate associated with breast cancer, it still represents the most frequently diagnosed cancer in women and the second leading cause of all cancer related deaths in women in North America [2, 3, 106].

Research advances in the field of cancer have generated a wealth of knowledge concerning how cancer initially develops and the potential targets worth exploiting. However, as we gain a greater understanding of the complexities of both the tumour and the tumour microenvironment, we are beginning to appreciate the vast heterogeneity that exists within the tumour population. This in part has led to many failed therapeutics and treatments in the metastatic setting, increasing the risk of relapse and cancer recurrence in patients. It is therefore paramount that we put forth efforts to better understand the mechanisms that determine why tumours spread in the patterns they do and ultimately how this metastatic process occurs once single cells reach secondary organs.

The lung is one of the most frequent sites of metastasis associated with breast cancer, as a result of its large surface area and dense capillary network that make it ideal for tumour cell stasis during circulation. Much work has been done investigating the genetic signatures of breast cancer cells associated with specific patterns of metastatic spread, specifically to the lung. This work, largely pioneered by Joan Massagué and related groups, has increased our understanding of the the genetic signatures that certain tumour cells acquire for lung-specific tropism [56]. However, genetics alone do not account for patterns of metastatic spread, and we are beginning to understand the profound influence of specific organ microenvironments and their relationship with tumour development. It has remained a technical challenge to understand the implications of both the soluble and insoluble microenvironments in

secondary organs, particularly in the lung as they relate to metastatic progression. Therefore, this study utilized a relatively new and innovative model system for studying the influence of the lung microenvironment on breast cancer cells. The pulmonary metastasis assay (PuMA) has allowed us to investigate the effect of both the soluble and insoluble lung microenvironments on the behaviour of breast cancer cells, specifically stem-like ALDH^{hi}CD44⁺ cells, from the single cell stage to multicellular colonies. This model will ultimately help elucidate how breast cancer cells interact with the lung during metastatic progression and allow us to develop methods of exploiting this microenvironment to limit growth and progression, with hopes of eventual translation to the clinic.

We set forth to test the hypothesis that stem-like ALDH^{hi}CD44⁺ breast cancer cells demonstrate increased growth and progression from a single cell stage within the PuMA compared to their non stem-like ALDH^{lo}CD44⁻ counterpart. To our knowledge, we are the first group to utilize this innovative *ex vivo* model system for tracking the metastatic behaviour of stem-like breast cancer cells within the lung in real time.

6.1. Summary of Experimental Findings

1. An innovative *ex vivo* pulmonary metastasis assay (PuMA) was established in our laboratory and demonstrated to maintain mouse lung viability and relevant lung architecture in culture for 21 days, as reported by previous studies [93, 102].
2. Whole population MDA-MB-468, SUM149 and MDA-MB-231 breast cancer cell lines differentially progressed within the PuMA with highly metastatic MDA-MB-231 cells actively proliferating and showing the greatest degree of growth.
3. ALDH^{hi}CD44⁺ breast cancer cells isolated from both SUM149 and MDA-MB-231 human cell lines showed increased growth and progression from single cells in the PuMA, relative to the non stem-like ALDH^{lo}CD44⁻ population.
4. ALDH^{hi}CD44⁺ breast cancer cells isolated from both SUM149 and MDA-MB-231 cell lines progressed from single cells (≤ 50 μm in diameter) to micrometastatic (100-400 μm) colonies within the PuMA, with MDA-MB-231 cells also progressing even further to macrometastatic colonies (>400 μm).

5. Basic fibroblast growth factor (bFGF) was shown to be present in both lung-CM and the intact lung microenvironment in the PuMA.
6. Depletion of bFGF from mouse lung-CM significantly reduced the proliferation of both SUM149 and MDA-MB-231 cells *in vitro*, but had no effect on cellular migration.
7. Blocking of either bFGF or its receptor CD44 did not significantly reduce cellular growth and progression in the context of the PuMA.

6.2. Advantages of the PuMA as a Model for Metastasis

Over 20 years ago, Siminski and colleagues successfully established a novel *ex vivo* model system for studying the pathogenesis of lung injury. They required a model system that accurately mimicked the *in vivo* environment of the lung, while at the same time being simple and practical. With their model, they were able to maintain normal pulmonary architecture and viability for up to 9 weeks in culture, in serum free conditions [102]. It wasn't until recently that this protocol was adapted to model cancer metastasis in a secondary environment.

To accurately study the biology of metastasis, an optimal assay would conveniently recapitulate the complexity of the cellular and non-cellular microenvironment, while at the same time allowing a “glass window” to observe metastatic progression. As a starting point, *in vitro* approaches are often employed. These techniques are rarely sufficient in modelling the complex interactions that occur between tumour cells and the host environment, both cellular and non-cellular. To complement this, *in vivo* models, most often in mice, are required. However, these models too often examine only the end-point of metastatic outcome (whether or not secondary tumours have been established) and the time to late-stage metastatic events [93, 107]. In order to bridge the gap between these traditional models of studying metastasis, Mendoza *et al.* adapted the *ex vivo* model system first put forth by Siminski some 20 years earlier. Their model, which they described as a pulmonary metastasis assay (PuMA), was able to effectively discriminate between both weakly and highly metastatic human and murine cancer cell lines that accurately modelled their behaviour previously observed *in vivo* [93]. Their study therefore introduced a

powerful tool for understanding the progression of metastasis in a secondary environment.

We therefore utilized this innovative assay in order to better understand breast cancer behaviour and metastatic progression in the context of the lung, a process often associated with high rates of mortality. We were able to effectively demonstrate that normal unseeded lung sections maintained in culture remained relatively healthy and intact throughout the 21 day period. Important to this assay was that the gross pulmonary architecture remained intact with no visible areas of collapse or loss of structure with the presence of structural components (muscle tissue and collagen) identified at each time point. Infusion of a 0.6% agarose solution prior to the extraction of lungs was key to maintaining airways in an expanded state throughout the duration of the assay. Other groups have demonstrated that without the inclusion of agarose, lung architecture is almost completely lost within the first 24 hours in culture [93]. In addition to intact pulmonary architecture, we have shown that cellularity also remains in the lung during the assay. Using H&E staining, there is evidence of cellular nuclei present throughout the lung at each time point of the assay. More specifically, we were able to identify and distinguish between type I and type II pneumocytes at the level of the alveoli at each time point throughout the assay. Although there was an overall qualitative loss of cellularity within the lung at days 14 and 21 compared to earlier time points as expected [93], the lung microarchitecture remained remarkably unchanged.

We next tested three breast cancer cell lines, each with varying degrees of metastatic behaviour *in vivo*: very weakly metastatic MDA-MB-468, weakly metastatic SUM149 and highly aggressive MDA-MB-231. Both MDA-MB-468 and MDA-MB-231 cells were originally derived from the pleural effusions of patients with breast cancer. In terms of molecular subtype, these cell lines are both classified as triple negative (TN) and have a EGFR⁺/TGF α ⁺/ER⁻/PR⁻/HER2⁻ phenotype [108, 109]. SUM149 cells were isolated from a patient with primary inflammatory breast cancer. These cells bear a EGFR⁺/HER2,3⁺/HER4⁻/ER⁻/PR⁻ phenotype [110]. Cell lines demonstrated growth patterns that accurately paralleled their metastatic behaviours *in vivo*. Previous studies have established the behaviours of these cell

lines *in vivo* and although MDA-MB-468 whole population and stem-like cells isolated based on an ALDH^{hi}CD44⁺CD133⁺ phenotype have produced lung tumours in mice injected by tail-vein, their mean metastatic burden (percentage of total lung) was quite low (<1%), indicating an inability of these cells to progress to macrometastatic colonies. Conversely, whole population and ALDH^{hi}CD44⁺CD24⁻ stem-like MDA-MB-231 cells have produced a much higher metastatic burden within the lung (>15%) and consistently produce macrometastases [52, 67]. Therefore, it's not surprising the MDA-MB-468 cell line produced the smallest degree of growth within the PuMA relative to the more aggressive SUM149 and MDA-MB-231 cell lines. Results of this study therefore validate this model as an effective surrogate for studying *in vivo* breast cancer metastasis. The PuMA provides an advantage over both *in vitro* and *in vivo* techniques for studying metastasis. Cells often behave quite differently when cultured on plastic compared to a native environment. For example, in one particular study, lung cancer cells grown in 2D tissue culture expressed significantly lower levels of MMP-1, 9, 10 and no expression of MMP-9 compared to the same cells grown in a native 3D lung matrix maintained in a bioreactor [111]. Therefore, the PuMA provides a more biologically relevant way for studying the behaviour of breast cancer within a secondary environment, something not always feasible with *in vitro* studies. Furthermore, the PuMA allows for the possibility of real-time assessment of metastatic progression at multiple time points using a single mouse lung. To accomplish this *in vivo* would require a vast number of mice as well as investigator time. In addition, studying metastatic progression from the single cell level is rarely achievable *in vivo* due to resolution limitations with current imaging techniques. Therefore, in this regard, the *ex vivo* PuMA provides a more efficient and cost effective strategy for evaluating metastatic progression in a native environment and allows for studying the behaviour of breast cancer from a single cell stage once cells have immediately reached the lung.

6.3. ALDH^{hi}CD44⁺ Breast Cancer Cells Drive Metastatic Progression Within the Lung Microenvironment

Evidence within the literature suggests that only a small subset of cells are able to successfully navigate the metastatic cascade to eventually initiate and form

secondary metastases. It has therefore been postulated that cancer stem cells (CSC) or stem-like cancer cells represent the subset of tumour cells responsible for metastatic disease [61, 112]. In breast cancer, the population of CSCs are traditionally isolated based on both surface markers (CD44⁺CD24⁻) and functional activity (ALDH^{hi}). The utilization of both functional activity in addition to surface markers increases the validity of isolation due to the inherent heterogeneity of tumour cell surface marker expression as a result of genetic instability [67, 113-115]. In this study, we isolated stem-like breast cancer cell populations using a two marker strategy. Therefore, we isolated stem-like cells using ALDH as a primary sort criteria and CD44 expression as secondary sort criteria. Previous studies have shown similar functional metastatic capabilities between cells isolated using an ALDH^{hi}CD44⁺ approach versus cells isolated using ALDH^{hi}CD44⁺CD24⁻ [65, 67], and we therefore did not include CD24 in our cell sorting criteria. Therefore, we are confident that the cells isolated from both cell lines used in this study represent the most aggressive and metastatic population.

Our specific interests relate to understanding the contribution of ALDH^{hi}CD44⁺ breast cancer cells during the process of metastasis, and how the lung microenvironment ultimately interacts with these cells to promote metastases formation once these cells immediately reach the lung. Although there is a wealth of knowledge concerning the existence of stem-like cancer cells in primary tumours, much less is known regarding the functional and mechanistic implications of these cells in mediating metastasis. Using the PuMA, we have evaluated the growth and progression patterns for both stem-like and non stem-like breast cancer cells within the native lung microenvironment. We have observed that breast cancer cell populations isolated based on an ALDH^{hi}CD44⁺ phenotype demonstrate increased growth over the course of 21 days compared to ALDH^{lo}CD44⁻ cells. Moreover, stem-like ALDH^{hi}CD44⁺ progressed within the PuMA from single cells once delivered to the lungs, to micrometastases (SUM149, MDA-MB-231) to macrometastases (MDA-MB-231), whereas the majority of non stem-like cells in both cell lines remained

predominantly as single cells, showing very little progression to the micrometastases stage, if any. Together these results indicate that breast cancer cells, specifically the stem-like ALDH^{hi}CD44⁺ population, are responsible for metastatic progression within the lung. Differences in growth are not a result of a discrepancy in cellular delivery, since a similar number of both ALDH^{hi}CD44⁺ and ALDH^{lo}CD44⁻ cells are able to reach the lungs initially at day 0. Therefore, it is specifically the stem-like population that is able to interact with the native lung microarchitecture to successfully establish secondary tumour populations, whereas the majority of non stem-like cells remain as single cells and fail to progress past the micrometastases stage. Importantly, the PuMA assay has allowed us to dissect out the role of the lung microenvironment in mediating the 2 most significant rate-limiting steps in metastasis (and those we hypothesize to be facilitated by stem-like cells): the transition from single cells to micrometastases, and from micrometastases to macrometastases [116, 117]. This is very difficult to do in real-time using *in vivo* models, since most imaging technologies do not have this degree of sensitivity, particularly in the lung.

6.4. The Complexity of the Lung Microenvironment

The microenvironment of organs is comprised of normal parenchymal cells, stromal cells and insoluble elements including the ECM and ECM-related factors as well as soluble factors [118]. We are beginning to appreciate how certain organ microenvironments can influence the biology of tumour growth and survival, a concept that's relatively new in the field of metastasis. As stated by Fidler in a review of the organ microenvironment and metastasis, the extent of tumour cell proliferation, invasion, angiogenesis and survival are in part determined by the specific organ microenvironment [48].

The lung microenvironment is no exception to this complexity. The lung is composed of a dense vascular network, surrounded by over 60 different cellular types including cells with sensory, secretory, mechanical and transport functions [119], each with distinct expression patterns for soluble factors. Moreover, the insoluble ECM and ECM-related components of the lung function as a scaffold for these cells. Therefore, there are many potential sources in the lung microenvironment that may

contribute to the metastatic behaviour of breast cancer cells once they reach the lung. Together, these factors probably do not influence the behaviour of breast cancer exclusively but rather, many of these components likely act together to drive the process of breast cancer metastasis within the lung. Previous work done in our lab has focused primarily on the soluble component of the lung microenvironment and thus was used as a potential target in this study.

Work done by Jenny Chu has identified over 70 soluble factors within the lung microenvironment that may be contributing to the growth and metastatic behaviour of breast cancer once they reach the lung [52]. This work predominantly concentrated on the soluble lung microenvironment and its role as a chemoattractant for breast cancer cells. Her work demonstrated that soluble factors within lung-CM including the CD44 ligands osteopontin (OPN) and L-selectin (SELP) mediated breast cancer cell migration *in vitro* [52]. Although her work led to a greater understanding of the contribution of the soluble lung microenvironment to the “getting there” stage of breast cancer metastasis, much less has been explored in terms of the “growing there” portion of breast cancer metastatic progression. One of the proteins previously identified within lung-CM and of particular interest to us was bFGF.

6.5. bFGF in the Lung Microenvironment

We were especially interested in the role of soluble bFGF and its influence on breast cancer cell metastatic behaviour and progression within the lung, particularly in the context of the *ex vivo* PuMA. bFGF is well known for its potent mitogenic effects, with many of its pro-proliferative activity linked to promoting growth and proliferation in primary precursor cells [120]. Coupled with the fact that this particular protein is involved in the maintenance of self-renewal in stem cells and often found in media for culturing stem cells [121], we sought to determine its influence on breast cancer cell behaviour both *in vitro* and in the PuMA. Therefore, bFGF represented an appropriate target worth exploring within the lung microenvironment especially since murine and human bFGF share a 97% amino acid sequence identity (UniProtKB/Swiss-Prot-P09038).

Using our previously described *ex vivo* murine model system for generating organ conditioned media [52], we were able to show that bFGF present in mouse

lung-CM increased the proliferation of both SUM149 and MDA-MB-231 whole cell populations as assessed by BrdU incorporation. Moreover, this increase in proliferative behaviour was abrogated following the immunodepletion of bFGF from lung-CM and could be rescued by re-introducing recombinant bFGF to immunodepleted media. Interestingly, we observed a lack of migratory responses towards bFGF using Transwell migration assays which indicated that this protein was more important for promoting proliferation versus migration of breast cancer cells. Taken together, these results suggest that bFGF may play more of a role in the “growing there” versus “getting there” stage of breast cancer metastasis. Although bFGF has previously been characterized as a chemoattractant, most of these studies have been in the context of evaluating the process of angiogenesis, using endothelial cell lines, not breast cancer cells [122].

Following *in vitro* experiments suggesting the role of bFGF in promoting proliferation of breast cancer cells, we aimed to target this protein in the PuMA to determine if we could interfere with breast cancer cell growth and progression. We chose to evaluate the response of highly metastatic MDA-MB-231 whole population cells due to their prominent growth observed in the PuMA compared to the other cell lines (MDA-MB-468 and SUM149). We first demonstrated the presence of bFGF in the intact lung used within the PuMA. Immunohistochemical staining for bFGF revealed a diffuse pattern of staining throughout the lung, with a high degree of positive staining surrounding vasculature. This pattern of staining was expected as bFGF is normally expressed ubiquitously and present in high amounts in the basement membranes and ECM of blood vessels [123]. We were also able to show that bFGF was present within the Gelfoam® that lung sections were grown on during the PuMA. Over the course of 21 days, there was an increase in the amount of bFGF detected at later time points, compared to earlier ones. This increase coincided with the length of time that lung sections spent on the Gelfoam® throughout the assay. Despite the changing of media every other day, an increase in concentration was still observed suggesting that bFGF was continuously secreted by the sections of lung grown on Gelfoam® and that secreted bFGF remained bound or stuck within the network of the Gelfoam®.

To determine the effect of bFGF in the *ex vivo* PuMA, we utilized antibody-mediated blocking of both mouse bFGF produced in the lung and CD44, a non-canonical bFGF receptor present on breast cancer cells. Although no significant reduction in breast cancer growth in the lung was observed, data indicated a general trend towards a reduction in growth of MDA-MB-231 cells. Due to the difficulty of blocking these proteins continuously over the course of 21 days, the negative results may be due to technical challenges rather than a lack of biological response. First, lung sections, although thin (~1 mm), still represent a significant area for penetration of antibody during the assay. Therefore, simply adding fresh antibody throughout the assay would not increase the exposure between antibody and tumour cells. Therefore, we opted to instead perfuse the lung with a mouse-specific neutralizing bFGF antibody prior to the removal of lungs from mice and pre-incubated cells with an anti-CD44 antibody prior to tail-vein injection. For bFGF blocking in the PuMA, we chose to use a concentration of antibody equal to the amount needed to successfully deplete lung-CM. Therefore, another potential source of negative response may be due to an ineffective concentration of neutralizing bFGF antibody initially used when perfusing the lung, or a diminishing biochemical activity of bFGF antibody throughout the assay. Unfortunately, there is very little data within the literature to suggest an appropriate starting point for antibody-mediated blocking using the PuMA since this is a relatively new model. Work that has been done regarding targeting within the PuMA is primarily focused on testing chemotherapeutics and not antibodies [93]. For CD44 blocking, cells were pre-incubated with an anti-CD44 antibody prior to injection. Therefore, a negative reduction in growth associated with blocked CD44 may indicate the antibody does not remain bound during the initial seeding to the lung or a diminishing biological activity throughout the assay. Another possible explanation is that breast cancer cells are able to compensate for decreased CD44 receptor activity in relation to bFGF by using its canonical receptor (FGFR1), normally expressed by MDA-MB-231 cells [85] or other receptors involved with fine-tuning bFGF signalling (integrin $\alpha v \beta 3$, heparin, thrombospondin, fibrinogen, PDGF) [83]. Ultimately, more work needs to be done with regards to optimization of antibody-mediated blocking techniques within the PuMA before we can confidently

rule out bFGF as a potential target within the native lung microenvironment that could reduce the metastatic behaviour of breast cancer cells.

7. POSSIBLE LIMITATIONS OF THE STUDY

Findings and subsequent conclusions made in this study are based upon certain assumptions, particularly concerning features of the presented *ex vivo* models. The PuMA represents an innovative model system for assessing growth and progression of cancer cells in real time within a native lung environment. While this model illustrates a promising approach for studying breast cancer metastasis in a secondary environment, like most models, it is not without its limitations.

The first assumption is that breast cancer cell growth and progression in the PuMA is not influenced by the immune system. This study utilized athymic Nude-*Foxn1^{nu}* mice which have an inhibited immune capacity due to a reduced number of mature T-cells. Because of this, they are unable to mount adaptive immune responses and are therefore ideal for studying the growth of solid tumours derived from humans [124]. Nude mice were also chosen to compare current and future results with previous *in vivo* findings using this mouse strain. In addition, in context of the PuMA, due to the excision of the lungs from nude mice and subsequent slicing of the lung, there is no active immune system regardless. While in theory, the advantage of the PuMA is that it accurately represents the pulmonary architecture that breast cancer cells would encounter physiologically, it still does not take into account the contribution and possible interaction of the immune system during immunosurveillance of tumour cells.

The second assumption is that murine secreted factors and insoluble matrix components interact with human cancer cells both in the PuMA and lung-CM. Traditionally, murine models are utilized because they are small, easy to handle and have consistent disease manifestations. More importantly, mice have over a 95% similarity to human genetics, with many genes showing high degrees of conservation between the two species. Despite the significant evolutionary genetic conservation

between mice and humans, certain ligand-receptor interactions may remain incompatible between the two species. However, many secreted murine factors are still able to stimulate cellular responses in human cells [125]. Ethically speaking, the collection of human lungs in lieu of murine lungs presents a challenge and is not feasible, thus the murine model system was both practical and essential.

The third assumption in terms of the *ex vivo* lung-CM model system is that lung-derived soluble factors are adequate for inducing changes in cellular behaviour, particularly migration and proliferation. In reality, the metastatic niche is composed of insoluble factors, ECM components and various cell types in addition to soluble factors. All of these factors can potentially contribute to tumour cell behaviour. Although, changes in cellular proliferation were seen in this study, results would have been strengthened with the addition of the ECM or ECM-related components to the assay outlined above.

Finally, as with most basic science cancer research, these studies relied on immortalized human cell lines rather than primary human breast cancer cells. While immortalized cells used in this study originated from primary patient samples, they have undergone significant mutations to become immortal. In addition, there still represents the potential for these cell lines to acquire additional mutations due to failures in DNA repair. Although immortalized cell lines are easy to obtain and maintain in culture, they still may not accurately represent the true behaviour present with primary patient-derived breast cancer cells.

8. FUTURE DIRECTIONS

As mentioned previously, the occurrence of lung metastases in breast cancer patients is often associated with high rates of mortality. This highlights the importance of understanding the contribution of the lung microenvironment as a whole in mediating lung related metastatic spread. Therefore, elucidating specific factors or signals involved in promoting lung specific tropism in breast cancer should remain a strong focus.

The molecular basis for organ-specific metastasis has started to gain significant attention amongst the scientific community, especially as we continue to discover the disparity between the behaviour of primary tumour cells and those in the metastatic setting. Traditionally, metastasis-related research tends to focus more on the end point, e.g. after a clinically detectable tumour has developed. This approach often overlooks the importance of the initial steps of tumour establishment and subsequent metastatic progression. One of the main advantages of the PuMA is that it shifts the focus from the end point of metastatic development by also incorporating the initial stages of metastatic progression. Therefore, future work should centre around determining aspects of the lung microenvironment responsible for promoting successful micrometastases development. This study in particular focuses on one soluble factor specifically, bFGF. Methods in addition to antibody-mediated targeting of bFGF, such as small molecule inhibitors should be utilized to determine the full extent of bFGF influence on breast cancer cell behaviour. For example, the chemical SSR128129E has been shown to effectively inhibit bFGF signalling by binding to the extracellular domain of FGFR receptors [126-128]. Additionally, selective FGFR1/3 small molecule inhibitors including PD173074 [129-131], and FGFR1 inhibitors including PD161570 [132, 133] also exist and provide another possible route of inhibition. These small molecule inhibitors have been used both *in vitro* and *in vivo* and show promise for decreasing the growth of certain cancers. However, these

molecular inhibitors have not been used in the context of either breast cancer or breast cancer metastasis, and thus provide encouraging methods for inhibiting bFGF within the PuMA. To further complement blocking of bFGF within the PuMA, future work in assessing bFGF could be better suited using a systemic bFGF knockout mouse model. The *Fgf2^{tm3Doe}/Fgf2^{tm3Doe}* mouse model provides a unique approach for evaluating the behaviour of breast cancer cells in an environment devoid of bFGF. These mice develop and age normally with a normal lifespan and exhibit regular organ architecture [134]. Therefore, these mice could be used in the context of the PuMA outlined above using syngeneic mouse breast cancer cell lines. Comparisons to mice with normal bFGF expression or to bFGF knockout mice with re-introduced bFGF (added to the infused agarose/media 1 solution) could be used to fully gauge the effect of bFGF on breast cancer cell behaviour in the lung.

However, many other soluble factors in addition to bFGF may be contributing to the metastatic behaviour of breast cancer within the lung. Therefore, the PuMA can be used as a high throughput screening tool in the future for inhibiting other soluble factors in the lung microenvironment that may have a contribution to the metastatic progression of breast cancer. The PuMA not only represents an innovative method for targeting specific soluble factors within the lung but also provides an avenue for screening potential therapeutics. One disadvantage of traditional *in vivo* screening of therapeutics is the sheer number of animals needed and the associated cost. With the PuMA, many sections of lung from the same mouse/animal can be used as a much cheaper high throughput technique for determining proper drug concentrations and dosing regimes with many different therapeutics at once. This also has an added advantage over traditional cell culture based screening as cells often behave differently within a native 3D environment opposed to on 2D tissue culture plastic. Therefore, the PuMA provides not only a unique *ex vivo* method for studying the behaviour of cancer cells in a native environment but also brings the ability to screen many different targeted and non-targeted therapeutics in a biologically relevant setting.

Finally, another advantage of the PuMA is that it provides an appropriate native 3D architecture onto which breast cancer cells interact. Since the PuMA is able

to maintain lung viability throughout the duration of the assay, the architecture on which breast cancer cells interact include both the soluble and the insoluble lung microenvironment. Although this study focuses on specific soluble factors present within the lung microenvironment that may be contributing to breast cancer cell growth and behaviour, we cannot discount the importance of the insoluble component, including the ECM. In fact, it has been shown that the ECM is a crucial component of the metastatic niche and plays an important role in mediating the metastatic progression of cancer [135]. A future goal of ours in collaboration with Dr. Lauren Flynn (Western University) is the development of a decellularization protocol to effectively eliminate the cellular presence within the lung, leaving only the insoluble ECM scaffold. We are particularly interested in the growth patterns of both whole population and stem-like ALDH^{hi}CD44⁺ breast cancer cells in the native lung versus a decellularized lung containing only a 3D matrix scaffold. In order to pursue this, we are looking at assessing breast cancer behaviour in a modified version of the PuMA. Traditionally in the PuMA, cells are seeded to the lung via the vasculature (tail-vein injection). However, in the context of comparing between native lung and a decellularized lung, there is no functional vasculature to utilize in seeding the lung. Therefore, cells should instead be seeded to the lung in both the native and decellularized lung by means of the trachea. Although this does not accurately recapitulate what occurs physiologically, it represents a more consistent way to compare between lung conditions. The seeding of decellularized lungs with lung cancer cells via the trachea has been accomplished successfully by other groups and we are confident this approach will provide an accurate avenue for comparing growth patterns between lung conditions [89]. This work is currently underway.

9. FINAL CONCLUSIONS

Since the majority of deaths associated with breast cancer can be attributed to metastasis, and more specifically to breast cancer that has spread to the lung, we sought to determine the influence of the native lung microenvironment on the behaviour of breast cancer cells. There are often many limitations associated with studying the progression of metastasis *in vitro*. This thesis made use of an innovative *ex vivo* pulmonary metastasis (PuMA) model to test the hypothesis that stem-like ALDH^{hi}CD44⁺ breast cancer cells demonstrate increased growth and progression from a single cell stage within the native lung in relation to their non stem-like ALDH^{lo}CD44⁻ counterparts. Although the PuMA has been used to study the behavioural differences between weakly and highly metastatic osteosarcoma cells within the lung, to our knowledge, we are the first group to utilize this unique *ex vivo* assay to model breast cancer metastasis within the lung, with a specific interest in the progression differences between stem-like and non stem-like cells. This study not only answers questions that we initially posed, but has provoked many additional questions for the future. Therefore, this study represents a novel stepping stone for the development of future research questions and studies.

Overall, this study supports evidence from both our lab and the literature suggesting that small subset of tumour cells, which bear similar characteristics to normal stem-cells, are ultimately responsible for the growth and progression of secondary tumours after they have spread beyond the initial site of origin. We have taken a unique approach in that we have tracked the progression of stem-like breast cancer cell growth from the single cell stage in real time once they've immediately reached the lung to study the initial steps of metastatic progression. This lung-specific model for breast cancer metastasis has the potential to uncover key processes during

the initial stages of lung metastasis and offers a valuable tool for future research geared towards exploring and targeting certain aspects of the lung microenvironment, including both the soluble and insoluble components to limit the extent of lung-related spread in breast cancer patients.

BIBLIOGRAPHY

1. Ferlay J, Shin HR, Bray F, Forman D, Mathers C, Parkin DM: Estimates of worldwide burden of cancer in 2008: GLOBOCAN 2008. *International journal of cancer Journal international du cancer* 2010, 127(12):2893-2917.
2. Jemal A, Bray F, Center MM, Ferlay J, Ward E, Forman D: Global cancer statistics. *CA: a cancer journal for clinicians* 2011, 61(2):69-90.
3. Statistics CCSsACoC: Canadian Cancer Statistics 2013. In. Edited by Society CC; 2013.
4. Siegel R, Ma J, Zou Z, Jemal A: Cancer statistics, 2014. *CA: a cancer journal for clinicians* 2014, 64(1):9-29.
5. Berry DA, Cronin KA, Plevritis SK, Fryback DG, Clarke L, Zelen M, Mandelblatt JS, Yakovlev AY, Habbema JD, Feuer EJ, Cancer I, Surveillance Modeling Network C: Effect of screening and adjuvant therapy on mortality from breast cancer. *The New England journal of medicine* 2005, 353(17):1784-1792.
6. DeSantis CE, Lin CC, Mariotto AB, Siegel RL, Stein KD, Kramer JL, Alteri R, Robbins AS, Jemal A: Cancer treatment and survivorship statistics, 2014. *CA: a cancer journal for clinicians* 2014, 64(4):252-271.
7. Hayat MJ, Howlader N, Reichman ME, Edwards BK: Cancer statistics, trends, and multiple primary cancer analyses from the Surveillance, Epidemiology, and End Results (SEER) Program. *Oncologist* 2007, 12(1):20-37.
8. Minn AJ, Kang Y, Serganova I, Gupta GP, Giri DD, Doubrovin M, Ponomarev V, Gerald WL, Blasberg R, Massague J: Distinct organ-specific metastatic potential of individual breast cancer cells and primary tumors. *The Journal of clinical investigation* 2005, 115(1):44-55.
9. Scully OJ, Bay BH, Yip G, Yu Y: Breast cancer metastasis. *Cancer Genomics Proteomics* 2012, 9(5):311-320.
10. Hanahan D, Weinberg RA: The hallmarks of cancer. *Cell* 2000, 100(1):57-70.
11. Hanahan D, Weinberg RA: Hallmarks of cancer: the next generation. *Cell* 2011, 144(5):646-674.
12. Croce CM: Oncogenes and cancer. *The New England journal of medicine* 2008, 358(5):502-511.
13. Sherr CJ: Principles of tumor suppression. *Cell* 2004, 116(2):235-246.

14. Knudson AG: Two genetic hits (more or less) to cancer. *Nature reviews Cancer* 2001, 1(2):157-162.
15. Baylin SB, Ohm JE: Epigenetic gene silencing in cancer - a mechanism for early oncogenic pathway addiction? *Nature reviews Cancer* 2006, 6(2): 107-116.
16. Golub TR, Slonim DK, Tamayo P, Huard C, Gaasenbeek M, Mesirov JP, Coller H, Loh ML, Downing JR, Caligiuri MA, Bloomfield CD, Lander ES: Molecular classification of cancer: class discovery and class prediction by gene expression monitoring. *Science* 1999, 286(5439):531-537.
17. Kalirai H, Clarke RB: Human breast epithelial stem cells and their regulation. *J Pathol* 2006, 208(1):7-16.
18. Watson CJ, Khaled WT: Mammary development in the embryo and adult: a journey of morphogenesis and commitment. *Development* 2008, 135(6): 995-1003.
19. Fata JE, Werb Z, Bissell MJ: Regulation of mammary gland branching morphogenesis by the extracellular matrix and its remodeling enzymes. *Breast cancer research : BCR* 2004, 6(1):1-11.
20. Sternlicht MD: Key stages in mammary gland development: the cues that regulate ductal branching morphogenesis. *Breast cancer research : BCR* 2006, 8(1):201.
21. Sariego J: Breast cancer in the young patient. *The American surgeon* 2010, 76(12):1397-1400.
22. Li CI, Uribe DJ, Daling JR: Clinical characteristics of different histologic types of breast cancer. *Br J Cancer* 2005, 93(9):1046-1052.
23. Stopeck ATC, P.; Thompson, P.A.: *Breast Cancer Pathophysiology*. In.: Medscape; 2015.
24. Sakorafas GH, Tsiotou AG: Ductal carcinoma in situ (DCIS) of the breast: evolving perspectives. *Cancer Treat Rev* 2000, 26(2):103-125.
25. Takahashi K, Saito M, Makita M, Tada T, Uchida Y, Yoshimoto M, Kasumi F, Akiyama F, Sakamoto G: Surgery for ductal carcinoma in situ. *Breast Cancer* 2000, 7(4):337-340.
26. Simpson PT, Gale T, Fulford LG, Reis-Filho JS, Lakhani SR: The diagnosis and management of pre-invasive breast disease: pathology of atypical lobular hyperplasia and lobular carcinoma in situ. *Breast cancer research : BCR* 2003, 5(5):258-262.

27. Bleiweiss IJ, Raptis G: Look again: the importance of second opinions in breast pathology. *Journal of clinical oncology : official journal of the American Society of Clinical Oncology* 2012, 30(18):2175-2176.
28. Chambers AF, Groom AC, MacDonald IC: Dissemination and growth of cancer cells in metastatic sites. *Nature reviews Cancer* 2002, 2(8):563-572.
29. Kennecke H, Yerushalmi R, Woods R, Cheang MC, Voduc D, Speers CH, Nielsen TO, Gelmon K: Metastatic behavior of breast cancer subtypes. *Journal of clinical oncology : official journal of the American Society of Clinical Oncology* 2010, 28(20):3271-3277.
30. Voduc KD, Cheang MC, Tyldesley S, Gelmon K, Nielsen TO, Kennecke H: Breast cancer subtypes and the risk of local and regional relapse. *Journal of clinical oncology : official journal of the American Society of Clinical Oncology* 2010, 28(10):1684-1691.
31. Cancer Genome Atlas N: Comprehensive molecular portraits of human breast tumours. *Nature* 2012, 490(7418):61-70.
32. Carey LA, Perou CM, Livasy CA, Dressler LG, Cowan D, Conway K, Karaca G, Troester MA, Tse CK, Edmiston S, Deming SL, Geradts J, Cheang MC, Nielsen TO, Moorman PG, Earp HS, Millikan RC: Race, breast cancer subtypes, and survival in the Carolina Breast Cancer Study. *JAMA* 2006, 295(21):2492-2502.
33. O'Brien KM, Cole SR, Tse CK, Perou CM, Carey LA, Foulkes WD, Dressler LG, Geradts J, Millikan RC: Intrinsic breast tumor subtypes, race, and long-term survival in the Carolina Breast Cancer Study. *Clinical cancer research : an official journal of the American Association for Cancer Research* 2010, 16(24):6100-6110.
34. Arvold ND, Taghian AG, Niemierko A, Abi Raad RF, Sreedhara M, Nguyen PL, Bellon JR, Wong JS, Smith BL, Harris JR: Age, breast cancer subtype approximation, and local recurrence after breast-conserving therapy. *Journal of clinical oncology : official journal of the American Society of Clinical Oncology* 2011, 29(29):3885-3891.
35. Metzger-Filho O, Sun Z, Viale G, Price KN, Crivellari D, Snyder RD, Gelber RD, Castiglione-Gertsch M, Coates AS, Goldhirsch A, Cardoso F: Patterns of Recurrence and outcome according to breast cancer subtypes in lymph node-negative disease: results from international breast cancer study group trials VIII and IX. *Journal of clinical oncology : official journal of the American Society of Clinical Oncology* 2013, 31(25):3083-3090.
36. Lund MJ, Butler EN, Hair BY, Ward KC, Andrews JH, Oprea-Ilie G, Bayakly AR, O'Regan RM, Vertino PM, Eley JW: Age/race differences in HER2

testing and in incidence rates for breast cancer triple subtypes: a population-based study and first report. *Cancer* 2010, 116(11):2549-2559.

37. Yang XR, Chang-Claude J, Goode EL, Couch FJ, Nevanlinna H, Milne RL, Gaudet M, Schmidt MK, Broeks A, Cox A, Fasching PA, Hein R, Spurdle AB, Blows F, Driver K, Flesch-Janys D, Heinz J, Sinn P, Vrieling A, Heikkinen T, Aittomaki K, Heikkila P, Blomqvist C, Lissowska J, Peplonska B, Chanock S, Figueroa J, Brinton L, Hall P, Czene K, Humphreys K, Darabi H, Liu J, Van 't Veer LJ, van Leeuwen FE, Andrulis IL, Glendon G, Knight JA, Mulligan AM, O'Malley FP, Weerasooriya N, John EM, Beckmann MW, Hartmann A, Weibrecht SB, Wachter DL, Jud SM, Loehberg CR, Baglietto L, English DR, Giles GG, McLean CA, Severi G, Lambrechts D, Vandrope T, Weltens C, Paridaens R, Smeets A, Neven P, Wildiers H, Wang X, Olson JE, Cafourek V, Fredericksen Z, Kosel M, Vachon C, Cramp HE, Connley D, Cross SS, Balasubramanian SP, Reed MW, Dork T, Bremer M, Meyer A, Karstens JH, Ay A, Park-Simon TW, Hillemanns P, Arias Perez JI, Menendez Rodriguez P, Zamora P, Benitez J, Ko YD, Fischer HP, Hamann U, Pesch B, Bruning T, Justenhoven C, Brauch H, Eccles DM, Tapper WJ, Gerty SM, Sawyer EJ, Tomlinson IP, Jones A, Kerin M, Miller N, McInerney N, Anton-Culver H, Ziogas A, Shen CY, Hsiung CN, Wu PE, Yang SL, Yu JC, Chen ST, Hsu GC, Haiman CA, Henderson BE, Le Marchand L, Kolonel LN, Lindblom A, Margolin S, Jakubowska A, Lubinski J, Huzarski T, Byrski T, Gorski B, Gronwald J, Hooning MJ, Hollestelle A, van den Ouweland AM, Jager A, Kriege M, Tilanus-Linthorst MM, Collee M, Wang-Gohrke S, Pylkas K, Jukkola-Vuorinen A, Mononen K, Grip M, Hirvikoski P, Winqvist R, Mannermaa A, Kosma VM, Kauppinen J, Kataja V, Auvinen P, Soini Y, Sironen R, Bojesen SE, Orsted DD, Kaur-Knudsen D, Flyger H, Nordestgaard BG, Holland H, Chenevix-Trench G, Manoukian S, Barile M, Radice P, Hankinson SE, Hunter DJ, Tamimi R, Sangrajrang S, Brennan P, McKay J, Odefrey F, Gaborieau V, Devilee P, Huijts PE, Tollenaar RA, Seynaeve C, Dite GS, Apicella C, Hopper JL, Hammet F, Tsimiklis H, Smith LD, Southey MC, Humphreys MK, Easton D, Pharoah P, Sherman ME, Garcia-Closas M: Associations of breast cancer risk factors with tumor subtypes: a pooled analysis from the Breast Cancer Association Consortium studies. *Journal of the National Cancer Institute* 2011, 103(3):250-263.
38. Kim MJ, Ro JY, Ahn SH, Kim HH, Kim SB, Gong G: Clinicopathologic significance of the basal-like subtype of breast cancer: a comparison with hormone receptor and Her2/neu-overexpressing phenotypes. *Hum Pathol* 2006, 37(9):1217-1226.
39. Potemski P, Kusinska R, Watala C, Pluciennik E, Bednarek AK, Kordek R: Prognostic relevance of basal cytokeratin expression in operable breast cancer. *Oncology* 2005, 69(6):478-485.

40. Millar EK, Graham PH, O'Toole SA, McNeil CM, Browne L, Morey AL, Eggleton S, Beretov J, Theocharous C, Capp A, Nasser E, Kearsley JH, Delaney G, Papadatos G, Fox C, Sutherland RL: Prediction of local recurrence, distant metastases, and death after breast-conserving therapy in early-stage invasive breast cancer using a five-biomarker panel. *Journal of clinical oncology : official journal of the American Society of Clinical Oncology* 2009, 27(28):4701-4708.
41. Parker JS, Mullins M, Cheang MC, Leung S, Voduc D, Vickery T, Davies S, Fauron C, He X, Hu Z, Quackenbush JF, Stijleman IJ, Palazzo J, Marron JS, Nobel AB, Mardis E, Nielsen TO, Ellis MJ, Perou CM, Bernard PS: Supervised risk predictor of breast cancer based on intrinsic subtypes. *Journal of clinical oncology : official journal of the American Society of Clinical Oncology* 2009, 27(8):1160-1167.
42. Liotta LA, Steeg PS, Stetler-Stevenson WG: Cancer metastasis and angiogenesis: an imbalance of positive and negative regulation. *Cell* 1991, 64(2):327-336.
43. Wyckoff JB, Jones JG, Condeelis JS, Segall JE: A critical step in metastasis: in vivo analysis of intravasation at the primary tumor. *Cancer research* 2000, 60(9):2504-2511.
44. Chambers AF, Naumov GN, Varghese HJ, Nadkarni KV, MacDonald IC, Groom AC: Critical steps in hematogenous metastasis: an overview. *Surg Oncol Clin N Am* 2001, 10(2):243-255, vii.
45. Chiang AC, Massague J: Molecular basis of metastasis. *The New England journal of medicine* 2008, 359(26):2814-2823.
46. Klein CA: Cancer. The metastasis cascade. *Science* 2008, 321(5897):1785-1787.
47. Wong CW, Lee A, Shientag L, Yu J, Dong Y, Kao G, Al-Mehdi AB, Bernhard EJ, Muschel RJ: Apoptosis: an early event in metastatic inefficiency. *Cancer research* 2001, 61(1):333-338.
48. Fidler IJ: The organ microenvironment and cancer metastasis. *Differentiation; research in biological diversity* 2002, 70(9-10):498-505.
49. Nguyen DX, Bos PD, Massague J: Metastasis: from dissemination to organ-specific colonization. *Nature reviews Cancer* 2009, 9(4):274-284.
50. Chu JE, Allan AL: The Role of Cancer Stem Cells in the Organ Tropism of Breast Cancer Metastasis: A Mechanistic Balance between the "Seed" and the "Soil"? *International journal of breast cancer* 2012, 2012:209748.

51. Paget S: The distribution of secondary growths in cancer of the breast. 1889. *Cancer metastasis reviews* 1989, 8(2):98-101.
52. Chu JE, Xia Y, Chin-Yee B, Goodale D, Croker AK, Allan AL: Lung-derived factors mediate breast cancer cell migration through CD44 receptor-ligand interactions in a novel ex vivo system for analysis of organ-specific soluble proteins. *Neoplasia* 2014, 16(2):180-191.
53. Piaseczny MM, Allan AL: Why does breast cancer often spread to the lung? *Women's health* 2014, 10(6):561-564.
54. Yokota J: Tumor progression and metastasis. *Carcinogenesis* 2000, 21(3):497-503.
55. Fidler IJ: The pathogenesis of cancer metastasis: the 'seed and soil' hypothesis revisited. *Nature reviews Cancer* 2003, 3(6):453-458.
56. Minn AJ, Gupta GP, Siegel PM, Bos PD, Shu W, Giri DD, Viale A, Olshen AB, Gerald WL, Massague J: Genes that mediate breast cancer metastasis to lung. *Nature* 2005, 436(7050):518-524.
57. Fidler IJ: Modulation of the organ microenvironment for treatment of cancer metastasis. *Journal of the National Cancer Institute* 1995, 87(21):1588-1592.
58. Gupta GP, Minn AJ, Kang Y, Siegel PM, Serganova I, Cordon-Cardo C, Olshen AB, Gerald WL, Massague J: Identifying site-specific metastasis genes and functions. *Cold Spring Harb Symp Quant Biol* 2005, 70:149-158.
59. Wilmanns C, Fan D, O'Brian CA, Bucana CD, Fidler IJ: Orthotopic and ectopic organ environments differentially influence the sensitivity of murine colon carcinoma cells to doxorubicin and 5-fluorouracil. *International journal of cancer Journal international du cancer* 1992, 52(1):98-104.
60. Louie E, Nik S, Chen JS, Schmidt M, Song B, Pacson C, Chen XF, Park S, Ju J, Chen EI: Identification of a stem-like cell population by exposing metastatic breast cancer cell lines to repetitive cycles of hypoxia and reoxygenation. *Breast cancer research : BCR* 2010, 12(6):R94.
61. Visvader JE, Lindeman GJ: Cancer stem cells in solid tumours: accumulating evidence and unresolved questions. *Nature reviews Cancer* 2008, 8(10):755-768.
62. Reya T, Morrison SJ, Clarke MF, Weissman IL: Stem cells, cancer, and cancer stem cells. *Nature* 2001, 414(6859):105-111.
63. Dick JE: Stem cell concepts renew cancer research. *Blood* 2008, 112(13):4793-4807.

64. Sheridan C, Kishimoto H, Fuchs RK, Mehrotra S, Bhat-Nakshatri P, Turner CH, Goulet R, Jr., Badve S, Nakshatri H: CD44+/CD24- breast cancer cells exhibit enhanced invasive properties: an early step necessary for metastasis. *Breast cancer research : BCR* 2006, 8(5):R59.
65. Ginestier C, Hur MH, Charafe-Jauffret E, Monville F, Dutcher J, Brown M, Jacquemier J, Viens P, Kleer CG, Liu S, Schott A, Hayes D, Birnbaum D, Wicha MS, Dontu G: ALDH1 is a marker of normal and malignant human mammary stem cells and a predictor of poor clinical outcome. *Cell stem cell* 2007, 1(5):555-567.
66. Dontu G: Breast cancer stem cell markers - the rocky road to clinical applications. *Breast cancer research : BCR* 2008, 10(5):110.
67. Croker AK, Goodale D, Chu J, Postenka C, Hedley BD, Hess DA, Allan AL: High aldehyde dehydrogenase and expression of cancer stem cell markers selects for breast cancer cells with enhanced malignant and metastatic ability. *Journal of cellular and molecular medicine* 2009, 13(8B):2236-2252.
68. Spring FA, Dalchau R, Daniels GL, Mallinson G, Judson PA, Parsons SF, Fabre JW, Anstee DJ: The Ina and Inb blood group antigens are located on a glycoprotein of 80,000 MW (the CDw44 glycoprotein) whose expression is influenced by the In(Lu) gene. *Immunology* 1988, 64(1):37-43.
69. van den Hoogen C, van der Horst G, Cheung H, Buijs JT, Lippitt JM, Guzman-Ramirez N, Hamdy FC, Eaton CL, Thalmann GN, Cecchini MG, Pelger RC, van der Pluijm G: High aldehyde dehydrogenase activity identifies tumor-initiating and metastasis-initiating cells in human prostate cancer. *Cancer research* 2010, 70(12):5163-5173.
70. Croker AK, Allan AL: Inhibition of aldehyde dehydrogenase (ALDH) activity reduces chemotherapy and radiation resistance of stem-like ALDHhiCD44(+) human breast cancer cells. *Breast Cancer Res Treat* 2012, 133(1):75-87.
71. Marcato P, Dean CA, Giacomantonio CA, Lee PW: Aldehyde dehydrogenase: its role as a cancer stem cell marker comes down to the specific isoform. *Cell cycle* 2011, 10(9):1378-1384.
72. Charafe-Jauffret E, Ginestier C, Iovino F, Tarpin C, Diebel M, Esterni B, Houvenaeghel G, Extra JM, Bertucci F, Jacquemier J, Xerri L, Dontu G, Stassi G, Xiao Y, Barsky SH, Birnbaum D, Viens P, Wicha MS: Aldehyde dehydrogenase 1-positive cancer stem cells mediate metastasis and poor clinical outcome in inflammatory breast cancer. *Clinical cancer research : an official journal of the American Association for Cancer Research* 2010, 16(1):45-55.

73. Charafe-Jauffret E, Ginestier C, Bertucci F, Cabaud O, Wicinski J, Finetti P, Josselin E, Adelaide J, Nguyen TT, Monville F, Jacquemier J, Thomassin-Piana J, Pinna G, Jalaguier A, Lambaudie E, Houvenaeghel G, Xerri L, Harel-Bellan A, Chaffanet M, Viens P, Birnbaum D: ALDH1-positive cancer stem cells predict engraftment of primary breast tumors and are governed by a common stem cell program. *Cancer Res* 2013.
74. Talmadge JE, Wolman SR, Fidler IJ: Evidence for the clonal origin of spontaneous metastases. *Science* 1982, 217(4557):361-363.
75. Fidler IJ: Orthotopic implantation of human colon carcinomas into nude mice provides a valuable model for the biology and therapy of metastasis. *Cancer metastasis reviews* 1991, 10(3):229-243.
76. Teicher BA, Herman TS, Holden SA, Wang YY, Pfeffer MR, Crawford JW, Frei E, 3rd: Tumor resistance to alkylating agents conferred by mechanisms operative only in vivo. *Science* 1990, 247(4949 Pt 1):1457-1461.
77. Mohammadi M, Olsen SK, Ibrahimi OA: Structural basis for fibroblast growth factor receptor activation. *Cytokine Growth Factor Rev* 2005, 16(2):107-137.
78. Su N, Du X, Chen L: FGF signaling: its role in bone development and human skeleton diseases. *Front Biosci* 2008, 13:2842-2865.
79. Turner N, Grose R: Fibroblast growth factor signalling: from development to cancer. *Nature reviews Cancer* 2010, 10(2):116-129.
80. Delrieu I: The high molecular weight isoforms of basic fibroblast growth factor (FGF-2): an insight into an intracrine mechanism. *FEBS Lett* 2000, 468(1): 6-10.
81. Reuss B, von Bohlen und Halbach O: Fibroblast growth factors and their receptors in the central nervous system. *Cell Tissue Res* 2003, 313(2): 139-157.
82. Kardami E, Jiang ZS, Jimenez SK, Hirst CJ, Sheikh F, Zahradka P, Cattini PA: Fibroblast growth factor 2 isoforms and cardiac hypertrophy. *Cardiovasc Res* 2004, 63(3):458-466.
83. Presta M, Dell'Era P, Mitola S, Moroni E, Ronca R, Rusnati M: Fibroblast growth factor/fibroblast growth factor receptor system in angiogenesis. *Cytokine Growth Factor Rev* 2005, 16(2):159-178.
84. Basilico C, Moscatelli D: The FGF family of growth factors and oncogenes. *Adv Cancer Res* 1992, 59:115-165.
85. Penault-Llorca F, Bertucci F, Adelaide J, Parc P, Coulier F, Jacquemier J, Birnbaum D, deLapeyriere O: Expression of FGF and FGF receptor genes in

- human breast cancer. *International journal of cancer Journal international du cancer* 1995, 61(2):170-176.
86. Johnstone RW, Cretney E, Smyth MJ: P-glycoprotein protects leukemia cells against caspase-dependent, but not caspase-independent, cell death. *Blood* 1999, 93(3):1075-1085.
 87. Franks TJ, Colby TV, Travis WD, Tuder RM, Reynolds HY, Brody AR, Cardoso WV, Crystal RG, Drake CJ, Engelhardt J, Frid M, Herzog E, Mason R, Phan SH, Randell SH, Rose MC, Stevens T, Serge J, Sunday ME, Voynow JA, Weinstein BM, Whitsett J, Williams MC: Resident cellular components of the human lung: current knowledge and goals for research on cell phenotyping and function. *Proceedings of the American Thoracic Society* 2008, 5(7): 763-766.
 88. Rintoul RC, Sethi T: The role of extracellular matrix in small-cell lung cancer. *Lancet Oncol* 2001, 2(7):437-442.
 89. Price AP, England KA, Matson AM, Blazar BR, Panoskaltsis-Mortari A: Development of a decellularized lung bioreactor system for bioengineering the lung: the matrix reloaded. *Tissue engineering Part A* 2010, 16(8): 2581-2591.
 90. Mishra DK, Thrall MJ, Baird BN, Ott HC, Blackmon SH, Kurie JM, Kim MP: Human lung cancer cells grown on acellular rat lung matrix create perfusable tumor nodules. *The Annals of thoracic surgery* 2012, 93(4):1075-1081.
 91. Rintoul RC, Sethi T: Extracellular matrix regulation of drug resistance in small-cell lung cancer. *Clinical science* 2002, 102(4):417-424.
 92. Frisch SM, Francis H: Disruption of epithelial cell-matrix interactions induces apoptosis. *The Journal of cell biology* 1994, 124(4):619-626.
 93. Mendoza A, Hong SH, Osborne T, Khan MA, Campbell K, Briggs J, Eleswarapu A, Buquo L, Ren L, Hewitt SM, Dakir el H, Garfield S, Walker R, Merlino G, Green JE, Hunter KW, Wakefield LM, Khanna C: Modeling metastasis biology and therapy in real time in the mouse lung. *The Journal of clinical investigation* 2010, 120(8):2979-2988.
 94. Massoud TF, Gambhir SS: Molecular imaging in living subjects: seeing fundamental biological processes in a new light. *Genes & development* 2003, 17(5):545-580.
 95. Henriquez NV, van Overveld PG, Que I, Buijs JT, Bachelier R, Kaijzel EL, Lowik CW, Clezardin P, van der Pluijm G: Advances in optical imaging and novel model systems for cancer metastasis research. *Clin Exp Metastasis* 2007, 24(8):699-705.

96. Wetterwald A, van der Pluijm G, Que I, Sijmons B, Buijs J, Karperien M, Lowik CW, Gautschi E, Thalmann GN, Cecchini MG: Optical imaging of cancer metastasis to bone marrow: a mouse model of minimal residual disease. *Am J Pathol* 2002, 160(3):1143-1153.
97. Jenkins DE, Oei Y, Hornig YS, Yu SF, Dusich J, Purchio T, Contag PR: Bioluminescent imaging (BLI) to improve and refine traditional murine models of tumor growth and metastasis. *Clin Exp Metastasis* 2003, 20(8):733-744.
98. Jain RK, Munn LL, Fukumura D: Dissecting tumour pathophysiology using intravital microscopy. *Nature reviews Cancer* 2002, 2(4):266-276.
99. Kan Z, Liu TJ: Video microscopy of tumor metastasis: using the green fluorescent protein (GFP) gene as a cancer-cell-labeling system. *Clin Exp Metastasis* 1999, 17(1):49-55.
100. Al-Mehdi AB, Tozawa K, Fisher AB, Shientag L, Lee A, Muschel RJ: Intravascular origin of metastasis from the proliferation of endothelium-attached tumor cells: a new model for metastasis. *Nature medicine* 2000, 6(1):100-102.
101. Chambers AF, MacDonald IC, Schmidt EE, Koop S, Morris VL, Khokha R, Groom AC: Steps in tumor metastasis: new concepts from intravital videomicroscopy. *Cancer metastasis reviews* 1995, 14(4):279-301.
102. Siminski JT, Kavanagh TJ, Chi E, Raghu G: Long-term maintenance of mature pulmonary parenchyma cultured in serum-free conditions. *The American journal of physiology* 1992, 262(1 Pt 1):L105-110.
103. Klauber-DeMore N, Van Zee KJ, Linkov I, Borgen PI, Gerald WL: Biological behavior of human breast cancer micrometastases. *Clinical cancer research : an official journal of the American Association for Cancer Research* 2001, 7(8):2434-2439.
104. Rutledge H, Davis J, Chiu R, Cibull M, Brill Y, McGrath P, Samayoa L: Sentinel node micrometastasis in breast carcinoma may not be an indication for complete axillary dissection. *Mod Pathol* 2005, 18(6):762-768.
105. Grimme HU, Termeer CC, Bennett KL, Weiss JM, Schopf E, Aruffo A, Simon JC: Colocalization of basic fibroblast growth factor and CD44 isoforms containing the variably spliced exon v3 (CD44v3) in normal skin and in epidermal skin cancers. *Br J Dermatol* 1999, 141(5):824-832.
106. Howlader, N., et al.: SEER Cancer Statistics Review, 1975-2012, National Cancer Institute. Bethesda, MD, http://seer.cancer.gov/csr/1975_2012/, based

on November 2014 SEER data submission, posted to the SEER web site, April 2015.

107. Welch DR: Technical considerations for studying cancer metastasis in vivo. *Clin Exp Metastasis* 1997, 15(3):272-306.
108. Cailleau R, Olive M, Cruciger QV: Long-term human breast carcinoma cell lines of metastatic origin: preliminary characterization. *In Vitro* 1978, 14(11): 911-915.
109. Price JE, Polyzos A, Zhang RD, Daniels LM: Tumorigenicity and metastasis of human breast carcinoma cell lines in nude mice. *Cancer research* 1990, 50(3): 717-721.
110. Forozan F, Veldman R, Ammerman CA, Parsa NZ, Kallioniemi A, Kallioniemi OP, Ethier SP: Molecular cytogenetic analysis of 11 new breast cancer cell lines. *Br J Cancer* 1999, 81(8):1328-1334.
111. Mishra DK, Sakamoto JH, Thrall MJ, Baird BN, Blackmon SH, Ferrari M, Kurie JM, Kim MP: Human lung cancer cells grown in an ex vivo 3D lung model produce matrix metalloproteinases not produced in 2D culture. *PLoS one* 2012, 7(9):e45308.
112. Rosen JM, Jordan CT: The increasing complexity of the cancer stem cell paradigm. *Science* 2009, 324(5935):1670-1673.
113. Clarke MF, Dick JE, Dirks PB, Eaves CJ, Jamieson CH, Jones DL, Visvader J, Weissman IL, Wahl GM: Cancer stem cells--perspectives on current status and future directions: AACR Workshop on cancer stem cells. *Cancer research* 2006, 66(19):9339-9344.
114. Fillmore C, Kuperwasser C: Human breast cancer stem cell markers CD44 and CD24: enriching for cells with functional properties in mice or in man? *Breast cancer research : BCR* 2007, 9(3):303.
115. Shipitsin M, Campbell LL, Argani P, Weremowicz S, Bloushtain-Qimron N, Yao J, Nikolskaya T, Serebryiskaya T, Beroukhim R, Hu M, Halushka MK, Sukumar S, Parker LM, Anderson KS, Harris LN, Garber JE, Richardson AL, Schnitt SJ, Nikolsky Y, Gelman RS, Polyak K: Molecular definition of breast tumor heterogeneity. *Cancer Cell* 2007, 11(3):259-273.
116. Luzzi KJ, MacDonald IC, Schmidt EE, Kerkvliet N, Morris VL, Chambers AF, Groom AC: Multistep nature of metastatic inefficiency: dormancy of solitary cells after successful extravasation and limited survival of early micrometastases. *Am J Pathol* 1998, 153(3):865-873.

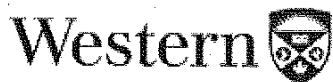
117. Croker AK, Allan AL: Cancer stem cells: implications for the progression and treatment of metastatic disease. *Journal of cellular and molecular medicine* 2008, 12(2):374-390.
118. Friedenstein AJ, Chailakhyan RK, Latsinik NV, Panasyuk AF, Keiliss-Borok IV: Stromal cells responsible for transferring the microenvironment of the hemopoietic tissues. Cloning in vitro and retransplantation in vivo. *Transplantation* 1974, 17(4):331-340.
119. Stone KC, Mercer RR, Gehr P, Stockstill B, Crapo JD: Allometric relationships of cell numbers and size in the mammalian lung. *Am J Respir Cell Mol Biol* 1992, 6(2):235-243.
120. Kitchens DL, Snyder EY, Gottlieb DI: FGF and EGF are mitogens for immortalized neural progenitors. *J Neurobiol* 1994, 25(7):797-807.
121. Xu C, Rosler E, Jiang J, Lebkowski JS, Gold JD, O'Sullivan C, Delavan-Boorsma K, Mok M, Bronstein A, Carpenter MK: Basic fibroblast growth factor supports undifferentiated human embryonic stem cell growth without conditioned medium. *Stem Cells* 2005, 23(3):315-323.
122. Yoshida A, Anand-Apte B, Zetter BR: Differential endothelial migration and proliferation to basic fibroblast growth factor and vascular endothelial growth factor. *Growth Factors* 1996, 13(1-2):57-64.
123. Montero A, Okada Y, Tomita M, Ito M, Tsurukami H, Nakamura T, Doetschman T, Coffin JD, Hurley MM: Disruption of the fibroblast growth factor-2 gene results in decreased bone mass and bone formation. *The Journal of clinical investigation* 2000, 105(8):1085-1093.
124. Frohlich M, Henke E, Arnold W, Naundorf H, Gens J: [Experimental research following intratumor bleomycin use in the nude mouse model of oral mucosa cancer and the clinical pilot study]. *Arch Geschwulstforsch* 1986, 56(2):125-134.
125. Gupta PBK, C.: Disease models of cancer: Breast cancer. *Drug Discov Today* 2004, 1:9-16.
126. Bono F, De Smet F, Herbert C, De Bock K, Georgiadou M, Fons P, Tjwa M, Alcouffe C, Ny A, Bianciotto M, Jonckx B, Murakami M, Lanahan AA, Michielsen C, Sibrac D, Dol-Gleizes F, Mazzone M, Zacchigna S, Herault JP, Fischer C, Rigon P, Ruiz de Almodovar C, Claes F, Blanc I, Poesen K, Zhang J, Segura I, Gueguen G, Bordes MF, Lambrechts D, Broussy R, van de Wouwer M, Michaux C, Shimada T, Jean I, Blacher S, Noel A, Motte P, Rom E, Rakic JM, Katsuma S, Schaeffer P, Yayon A, Van Schepdael A, Schwalbe H, Gervasio FL, Carmeliet G, Rozensky J, Dewerchin M, Simons M, Christopoulos A, Herbert JM, Carmeliet P: Inhibition of tumor angiogenesis

- and growth by a small-molecule multi-FGF receptor blocker with allosteric properties. *Cancer Cell* 2013, 23(4):477-488.
127. Herbert C, Alcouffe C, Bono F: [SSR128129E, an extracellularly acting, small-molecule, allosteric inhibitor of FGF receptor signaling]. *Med Sci (Paris)* 2013, 29(10):834-836.
 128. Herbert C, Schieborr U, Saxena K, Juraszek J, De Smet F, Alcouffe C, Bianciotto M, Saladino G, Sibrac D, Kudlinzki D, Sreeramulu S, Brown A, Rigon P, Herault JP, Lassalle G, Blundell TL, Rousseau F, Gils A, Schymkowitz J, Tompa P, Herbert JM, Carmeliet P, Gervasio FL, Schwalbe H, Bono F: Molecular mechanism of SSR128129E, an extracellularly acting, small-molecule, allosteric inhibitor of FGF receptor signaling. *Cancer Cell* 2013, 23(4):489-501.
 129. Bansal R, Magge S, Winkler S: Specific inhibitor of FGF receptor signaling: FGF-2-mediated effects on proliferation, differentiation, and MAPK activation are inhibited by PD173074 in oligodendrocyte-lineage cells. *J Neurosci Res* 2003, 74(4):486-493.
 130. Pardo OE, Latigo J, Jeffery RE, Nye E, Poulsom R, Spencer-Dene B, Lemoine NR, Stamp GW, Aboagye EO, Seckl MJ: The fibroblast growth factor receptor inhibitor PD173074 blocks small cell lung cancer growth in vitro and in vivo. *Cancer research* 2009, 69(22):8645-8651.
 131. Miyake M, Ishii M, Koyama N, Kawashima K, Kodama T, Anai S, Fujimoto K, Hirao Y, Sugano K: 1-tert-butyl-3-[6-(3,5-dimethoxy-phenyl)-2-(4-diethylamino-butylamino)-pyrido[2,3 -d]pyrimidin-7-yl]-urea (PD173074), a selective tyrosine kinase inhibitor of fibroblast growth factor receptor-3 (FGFR3), inhibits cell proliferation of bladder cancer carrying the FGFR3 gene mutation along with up-regulation of p27/Kip1 and G1/G0 arrest. *J Pharmacol Exp Ther* 2010, 332(3):795-802.
 132. Hamby JM, Connolly CJ, Schroeder MC, Winters RT, Showalter HD, Panek RL, Major TC, Olsewski B, Ryan MJ, Dahring T, Lu GH, Keiser J, Amar A, Shen C, Kraker AJ, Slintak V, Nelson JM, Fry DW, Bradford L, Hallak H, Doherty AM: Structure-activity relationships for a novel series of pyrido[2,3-d]pyrimidine tyrosine kinase inhibitors. *J Med Chem* 1997, 40(15):2296-2303.
 133. Batley BL, Doherty AM, Hamby JM, Lu GH, Keller P, Dahring TK, Hwang O, Crickard K, Panek RL: Inhibition of FGF-1 receptor tyrosine kinase activity by PD 161570, a new protein-tyrosine kinase inhibitor. *Life Sci* 1998, 62(2):143-150.
 134. Itoh N, Ornitz DM: Functional evolutionary history of the mouse Fgf gene family. *Dev Dyn* 2008, 237(1):18-27.

135. Bonnans C, Chou J, Werb Z: Remodelling the extracellular matrix in development and disease. *Nat Rev Mol Cell Biol* 2014, 15(12):786-801.

APPENDICES

Appendix 1. Approved animal use protocol



AUP Number: 2009-064

AUP Title: Role of ALDH+/CD44+ stem-like cells in breast cancer progression and treatment

Yearly Renewal Date: 10/01/2014

The YEARLY RENEWAL to Animal Use Protocol (AUP) 2009-064 has been approved, and will be approved for one year following the above review date.

This AUP number must be indicated when ordering animals for this project.

Animals for other projects may not be ordered under this AUP number.

Purchases of animals other than through this system must be cleared through the ACVS office.

Health certificates will be required.

REQUIREMENTS/COMMENTS

Please ensure that individual(s) performing procedures on live animals, as described in this protocol, are familiar with the contents of this document.

The holder of this Animal Use Protocol is responsible to ensure that all associated safety components (biosafety, radiation safety, general laboratory safety) comply with institutional safety standards and have received all necessary approvals.

Please consult directly with your institutional safety officers.

Submitted by: Kinchlea, Will D

on behalf of the Animal Use Subcommittee

CURRICULUM VITAE

Matthew Michael Piaseczny

EDUCATIONAL

- Master of Science (MSc) - Anatomy and Cell Biology
University of Western Ontario - London, ON, Canada **Sept 2013 - June 2015**
(intended)
- Bachelor of Medical Sciences (BMSc) - Honours
Specialization Microbiology and Immunology
University of Western Ontario - London, ON, Canada **Sept 2009 - April 2013**

RESEARCH AND RELATED EXPERIENCE

- Graduate Research Assistant (MSc Thesis)
University of Western Ontario - London, ON, Canada **Sept 2013 - June 2015**
Supervisor: Dr. Alison Allan (intended)
- Graduate Teaching Assistant **Sept 2013 - April 2015**
Medical Sciences 4930F/G
- Clinical Research Assistant **Sept 2013 - May 2015**
Paediatric E.R., Victoria Hospital - London, ON, Canada
Principle Investigator: Dr. Roger Zemek
Supervisor: Dr. Gurinder Sangha
- Honours Thesis Project (undergraduate, fourth year) **Sept 2012 - April 2013**
University of Western Ontario - London, ON, Canada
Supervisor: Dr. Lynne Postovit
- Scholar's Electives Research Project (undergraduate, third year) **Sept 2011 - April 2012**
University of Western Ontario - London, ON, Canada
Supervisor: Dr. Lynne Postovit
- Scholar's Electives Research Project (undergraduate, second year) **Sept 2010 - April 2011**
University of Western Ontario - London, ON, Canada
Supervisor: Dr. Lynne Postovit

ACADEMIC AWARDS AND SCHOLARSHIPS

CIHR Institute Community Support (ICS) Travel Award Amount: \$1,000	April 2015
CIHR Fredrick Banting and Charles Best Canada Graduate Scholarship Amount: \$17,500	Sept 2014 - Aug 2015
CIHR Strategic Training Program in Cancer Research Studentship Amount: \$300 (co-funded by the Translational Breast Cancer Research Unit)	Sept 2014 - Aug 2015
Translational Breast Cancer Research Unit Studentship Amount: \$300 (co-funded by the CIHR-Strategic Training Program)	Sept 2014 - Aug 2015
Western Graduate Research Scholarship Amount: \$4,500	Sept 2013 - Aug 2015
CIHR Strategic Training Program in Cancer Research Studentship Amount: \$9,050 (co-funded by the Translational Breast Cancer Research Unit)	Sept 2013 - Aug 2014
Translational Breast Cancer Research Unit Studentship Amount: \$9,050 (co-funded by the CIHR-Strategic Training Program)	Sept 2013 - Aug 2014
Scholar's Electives Program - University of Western Ontario	Sept 2009 - April 2013
OSSTF Teaching Promise Award Amount: \$250	Oct 2009

PUBLICATIONS

Pio, G., Piaseczny, MM. , Xia, Y., Goodale, D., Chu, JE and Allan, AL Soluble bone-derived osteopontin mediates migration and stem-like growth of human breast cancer cells via integrin and CD44 signaling. In preparation for <i>Journal of Biological Chemistry</i> , April 2015.	April 2015
Piaseczny MM , Allan AL. Why Does Breast Cancer Often Spread to the Lung? <i>Women's Health</i> . 2014; 10(6):561-564.	Sept 2014

ORAL PRESENTATIONS

- Piaseczny, MM**, Goodale, D, Allan, AL. “The lung microenvironment influences the metastatic behaviour of ALDH^{hi}CD44⁺ breast cancer cells in an innovative *ex vivo* pulmonary metastasis model. Cancer Research Laboratory Program Seminar Series, London Regional Cancer Centre, London, ON **March 2015**
- Piaseczny, MM**, Allan, AL. “Effect of soluble lung-derived factors on ALDH^{hi}CD44⁺ breast cancer cell metastatic behaviour and treatment resistance. Cancer Research Laboratory Program Seminar Series, London Regional Cancer Centre, London, ON **March 2014**

ABSTRACTS/POSTER PRESENTATIONS

- Piaseczny, MM.**, Goodale, D., and Allan, A.L. The lung microenvironment influences metastatic behavior of breast cancer cells in an innovative 3D *ex vivo* pulmonary metastasis model. 2015 American Association of Cancer Research (AACR) Annual Meeting, Philadelphia, PA, April 2015. **April 2015**
- Pio, G., **Piaseczny, MM.**, Xia, Y., Goodale, D., Chu, J.E. and Allan, A.L. Soluble bone-derived osteopontin mediates migration and stem-like growth of human breast cancer cells via integrin and CD44 signaling. 2015 American Association of Cancer Research (AACR) Annual Meeting, Philadelphia, PA, April 2015. **April 2015**
- Piaseczny, MM.**, Goodale, D., and Allan, A.L. The lung microenvironment influences metastatic behavior of breast cancer cells in an innovative 3D *ex vivo* pulmonary metastasis model. London Health Research Day, London, ON **April 2015**
- Zhang G, **Piaseczny M**, Findlay S, Jewer M, Vincent K, Postovit LM **Nov 2014**
The effect of Nodal on human fibroblast. CRINA Research Day, Edmonton, AB
- Piaseczny, MM.**, Goodale, D., and Allan, A.L. The lung microenvironment influences metastatic behavior of breast cancer cells in an innovative 3D *ex vivo* pulmonary metastasis model. ACB Research Day, University of Western Ontario, London, ON **Oct 2014**
- Piaseczny, MM**, Allan, AL. “Effect of soluble lung-derived factors on ALDH^{hi}CD44⁺ breast cancer cell metastatic behaviour and treatment resistance. Oncology Research and Education Day, London, ON **June 2014**
- Piaseczny, MM**, Allan, AL. “Effect of soluble lung-derived factors on ALDH^{hi}CD44⁺ breast cancer cell metastatic behaviour and treatment resistance. London Health Research Day, London, ON **April 2014**